The Calern Asteroid Polarisation Survey : state of the art

Ph. Bendjoya, A. Cellino, Jean-Pierre Rivet, M. Devogèle, S. Bagnulo, L. Abe, D. Vernet, R. Gil-Hutton, A. Veneziani

Astronomy & Astrophysics manuscript no. output
May 9, 2022

The Calern Asteroid Polarisation Survey: state of the art

An updated catalogue of asteroid polarimetric data

Ph. Bendjoya[1], A. Cellino[2], J.-P. Rivet[1], M. Devogèle[3], S. Bagnulo[4], L. Abe[1], D. Vernet[1], R. Gil-Hutton[5], and A. Veneziani[6]

[1] Université Côte d'Azur, Observatoire de la Côte d'Azur, CNRS, Laboratoire Lagrange, Boulevard de l'Observatoire, CS34229, 06304, Nice Cedex 4, France
e-mail: bendjoya@oca.eu
[2] INAF, Osservatorio Astrofisico di Torino, via Osservatorio 20, 10025 Pino Torinese, Italy
e-mail: alberto.cellino@inaf.it
[3] Lowell Observatory, 1400 W. Mars Hill Road, Flagstaff, AZ 86001, USA
e-mail: mdevogele@lowell.edu
[4] Armagh Observatory and Planetarium, College Hill, Armagh BT61 9DG, UK
e-mail: Stefano.Bagnulo@Armagh.ac.uk
[5] Grupo de Ciencias Planetarias, Departamento de Geofísica y Astronomía, Facultad de Ciencias Exactas, Físicas y Naturales, Universidad Nacional de San Juan - CONICET,
Av. J. I. de La Roza 590 Oeste, J5402DCS Rivadavia, San Juan, Argentina
e-mail: ricardo.gil-hutton@conicet.gov.ar
[6] Physics department, Torino University, via Pietro Giuria 1, 10025 Torino
e-mail: andrea.veneziani@edu.unito.it

Received ..., 2020; accepted ..., 2020

ABSTRACT

Context. The Calern Asteroid Polarimetric Survey (CAPS), a collaboration between the INAF, Astrophysical Observatory of Torino (Italy) and the Observatoire de la Côte d'Azur (Nice, France) has produced new asteroid polarimetric data for some years, and is one of the most important, currently active projects of asteroid polarimetry.
Aims. The purpose of this paper is to make public the CAPS data collected so far, to explain the adopted techniques of data reduction and computation of phase-polarisation curves for the measured objects, and explain, by means of some examples, the importance of the CAPS database.
Methods. The pipeline of data reduction has been recently updated and made as much automatic as possible, using numerical algorithms developed specifically for the purposes of CAPS. The derivation of phase-polarisation curves for the observed asteroids is done using established criteria and algorithms that have been recently slightly improved and are also summarized.
Results. The CAPS catalogue is a steadily growing source of information which can be exploited for different purposes, including but not limited to an updated calibration of the relations existing between different polarimetric parameters and the geometric albedo of the objects, and a study of classes of objects that can be most easily identified by means of polarimetric properties. These subjects will be more specifically discussed in separate papers.
Conclusions. Asteroid polarimetry data very nicely complement the results of other more commonly used techniques, including visible and IR photometry and spectroscopy. CAPS contains a lot of much desired information about physical properties which can hardly be inferred by means of other techniques.

Key words. Asteroids: general – Techniques: polarimetric –data analysis

1. Introduction

Polarimetry is an important tool to derive information about physical properties of the asteroids and other small bodies of the solar system. The state of partial linear polarisation of the sunlight scattered by asteroid surfaces, changes in different illumination conditions described by the so-called phase angle[1]. The fraction of linear polarisation and the orientation of the polarisation plane depend upon properties of the surface regolith, including geometric albedo, refractive index, packing density and size distribution of surface regolith particles, (see, for instance, Cellino et al. 2015a; Belskaya et al. 2015). The polarimetric behaviour is determined by the interplay of different physical mechanisms, including the so-called coherent backscattering, that is thought to be important also to explain some photometric properties of atmosphereless solar system bodies (Muinonen et al. 2002). The observed variety of polarimetric behaviour characterizing objects exhibiting different reflectance spectra, makes polarimetry a very useful complement to asteroid spectroscopy, and in some cases it makes it possible to identify more easily classes of objects that are more difficult to discover based on data obtained by other techniques. Examples are given by the so-called Barbarians (Cellino et al. 2006; Devogèle et al. 2018) and by some partially active asteroids (Devogèle et al. 2018; Cellino

[1] The phase angle is the angle between the directions to the Sun and to the observer as seen by the object.

et al. 2018). An analysis of the polarimetric properties of the asteroid (4) Vesta, visited by the DAWN space probe, has recently made it possible to more directly link the polarimetric behaviour to well-characterized properties of the surface, at least in this particular case (Cellino et al. 2016b)

The Calern Asteroid Polarimetric Survey (hereinafter CAPS) is a project of collaboration between the INAF - Astrophysical Observatory of Torino (Italy) and the Observatory of the Côte d'Azur (OCA) in Nice, (France). It is aimed at obtaining asteroid polarimetric data using a polarimeter built at the Torino Observatory, mounted on the Cassegrain focus of the 1.04-m Omicron (West) telescope of the Centre Pedagogique Planéte et Univers (C2PU) facility, located on the Calern plateau (southern France, MPC code 010) and managed by the OCA.

The purposes of CAPS, as well as a description of the instrument and a preliminary assessment of its performances have been described by Devogèle (2017b). Since 2017, and until December, 2021, CAPS has produced more than 2100 single measurements for about 600 asteroids (a first observing run carried out in 2022 has produced new data that are still under reduction). This is an important contribution in the field of asteroid polarimetry. As a comparison, the largest database currently available, namely the Asteroid Polarimetric Database (APD) maintained by D.F. Lupishko and available at the NASA *Planetary Data System* (PDS, Lupishko (2014)) at the URL address http://pds.jpl.nasa.gov/, includes little more than 5100 single measurements obtained by many authors over a much longer time span, starting since the early 70s. One of the main purposes of the present paper is to make the current CAPS database publicly available. Recently, the whole CAPS data reduction pipeline has been extensively re-designed to make most of the needed procedures automatic and faster, and improve the overall measurement accuracy, by devoting particular attention to the determination of instrumental polarisation. Moreover, some minor improvements of the criteria used to compute asteroid polarisation - phase curves using the so-called exponential-linear representation, as previously described by Cellino et al. (2015b, 2016a), have also been made.

New best-fit phase - polarisation curves have been obtained for a large sample of objects, combining CAPS data together with data available in the literature. The latter include primarily data listed in the previously mentioned APD database, as well as in the Belskaya Asteroid Polarimetry V1.0 database (Lupishko 2014; Belskaya et al. 2010). In addition, several measurements have been taken from a number of articles published by different authors. Among them, several papers were based upon data obtained at the Complejo Astronómico El Leoncito (CASLEO), managed by the Universities of La Plata, Córdoba and San Juan (Argentina), and the Argentinian scientific and technical research council (CONICET) (Gil-Hutton and Cañada-Assandri 2011, 2012; Cañada-Assandri et al. 2012). Several data were obtained in the framework of a long-lasting collaboration between the Torino Astrophysical Observatory and CASLEO started in the late 90s. Most obtained measurements were published in several papers, including Gil-Hutton et al. (2014); Gil Hutton et al. (2008); Cellino et al. (2005a,b, 1999, 2006); Belskaya et al. (2017). However, some of the CASLEO measurements, in UBVRI colours, have never been published before. Because in our computations of phase-polarisation curves described in the next Sections we use at least some of our old CASLEO measurements (taking them when needed from a private data file including all of them), after an overall check of the situation made by two of us (AC and RGH), we have decided to list CASLEO unpublished data in Appendix B

In this paper we present the current CAPS database and the techniques adopted for data analysis. We will devote separate papers (currently in preparation) to analyze specific issues based on the data presented here, including, but not limited to, the problem of a better determination of the geometric albedo of many objects. We present in the Appendix A the whole CAPS database, but in the text we only discuss some selected **subsets** of obtained data, in order to show the importance of CAPS, and give an idea of the advancements we can expect from a proper exploitation of this data set. We also briefly discuss the existence of measurement errors affecting both the CAPS database and the data available in the literature, and we list some explanations for the presence of such errors.

In this respect, it is important to note that, as described in Section 2, a new assessment of the variability of the instrumental polarisation affecting CAPS measurements, led us to revise and increase our estimates of CAPS measurement errors. In the cases of measurements published in previous papers, including those currently included in the APD database, the published values of linear polarisation do not change, but the updated values of the associated errors given in the Appendix A of this paper should supersede previous versions.

This paper is organized as follows: in Section 2, we present the reduction pipeline developed for the CAPS data. In Section 3 we mention some recent improvements of the criteria adopted to select the objects for which a reliable phase-polarisation curve can be obtained, and we summarize the algorithms developed to fit the obtained phase-polarisation curves using the so-called exponential-linear data representation. In Section 4 we show the good agreement between CAPS data and those present in the literature, and we stress the importance of adding such a large amount of CAPS data to improve the state of the art in asteroid polarimetry. In Section 5 we discuss some possible explanations for the existence of measurements that seem to be clearly affected by large errors, both among those available in the literature, as well as in a limited number of CAPS data. In Section 6 we show some preliminary examples of applications of the CAPS database to different problems encountered in asteroid polarimetry. A few final conclusions are summarized in Section 7.

2. Data Reduction

The Torino polarimeter (ToPol) makes use of a Wedged Double Wollaston configuration to split the incoming light into different polarisation components. It produces four separate replicas of the target field of view, corresponding to four orientations of linear polarisation (0°, 45°, 90°, and 135°). Therefore, the I, Q, and U Stokes parameters can be computed in one single shot (Pernechele et al. 2012; Oliva 1997).

Details on the general CAPS observation and data analysis procedures have been published by Devogèle et al. (2017a). The detector is a QSI632 CCD camera. Each night of CAPS operations includes measurements of a set of scientific targets (in nearly all cases asteroids) and a set of both zero-polarisation and highly-polarised polarimetric standard stars, for the purposes of instrumental calibration. In addition, CCD calibration measurements (bias, darks) are also carried out. No flat-field images are taken, however. In principle, these would be important for calibration purposes, but some problems have been evidenced after the publication of the Devogèle et al. (2017a) paper. In particular, it has been found that there are non-negligible internal reflections inside the ToPol that results in "leakages" between the four replicas of the field of view (the bottom part of a upper replica is leaking to the upper part of a bottom replica and vice-versa).

In the case of a fully illuminated field of view (needed to measure a flat field), these leakages are important and the normalized flat field images are noticeably affected. On the other hand, for a field of view mostly consisting of low level sky background these leakages are negligible (see section 4.1 of Devogèle (2017b) for a detailed analysis of the flat fielding and internal reflections of the ToPol). To compensate from the lack of flat fielding, the observing procedure imposes that the targets are always kept centered into the same pixels to avoid field-dependent variation of the recorded flux. This is always done with the maximum possible accuracy according to the observing circumstances (pointing and tracking accuracy of the telescope). Of course, the centering of the target cannot be considered always perfect, in spite of the fact that the moving targets (asteroids) are always observed using telescope differential tracking. However, this effect, that certainly contributes to the overall budget error, does not seem to be the main responsible of the amount of variable instrumental polarisation described in what follows.

All standard stars used for CAPS have been obtained from Hsu and Breger (1982) and Gehrels (1974). They are bright (generally between V magnitudes between 4 and 7) and require very short exposure times (rarely above a couple of seconds). Each measurement typically consists of 30 individual acquisitions to account for scintillation noise and other type of noise associated with short exposure acquisitions of bright objects.

Asteroid targets are generally much fainter and require longer exposure times, up to half an hour or more in the most challenging cases) to achieve a reasonable SNR. Each measurement consists of at least 10 individual acquisitions (more for relatively bright targets). We remind here that, opposite to the case of most polarimeters used for asteroid investigations, each acquisition provide the full set of Stokes parameters. Thus, the 10 individual acquisitions provide 10 independent measurements of the target polarisation.

Another change in the data reduction procedure with respect to the situation described by Devogèle et al. (2017a), is that the field mask has been reduced from a field of view of 5.31×0.95" to a field of view of 2.65×0.95. This change has been implemented to avoid or minimize internal reflections inside the instrument. Such reflections have been found to be symmetric with respect to the x-axis of the field of view. By covering one half of the field of view, internal reflections of the flux from bright targets are minimized, down to mostly negligible levels (more detail can be found in Devogèle (2017b)).

Up to around mid-2018, data reduction was carried out manually using the AstroImageJ image processing software (Collins et al. 2017) and a suite of Matlab codes developed for ToPol. These tasks were highly time consuming and needed to be upgraded to be able to process large number of data in a timely manner. More recently, a partially automated reduction pipeline has been developed in Python, making use of the publicly available modules: matplotlib, argparse, numpy, operator, astroquery, os, photutil, sys, glob, astropy, scipy, and tkinter.

The general procedure for any observed target (in the case of CAPS, this means solar system objects and polarisation standard stars) consists of three main steps.

1. Creation of the master dark for each exposure time and CCD temperature and correction of the science frames from the master dark. All the observations are performed at the same fixed CCD temperature. This is checked by the data reduction pipeline, which automatically checks the CCD temperature keyword in each dark and science frame. Each science frame is then corrected **for** the dark by looking for the closest in time master dark frame (of the same CCD temperature) for each science frame.
2. Due to the small field of view ($0.95' \times 2.65'$), no automatic, astrometric-based identification of the sources present in the CCD frame can be performed, as most of the time only the target and no more than one or two extra stars are detected in the field of view. This prevents the user from having an automatic selection of the target based on its sky position. As a consequence, one has to manually identify the target in the uppermost replica of the first acquisition. Since the offsets between the replicas are fixed, the three other replicas are automatically selected. Then, the pipeline will automatically detect the target in all the acquisition series (typically, 10 frames per target). The user can then verify that the correct target has been selected in all individual frames and modify manually the selection for each individual frame whenever necessary. One should note that, in the case of asteroids, the danger of mistakenly select a wrong target (like a star) is extremely unlikely if not impossible, because the asteroid is the only object that remains stationary in the field of view from frame to frame, as a consequence of the telescope tracking the desired target at a non-sidereal rate matching its motion. The target location on the CCD frame is accurately estimated by fitting a MOFFAT function to each individual replicas of the asteroid. Once the target has been correctly identified in each frame, a photometric analysis using a curve of growth technique (increasing aperture photometry) is performed.
3. The third step consists of an analysis of the photometric curve of growth obtained for each individual observation. The aperture photometry provides the counts in Analog Digital Units (ADU) for each of the four images: $I(d)$, where d= 0°, 45°, 90°, 135°. From these, the reduced Stokes parameters

$$q = \frac{I(0) - I(90)}{I(0) + I(90)}$$

and

$$u = \frac{I(45) - I(135)}{I(45) + I(135)}$$

can be derived. A plot of the mean value of the $q = Q/I$ and $u = U/I$ reduced Stokes parameters (taking into account all the frames) as a function of aperture size is presented to the users for selection of the optimal aperture size. The latter is the smallest aperture for which the curve of growth reaches a plateau and minimizes the deviation of the individual curves of growth of each of the four separate images produced on the focal plane. This approach is discussed in detail by Bagnulo et al. (2016) and has been systematically adopted for CAPS data (Devogèle et al. 2017a).

The three steps described above produce preliminary polarimetric measurements of the target.

The next step is the determination of the orientation in sky of the optical axis of the polarimeter. **If** $\overline{q_{\rm high}}$ (and $\overline{u_{\rm high}}$), are the mean value of $q_{\rm high} - \overline{q_{\rm zero}}$ (and $u_{\rm high} - \overline{u_{\rm zero}}$), where the index "high" stands for an observed high polarisation standard star, the instrumental polarisation angle is computed as:

$$\theta_{\rm exp} = 0.5 \arctan \frac{\overline{u_{\rm high}}}{\overline{q_{\rm high}}} + \theta_0$$

where (see Bagnulo et al. (2006))

$\theta_0 = 0°$ if $\overline{\rm q_{high}} > 0$ and $\overline{\rm u_{high}} > 0$,

$\theta_0 = 180^\circ$ if $\overline{q_{\rm high}} > 0$ and $\overline{u_{\rm high}} < 0$,

$\theta_0 = 90^\circ$ if $\overline{q_{\rm high}} < 0$,

$\theta_0 = 45^\circ$ if $\overline{q_{\rm high}} = 0$ and $\overline{u_{\rm high}} > 0$, and

$\theta_0 = 135^\circ$ if $\overline{q_{\rm high}} = 0$ and $\overline{u_{\rm high}} < 0$.

From the known value of the polarisation angle of the standard star $\theta_{\rm stand}$ the correction angle $\Delta\theta = \theta_{\rm stand} - \theta_{\rm exp}$ is determined.

The ToPol instrument is attached to the telescope in a fixed position, and is not subject to any rotation. This means that, once the above mentioned correction angle has been determined with high accuracy, it is supposed to remain constant from night to night. We use therefore for each observing run (lasting generally between one and two weeks) a fixed $\Delta\theta$ resulting from the measurements of all high-polarisation standard stars obtained in all the nights of the same observation run.

The final step is the computation of the so-called $P_{\rm r}$ parameter, which is generally used to describe the state of linear polarisation of planetary objects (see, also, Section 3). This is done by applying a rotation to the Stokes parameters such that $q_{\rm aster} = P_{\rm r}$ represents the polarisation in the scattering plane[2] and the plane perpendicular to the scattering plane. In this reference system, the $u_{\rm aster}$ Stokes parameters is expected to be equal or nearly equal to zero. This rotation is performed automatically by pulling the "Sun-Target radial (ϕ)" information about the target, available from the JPL Horizons service. The astroquery.jplhorizons python package is used to obtain these information automatically and accurately for each individual frame. The $P_{\rm r}$ can be finally computed as

$$P_{\rm r} = \cos(2(\Phi + \pi/2))\overline{q'} + \sin(2(\Phi + \pi/2))\overline{u'}$$

where $\Phi = \phi + \Delta\theta$ is the angle (corrected from the polarimeter orientation on sky) between the direction Object-North Pole and the direction Object-Sun. The Φ' angle can be computed from trivial formulas valid for the spherical triangle defined by the object, the Sun and the North celestial pole. The necessary information about the Sun coordinates and asteroid phase angle for any epoch of observation is also obtained automatically through a request to the Horizon JPL data server.
Finally, the uncertainty on $P_{\rm r}$ is computed by error propagation assuming that the errors of q and u are uncorrelated.

As mentioned above, a typical asteroid measurement consists of at least $N = 10$ individual exposures. During the various exposures, the target polarisation is supposed to remain constant, so that the scattering of the measurements about their average provides an external error estimate, which is practically dominated by photon-noise error.

The results, however, are affected by instrumental polarisation produced by the optical components of the system. To correct for instrumental polarisation, two or more unpolarised standard stars are observed every night. For these stars, it can be assumed that any measured values of q and $u \neq 0$ are spurious, being produced by instrumental polarisation. Assuming that q and u are the raw Stokes parameter, while $\overline{q_{\rm zero}}$ and $\overline{u_{\rm zero}}$ are the mean polarisation measured from several unpolarised standard stars observed during the same night, a preliminary correction of the measured polarisation is computed as:

$$q' = q - \overline{q_{\rm zero}}$$

and

$$u' = u - \overline{u_{\rm zero}}$$

Measurements of unpolarised stars allow us to estimate and monitor the instrumental polarisation at different epochs. This has been found to be slightly variable in time. In particular, an extensive inspection of the scattering of measurements of unpolarised stars around nightly average values over a time span covering several years led us to conclude that in any given night the instrumental polarisation may be determined with an uncertainty of the order of 0.08 %, which has to be quadratically added to the photon-noise error.

3. Mathematical representation of obtained phase-polarisation curves

The scattered sunlight we receive from atmosphereless Solar system bodies is in a state of partial linear polarisation, and the linear polarisation plane is always found to be either parallel or perpendicular to the scattering plane, namely the plane containing the Sun, the observer and the object. In asteroid polarimetry the degree of linear polarisation is usually defined as the ratio of the difference of intensity of the light beam component $I_\perp$ having the electric vector aligned along the plane perpendicular to the scattering plane minus the intensity $I_\parallel$ of the component having the electric vector aligned parallel to that plane, divided by the sum of the two intensities. This parameter, already mentioned in Section 2, is usually indicated as $P_{\rm r}$ in the literature, and the definition just given above, expressed as:

$$P_{\rm r} = \frac{(I_\perp - I_\parallel)}{(I_\perp + I_\parallel)},$$

is just another equivalent way to express it.

We will always use the $P_{\rm r}$ parameter to indicate the measured linear polarisation of asteroids throughout this paper. Its value will always be expressed (and plotted in our figures) in percent (%). Due to the two possible orientations of the plane of linear polarisation, as mentioned above, $P_{\rm r}$ has by definition the meaning of a fraction of linear polarisation, with its sign providing information about the orientation of the polarisation plane.

The fundamental property of $P_{\rm r}$, as already mentioned in Section 1, is that it changes as a function of the phase angle at the epoch of observation. By observing the same object at different epochs and correspondingly different phase angles, one derives its so-called phase-polarisation curve. These curves are characterized by the fact that $P_{\rm r}$ is found to be always negative in a range of phase angles between 0° and a so-called "inversion angle" $\alpha_{\rm inv}$, generally close to 20°. The interval of phase angles in which $P_{\rm r}$ is negative is generally called "negative polarisation branch" (see, for instance, Cellino et al. 2015a, and references therein).

Here, we follow the same approach adopted in some previous papers (Cellino et al. 2015b, 2016a, 2018), and we use the following exponential-linear function to represent the observed trend of the relation between $P_{\rm r}$ and the phase angle α:

$$P_{\rm r}(\alpha) = A(e^{-\alpha/B} - 1) + C \cdot \alpha \quad (1)$$

where A, B, C are free parameters to be determined by means of best-fit techniques. According to its mathematical representation, when the parameters A, B, C are all positive, the exponential-linear relation describes a curve which starts at zero for zero phase angle, then reaches increasingly negative values in

[2] the scattering plane is the plane containing the Sun, the observer, and the observed planetary object

the negative polarisation branch, up to a value generally named $P_{\rm min}$. As the phase angle increases, the derivative of the curve changes its sign, $P_{\rm r}$ starts to have decreasingly negative values and reaches zero at the so-called inversion angle $\alpha_{\rm inv}$. At larger phase angles $P_{\rm r}$ tends to increase linearly, as the exponential term tends quickly to zero. Note that this exponential-linear representation is very satisfactory only up to moderate values of the phase angle, corresponding to the extreme values achievable by main-belt asteroids, which are rarely visible at phase angles larger than about 30°. Much larger values of the phase angle can be attained by near-Earth objects, which may visible up to phase angles around 100°, depending upon the distance from the Earth. In those cases, different representations of the phase - polarisation curve are used, as mentioned in Section 5.

The computation of the best-fit representation of phase-polarisation curves using Eqn. 1 can be done in many ways. As explained in previous papers (Cellino et al. 2015b, 2016a) we use a genetic algorithm, which, starting from a random set of A, B, C values, explores the space of possible solution parameters and finds the set of A, B, C values producing the smallest possible residuals with a given set of phase-polarisation data.

The adopted genetic algorithm takes its name by the particular way it explores the space of unknown parameters. It considers any given set of A, B, C values as the "DNA" characterizing a particular solution. The "fitness" of any given individual solution is assumed to be the value of its residuals with respect to the set of real data characterizing the observed phase-polarisation curve under scrutiny. Starting from an initial population of individual solutions each one characterized by a fully-random set of A, B, C, the algorithm simulates an "evolution" of the population, in which the rule is the survival of the fittest. In other words, at each step, a number of solutions coming from the previous generation are taken, and each one is modified either by "mating" with another solution, randomly exchanging their their A, B, C values, or by having one single random variation of the "DNA" of a single solution. Each newly considered "baby" solution is evaluated in terms of residuals with respect to the real data, and is kept in the population ("it survives") only if it is found to give residuals better than those of some member of the previous generation (which is removed). As increasingly better solutions are retained in the solution population, the worst members of the previous generations are removed. This process is repeated until some solution is found to give very low residuals, and this solution cannot be further improved.

Due to the intrinsic properties of a genetic approach, the algorithm is executed several times, in order to have a correspondingly high number of solutions, in order to ensure that the best possible solution is not missed. What generally happens is that the same solution is obtained several times, with very small differences in the resulting values of the A, B, C solution parameters. These differences are used to estimate the uncertainty in the determination of each parameter. The total execution time is generally only a few seconds.

We limit the computation of best-fit curves only to cases when available data are of sufficiently good quality and sample satisfactorily the interval of possible phase angles. This means that we impose some strict constraints on the selection of the objects for which we make a best-fit computation. In this respect, we have recently made some mild improvements in our adopted selection criteria, with respect to those described in Cellino et al. (2015b), In particular, our current criteria are the following:

- we exclude *a priori* from our analysis all measurements having a nominal accuracy of $P_{\rm r}$ worse than 0.20%.
- we require to have at least 4 accepted measurements taken at phase angles > 2°.
- we require to have at least 1 accepted measurement taken at phase angles ≥ 17°.
- we require to have at least 1 accepted measurement taken at phase angles < 14°.
- we require to have at least 3 accepted measurements taken at phase angles < 30°.
- we require to have at least 1 accepted measurements taken at phase angles < 10°
- we require to have at least 1 accepted measurement taken at a phase angle between 6° and 20°.

The above criteria are similar to those adopted by Cellino et al. (2015b), but they include some refinements chosen in such a way to have a better automatic rejection of not adequately sampled phase-polarisation curves.

In what follows we will show many figures displaying asteroid phase - polarisation data, and we will use different colours to distinguish CAPS measurements from available literature data. Whenever possible, best-fit curves computed according to the exponential-linear representation will be displayed together with available data.

Finally, as in the case of previous papers, we limit our analysis to available data obtained in the standard V filter, only. Polarimetric data obtained in other colours are not so abundant. In previous papers, we rarely merged V and R measurements, only in very few cases (Cellino et al. 2014, 2019), in which only few observations of faint objects were available. It is known, in fact, that polarimetric data of asteroids are wavelength-dependent (Bagnulo et al. 2015), and in some cases the detected gradient can be sufficiently steep to suggest to avoid to mix together data obtained using different filters.

4. Exploring the CAPS database

Our purpose is to present **in this paper** the current CAPS catalogue of asteroid polarimetric measurements. This includes some data that were already published in the past (Devogèle et al. 2017a, 2018) as well as a large amount of unpublished data obtained in several observing runs, up to Dec, 2021 (the observational work having experienced in 2020 some interruptions due to the COVID-19 pandemics). The whole catalogue is given in the Appendix A. For each measurement, the Table lists the object identification number, the epoch of observation (year, month, day and the time of the measurement expressed as a fraction of day, the phase angle, the measured value of $P_{\rm r}$ with its nominal error determined by data reduction, and the filter used in the measurement (B, V, R or I in the Johnson-Cousin photometric system). Every line in this Table corresponds to an average of all the single measurements of a given object in the same filter obtained in the indicated night. The indicated epoch of observation corresponds to the mean of the instants of beginning of different measurements of the same target.

The first obvious test we did, was aimed at checking that CAPS measurements are in agreement with those obtained for objects observed many times in the past by other authors using different instruments. Fig. 1 shows the cases of the dwarf-planet (1) Ceres and of the asteroids (2) Pallas, (4) Vesta, (6) Hebe, (16) Psyche and (44) Nysa. These are objects for which several CAPS data are added to many polarimetric data already available in the literature (the sources of these data are summarized in Section 1). We find that for these asteroids, CAPS measurements very nicely fit and complement the data available in the literature. We note

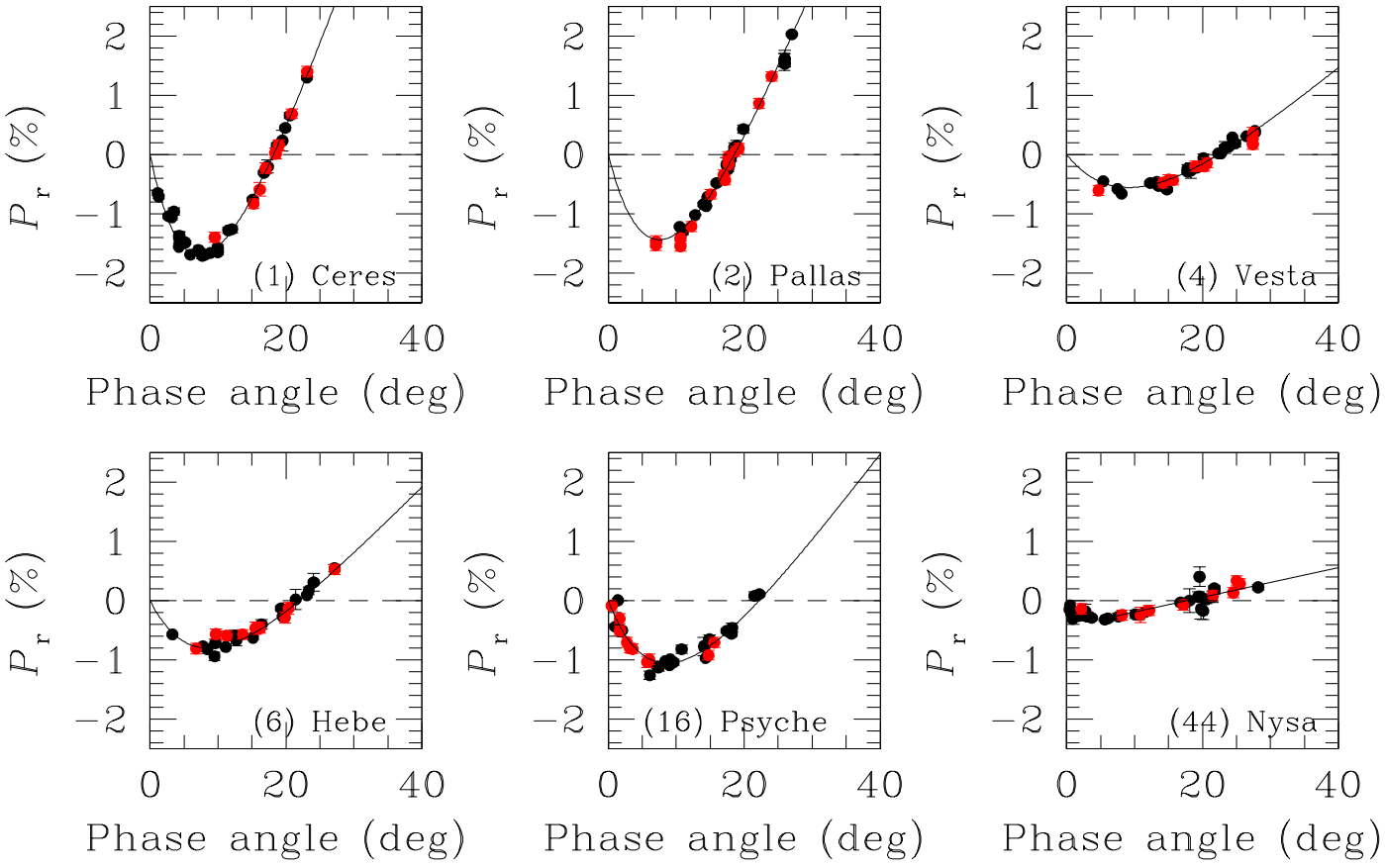

Fig. 1. Phase-polarisation curves for the dwarf-planet (1) Ceres and the asteroids (2) Pallas, (4) Vesta, (6) Hebe, (16) Psyche and (44) Nysa. CAPS measurements are plotted using red symbols, whereas literature data are plotted in black. The nominal error bars of all the measurements are shown, but are often not larger than the size of the symbols used to display the data.

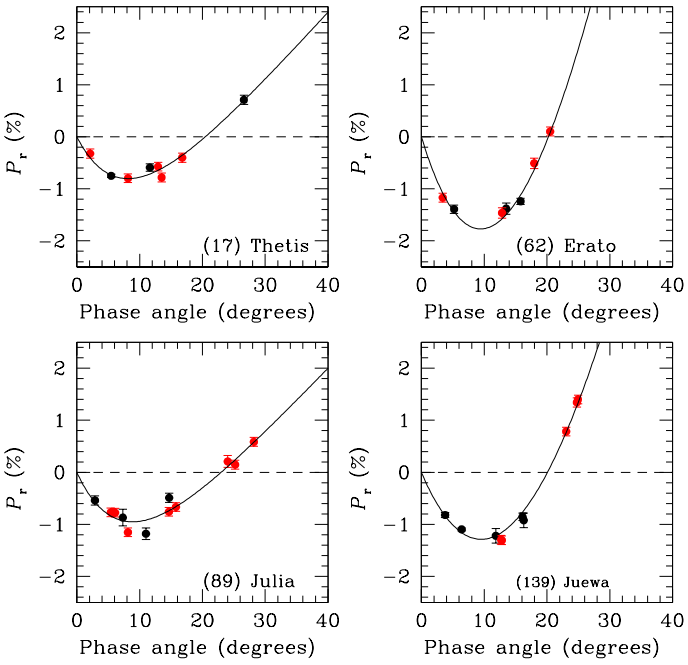

Fig. 2. The same as Fig. 1, but for the asteroids (17) Thetis, (62) Erato, (89) Julia and (139) Juewa.

that all the best-fit curves, in this and all the other figures shown below, have been obtained using all the available data (from the literature and from CAPS), without any *a priori* removal of discrepant measurements.

Fig. 2 shows the phase polarisation curves of the asteroids (17) Thetis, (62) Erato, (89) Julia and (139) Juewa. These are examples of cases in which CAPS data, due to scarcity of measurements coming from other sources, are essential to compute new phase-polarisation curves. In these cases, even a small number of additional CAPS measurements produce a decisive improvement of the interval of phase angle covered by the observations.

CAPS allow us in many cases to derive for the first time new, satisfactory phase-polarisation curves of asteroids for which no data coming from other sources were previously available. A few examples are given in Fig. 3, showing the cases of (28) Bellona, (57) Mnemosyne, (60) Echo and (510) Mabella.

CAPS data have been obtained for asteroids belonging to a large variety of taxonomic classes, as defined on the basis of their reflectance spectra. Although asteroid phase-polarisation curves can be represented using one single mathematical representation (as the one given by Eqn. 1), it is known that different taxonomic classes exhibit differences in the details of the morphology of their phase-polarisation curves. These differences include the position and depth of the extreme value of negative polarisation (the latter being usually indicated as $P_{\rm min}$), the value of the polarisation inversion angle $\alpha_{\rm inv}$, the slope of the curve around $\alpha_{\rm inv}$, and the so-called Ψ parameter, corresponding to the difference in P_r measured at the phase angles of 30° and 10° (Cellino et al. 2015b).

The variety of polarimetric behaviour of different classes of asteroids is generally thought to be a consequence of differences

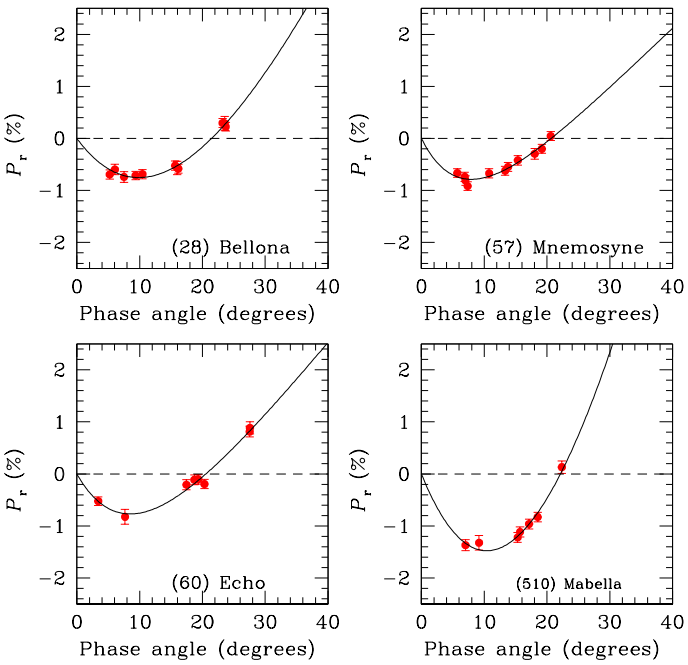

Fig. 3. The same as Fig. 1, but for the asteroids (28) Bellona, (57) Mnemosyne, (194) Prokne and (510) Mabella.

in surface properties, including primarily, but not limited to, the geometric albedo (see, for instance, Cellino et al. 2015b, 2016a). This subject will not be specifically analyzed in this paper, since it deserves more specific and detailed investigations to be postponed to forthcoming studies.

In choosing the targets of CAPS observing runs, particular attention is devoted to the members of dynamical families (Milani et al. 2014). These are groups of asteroids issued from energetic collisional events. It is therefore interesting to study the surface properties of these objects, that were previously parts of the internal layers of their parent bodies. We present a few preliminary results for some particular case in Section 6.4.

5. Noisy phase-polarisation curves

In the absence of very robust predictions based on theoretical considerations, we are forced to fit asteroid phase-polarisation curves using empirical relations like the one expressed by Eqn. 1. Other empirical functions have also been used in the past, including the following trigonometric representation originally proposed by Lumme and Muinonen (1993):

$$P_{\rm r}(\alpha) = K\ \sin^{L}(\alpha) \cdot \cos^{M}(\alpha/2) \cdot \sin\left(\alpha - \alpha_{inv}\right) \qquad (2)$$

where α is the phase angle, $\alpha_{\rm inv}$is the value of the inversion angle of polarisation, and K, L, and M are coefficients to be computed by means of least-squares fits. This mathematical representation has been found to provide very reasonable fits of the measured phase-polarisation curves of near-Earth objects, which are observable over a much wider range of phase angles than in the case of main-belt asteroids. A recent application of this relation can be found in Devogèle et al. (2018).

We emphasize the empirical nature of Eqns. 1 or 2 because it turns out that the best-fit solutions based on the above representations usually do not pass a Chi-square test. This means that the adopted empirical relations may be wrong, and/or that there are problems affecting several measurements of asteroid linear polarisation and the corresponding errors affecting these measurements. If we examine some Figures shown in the previous Section, actually, we see that there are objects for which some single polarimetric measurements turn out to be well above or below the expected value, according to the best-fit phase-polarisation curve. Such discrepancies can be much larger than the nominal error bars of the measurements.

It is therefore reasonable to explain the sporadic presence of evident outlier values in asteroid phase-polarisation curves as due to important observation errors and strong underestimates of their associated errors.

In general terms, because bad data appear to be unusual, they can be easily identified when the phase-polarisation of a given asteroid is computed on the basis of several available measurements. In these cases, the behaviour of the phase-polarisation curve is dominated by good-quality data points, and the presence of one or few bad measurements has not a strong effect on the computation of the best-fit curve. The situation is much worse whenever only small numbers of observations are available, since in these cases one or two bad measurements can lead to compute wrong phase-polarisation curves. This is the reason why we put a number of constraints upon the number and distribution of polarimetric measurements required for the computation of a phase-polarisation curve, as explained in Section 3.

As an alternative point of view, it could be tempting in some cases to interpret a noisy phase-polarisation curve as diagnostic of large-scale surface heterogeneity of the observed asteroid. In fact, in computing best-fit curves we are merging together data obtained in different observing circumstances, in terms not only of illumination conditions, but also of illuminated area facing the observers. This is a major point in asteroid polarimetry. Very similar values of linear polarisation are usually measured at very different epochs, when the object is observed in different viewing conditions, but at the same phase angle. This suggests that, although the detailed morphology of the phase-polarisation curve of any given asteroid is certainly determined by its individual surface properties, these properties tend to be very homogeneous across its surface.

Moreover, it seems very unlikely that the phase-polarisation curves of some asteroids might be characterized by so abrupt variations to be hardly represented using a continuous function. Nor should we forget that ground-based asteroid polarimetric measurements are disk-integrated. This tends to smooth out any abrupt variation that in principle might be due to local surface features.

In fact, there is only one asteroid for which large-scale surface heterogeneity has been definitely proven to exist and produce easily measurable effects on the resulting linear polarisation. This is the big asteroid (4) Vesta, which has been extensively investigated by different authors (see Cellino et al. 2016b, and references therein). Sets of measurement sequences covering intervals of time comparable to the known, 5.342 hours spin period of Vesta have been analyzed. This led to confirm the expected dependence of linear polarisation upon the average composition and regolith properties of Vesta, which is characterized by large-scale surface heterogeneity, as accurately determined by the DAWN space probe (Cellino et al. 2016b).

Apart from (4) Vesta, another exception may be given by the small (around 5 km in size) near-Earth asteroid (3200) Phaethon. This object was extensively observed by different teams during its last apparition in 2017, when it was visible at high phase angles, mostly larger than 40°. Due to its fast motion on the celestial sphere, the phase angle was rapidly changing from day to day and even during each single night. A modulation of linear polarisation roughly corresponding to the known rotation period

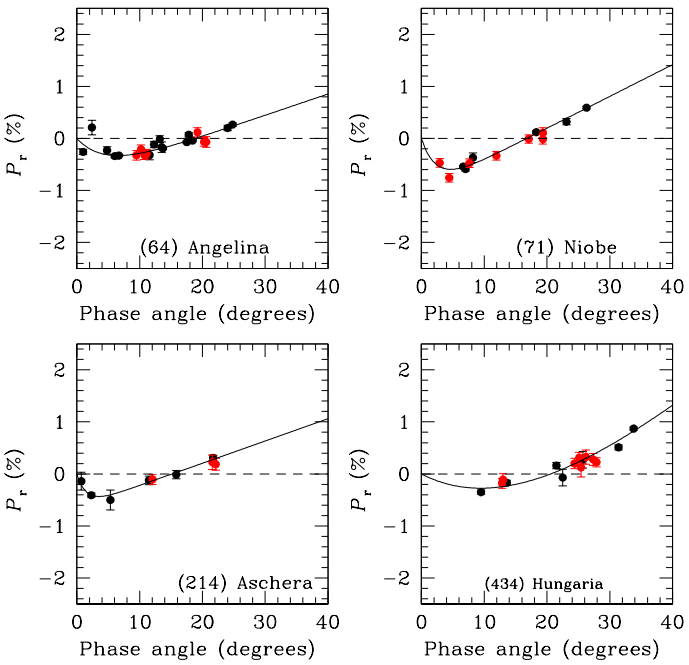

Fig. 4. The shallow phase-polarisation curves for the asteroids (64) Angelina, (71) Niobe, (214) Aschera and (434) Hungaria. The meaning of the symbols is the same as in Fig. 1.

of 3.604 h was found by Borisov et al. (2018, see also references therein). The same authors noted that no colour variation was measured during the observations, suggesting that the measured polarimetric variation could be due to regolith texture heterogeneity rather than to surface composition variegation. We can hope that more solid conclusions will be obtained during the next apparition of (3200) Phaethon in 2026.

A few other interesting cases have been more recently found by Wictorowicz & Masiero (2017) for (1) Ceres and (7) Iris, using hyper-accurate polarisation measurements. Another possible, but more uncertain case might be that of (6) Hebe, according to some old findings by Migliorini et al. (1997) that have not been confirmed so far. In the cases of Ceres and Isis, however, the measured modulation of the linear polarisation is extremely weak (Wictorowicz & Masiero 2017), and was found by an investigation specifically aimed at detecting such effect, using a 3-m telescope, and a polarimeter producing ultra-precise measurements.

It seems, therefore, that in the vast majority of cases surface heterogeneity seems not sufficient to alter significantly the nightly average of polarisation in such a way as to produce relevant noise or discontinuities in the phase-polarisation curve. We are led to conclude that no evidence of surface albedo heterogeneity can be reliably inferred by purely looking at the properties of phase-polarisation curves obtained using nightly averaged values of polarisation measured at different epochs.

There are, in fact, many possible sources of error which can sometimes produce low-quality asteroid polarimetric measurements. These can be identified when phase-polarisation curves of generally good quality are available.

The bottom line of this discussion is that bad measurements do occur, and this enhances the importance of deriving asteroid phase-polarisation curves from large datasets. In this respect, the purpose of CAPS is to strongly increase the number of available asteroid polarisation measurements. This perfectly fits one of the major challenges of modern asteroid polarimetric studies.

6. Some interesting cases

6.1. Shallow phase-polarisation curves

Fig. 4 shows the phase-polarisation curves of asteroids (64) Angelina, (71) Niobe, (214) Aschera and (434) Hungaria. We note that (434) Hungaria is the lowest-numbered member of an asteroid dynamical family located in the so-called Hungaria region, which is found at heliocentric distances between 1.8 and 2.0 AU, smaller than the inner edge of the classical asteroid main belt (Milani et al. 2014).

With the only exception of (214) Aschera, classified as *Xc*, the asteroids plotted in Fig. 4 are classified as members of the *Xe* class defined in the SMASS taxonomic classification (Bus & Binzel 2002). This class, which currently replaces the older *E* class of the Tholen taxonomy developed in the 80s (Tholen 1984, 1989), is known to consist of very high-albedo objects, according to polarimetric evidence. In fact, the so-called Umov "law", an inverse relation between degree of polarisation and albedo (see, for instance, Cellino et al. 2015b, and references therein), predicts shallow phase-polarisation curves for bright asteroids. NEOWISE thermal IR data (Masiero et al. 2014) for the asteroids shown in Fig. 4 suggest high albedo values generally above 0.4, with the only one exception of Niobe, for which a more moderate value slightly above 0.3 has been derived.

Interestingly, the above mentioned SMASS classification of (214) Aschera (*Xc*), based on its spectral reflectance properties would suggest this asteroid to be a low-albedo object, in agreement also with its *Cgh* classification in the DeMeo (DeMeo et al. 2009) taxonomy (an extension of SMASS, based on additional data obtained at near-IR wavelengths). This is in disagreeement with the Tholen classification of Aschera, Angelina and Hungaria, as members of the *E* class. As for Niobe, its Tholen classification was *S*, implying a moderate albedo.

Looking at Fig. 4, we find that new CAPS measurements of the above mentioned asteroids confirm their very shallow phase-polarisation curves, typical of high-albedo objects. We are then led to conclude that polarimetric data do not support the SMASS and DeMeo classifications of (214) Aschera as low-albedo asteroid, whereas they are in agreement with the older Tholen classification as *E*-type and with thermal IR albedo estimates. On the other hand, the polarimetric data for (71) Niobe tend to confirm the modern *Xe* classification and a moderate-to-high albedo.

Fig. 5 shows the phase-polarisation data for the asteroids (246) Asporina, (289) Nenetta, (354) Eleonora, (863) Benkoela. These asteroids belong to rare *A* taxonomic class, defined on the basis of spectral reflectance properties suggesting a high-abundance of the olivine silicate (Tholen 1989, and references therein). While (246) Asporina, (289) Nenetta, and (863) Benkoela are classified as *A*-type in the Tholen, SMASS and DeMeo taxonomies, in the case of (354) Eleonora there are classification differences: it is classified as *A*-class in the DeMeo taxonomy, but as *S* in the Tholen taxonomy, and *Sl* (one of the different sub-classes of the *S* complex), in the SMASS taxonomy. Fig. 5 shows a first example of noisy phase-polarisation curve, that of (246) Asporina, in which a general disagreement between CAPS and other literature data is apparent. In particular, CAPS data seem to be more compatible with a quite shallow curve, whereas literature data seem to suggest a slightly deeper negative polarisation branch. It is clear that more observations of this object are needed. Apart from the uncertain case of Asporina, the other three asteroids in Fig. 5 exhibit very shallow curves and look quite similar to each other, in spite of some noisy data of (863) Benkoela, which make more uncertain the determi-

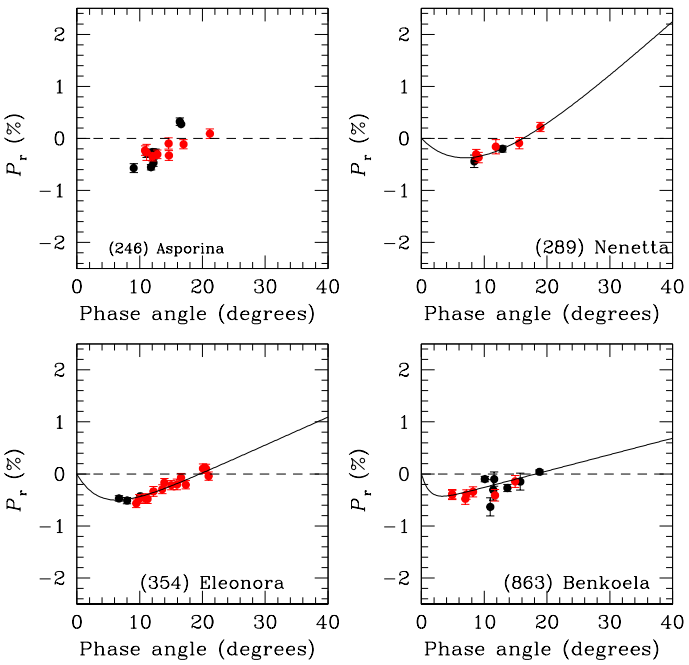

Fig. 5. Phase-polarisation data for the asteroids (354) Eleonora, (289) Nenetta, (625) Xenia and (863) Benkoela. The meaning of the symbols is the same as in Fig. 1.

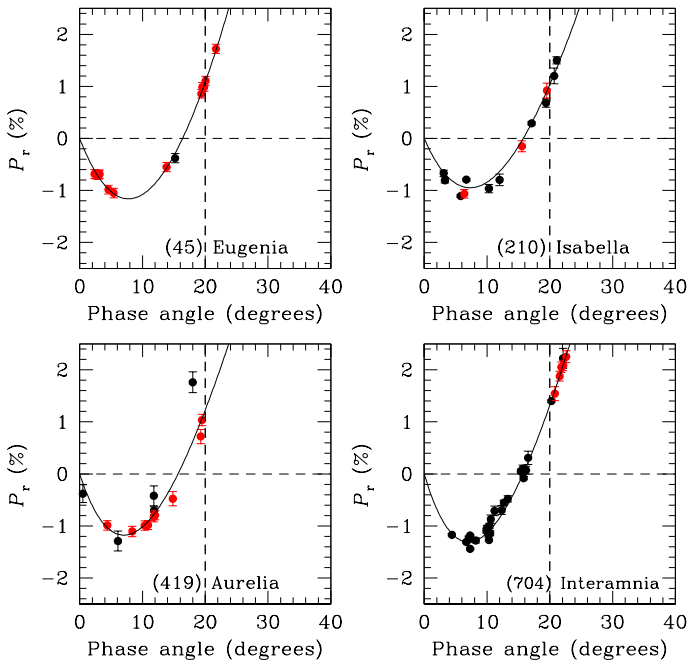

Fig. 6. Phase-polarisation data for the asteroids (45) Eugenia, (210) Isabella, (419) Aurelia and (704) Interamnia, all of them belonging to the *F* taxonomic class. The meaning of the symbols is the same as in Fig. 1. The vertical lines at the phase angle of 20° (corresponding to the typical value of the polarisation inversion angle of most asteroid taxonomic classes) are drawn as a reference to illustrate the anomanously low values of the inversion angle characterizing this taxonomic class (see text).

nation of the phase angle corresponding to the extreme value of negative polarization .

There are NEOWISE albedo estimates of 0.31 ± 0.05, 0.20 ± 0.05, and 0.29 ± 0.03 for (246) Asporina, (354) Eleonora and (863) Benkoela, respectively, according to the most recent online version of the catalogue, originally published by Masiero et al. (2014). The agreement of the fairly high values for Asporina and Benkoela is very good, whereas the lower albedo found for (354) Eleonora is more common among asteroids belonging to the *S* class. All these values might look a little underestimated for objects exhibiting such shallow phase-polarisation curves, which look similar to those of high-albedo asteroids shown in Fig. 4. This is a potentially interesting result, but, as already mentioned, we will postpone a more specific analysis of the determination of the geometric albedo from polarimetric data, and of the polarimetric properties of different asteroid taxonomic classes, to a forthcoming paper.

6.2. Curves with low inversion angles

The phase-polarisation curves of asteroids are very useful to identify particular classes of objects exhibiting unusual polarimetric properties. These properties can be diagnostic of a physical behaviour which can be hardly detectable based on data coming from other techniques. A classical example is given by the recovery of the previously known *F* taxonomic class.

This taxonomic class was first introduced by Gradie and Tedesco (1982). It included asteroids exhibiting a flat (that is why F) reflectance spectrum in the wavelength range from 0.3 to 1.1 μm, characterized by an overall lack of absorption features.

F-class asteroids are rare. In the classical asteroid taxonomy classification by Tholen (1984), only 27 asteroids, corresponding to about 3% of all classified objects, were found to belong to this class. Most interestingly, the *F*-class was known to include some objects, including the active asteroid (4015) Wilson-Harrington, showing episodes of surface activity, and therefore suspected to have a cometary origin (see, for instance, Devogèle et al. 2018, and references therein). This possibility was strengthened by the fact that the typical polarimetric property of *F*-class asteroids, namely an anomalously low value of the polarisation inversion angle $\alpha_{\rm inv}$, well below 20° (Belskaya et al. 2005, 2017), was found to be shared also by the nucleus of comet 133P/Elst-Pizarro according to (Bagnulo et al. 2010).

The most modern taxonomic classifications (Bus & Binzel 2002; DeMeo et al. 2009) are based on reflectance spectra obtained using CCD detectors, which do not cover adequately the UB spectral region. For this reason, objects previously classified as *F*-class are now merged together with asteroids previously belonging to a different Tholen class, named *B*, in what is the modern taxonomic *B*-class. The determination of the polarimetric inversion angle $\alpha_{\rm inv}$is currently the most effective tool to identify *F* class objects included in the modern *B* class.

More recently, the possibility that *F*-class asteroids can be borderline objects between asteroids and comets has been nicely confirmed by Cellino et al. (2018), who demonstrated that the near-Earth asteroid (101955) Bennu, the target of the space mission OSIRIS-REx, exhibits a low value of the polarimetric inversion angle, typical of the *F*-class. This is an important discovery, because Bennu has been found by OSIRIS-REx to display previously unexpected phenomena of surface activity (Hergenrother et al. 2019; Lauretta et al. 2019) and abundance of hydrated minerals (Hamilton et al. 2019) .

An extensive analysis of *F*-class asteroids cannot be presented in this paper. Available polarimetric data are still not sufficient. There are some preliminary indications that not all the asteroids classified as *F*-class by Tholen (1984) exhibit a sharply low value of the polarimetric inversion angle. This is not unexpected, taking into account possible cases of taxonomic misclassification, and the fact that there were in the Tholen (1984)

taxonomy several cases of uncertain, non univocal classifications (*CF*, *FC*, etc.). Moreover, recent polarisation measurements of the near-Earth asteroid (3200) Phaethon, the likely parent body of the Geminid meteor shower, and therefore an excellent candidate to be an active asteroid, have not produced conclusive evidence of a small value of $\alpha_{\rm inv}$(Devogèle et al. 2018). In general terms, the work of polarimetric analysis of the *F* taxonomic class is still in progress. One of the goals of current investigations, which will be presented in forthcoming papers, is to check whether the *F* class is sharply distinguishable, in terms of polarimetric properties, from asteroids displaying a similar reflectance spectrum at visible wavelengths, or, as it might be possible, there is a continuum in the transition from clearly *F*-like objects, to modern *B*-class asteroids.

In Fig. 6 we limit ourselves to present the cases of four asteroids, (45) Eugenia, (210) Isabella, (419) Aurelia and (704) Interamnia, clearly exhibiting a low value of $\alpha_{\rm inv}$, well below 20°, typical of the *F* class. In all these cases, CAPS observations play a relevant if not fundamental role to constrain the polarimetric behaviour of these objects.

6.3. Barbarians

The so-called Barbarian asteroids are a class of objects exhibiting an anomalous polarimetric behaviour, characterized by an unusually large value of the inversion angle $\alpha_{\rm inv}$. In this respect, their polarimetric behaviour is opposite to that of *F*-class asteroids. The prototype of the class is (234) Barbara, whose anomalous phase-polarisation curve was first discovered by Cellino et al. (2006). Since the beginning, Barbarians have been high priority targets for CAPS observations. The reason is that these objects are rare and extremely interesting, because some evidence suggests that they could be extremely primitive. In fact, spectroscopic observations have revealed that Barbarians, which are characterized by reddish reflectance spectra showing strong absorption bands in the near-IR around 2 μm, have surfaces which look extremely enriched in highly refractory compounds, especially the spinel mineral (Sunshine et al. 2008). Spinel is present in Calcium-Aluminum-rich inclusions (CAIs) found in some meteorites. CAIs are among the oldest samples of solid matter known in the Solar system, and their formation might date back to the early stages of planetesimal growth, or even before (see, for instance Cellino et al. 2015a, and references therein).

Barbarians have been extensively investigated by Devogèle et al. (2018), who carried out dedicated spectroscopic and polarimetric investigations of these objects. Among their main results, the authors proposed an explanation of the observed polarimetric behaviour as due to the refractive index of the spinel mineral, found to be anomalously abundant on Barbarian surfaces. Moreover, the above authors found evidence that that all the observed Barbarians turn out to be members of the *L* taxonomic class defined by DeMeo et al. (2009), based on reflectance spectra at visible and near-IR wavelengths. The analysis carried out by Devogèle et al. (2018) was based on the evidence coming from both spectroscopic and polarimetric data, and included an attempt to interpret the observed visible and near-IR reflectance spectra in terms of surface composition and space weathering effects. In this paper, instead, we focus more on details of the polarimetric properties, taking profit of the much improved database that is now available, including a large number of new CAPS measurements.

Figure 7 shows the available phase-polarisation data in V filter for a nearly all the known Barbarians larger than some tens of km. Smaller Barbarians exist, but they have been found to consist only of small members (a few km in size) of a couple of families having a Barbarian largest remnant, as will be mentioned below. The only one sizeable object which is not shown in 7 is (2085) Henan, for which we have so far only a couple of polarimetric measurements, suggesting a deep negative polarisation branch. Only three asteroids shown in 7 are not included in the DeMeo et al. (2009) taxonomy. They were previously classified as *L*-type by Bus & Binzel (2002). These three asteroids are (172) Baucis, (611) Valeria and (980) Anacostia.

By looking at Figure 7, one can conclude that there is not evidence of any systematic difference between Barbarians which are known members of the DeMeo et al. (2009) **L** class and those which are not included in the DeMeo et al. (2009) classification. This is not surprising: in the case of (387) Aquitania and (980) Anacostia, for instance, their close similarity in terms of spectral reflectance data had been known since a longtime (Burbine et al. 1992), and it was just the fact that (980) Anacostia had been found to be a Barbarian in terms of polarimetric properties, which led Masiero & Cellino (2009) to observe (387) Aquitania, leading to the discovery of the Barbarian polarimetric behaviour of this object.

It should also be noted that (729) Watsonia, whose phase-polarisation curve is shown in Fig. 7, is the largest remnant of the first dynamical family discovered to consist of small Barbarian members (not shown in our Figure), according to Cellino et al. (2014). This was an important discovery, because dynamical families are the currently observable outcomes of energetic collisional phenomena which produced in the past the partial or complete disruption of single parent bodies. As a consequence, current members of the Watsonia family include objects that were buried inside their parent body before the collision. In turn, the fact that the observed Watsonia members display the polarimetric properties typical of Barbarians, means that these properties are not simply due to surface processing mechanisms, but to unusual bulk compositions. The Watsonia family is important also for another reason. It is surrounded by three large Barbarians, (387) Aquitania, (599) Luisa and (980) Anacostia, which are not official members of the Watsonia family, but are so close in the space of orbital proper elements to suggest that this cannot be due to chance. The most natural explanation (Cellino et al. 2014) seems to be that in a very remote epoch one single big Barbarian parent body was completely shattered by a collision, which produced four large fragments: Aquitania, Luisa, Anacostia and Watsonia. Only at a subsequent epoch Watsonia experienced in turn another collision that produced its currently identified family. If this interpretation is correct, we can expect a close similarity between Aquitania, Luisa, Anacostia and Watsonia. Figure 7 confirms the close resemblance of the phase-polarisation curves of these four asteroids. Only in the case of (599) Luisa, it seems that the asteroid displays a slightly deeper negative polarisation branch, but this has to be confirmed by additional data. We have already mentioned the very close similarity of Aquitania and Anacostia, including also their unusual reflectance spectra.

There are, however, some questions deserving further scrutiny. Looking at Fig. 7, it seems that we can tentatively separate the objects into two different subclasses. The first and much more populous subclass, which we call "classical Barbarians", is characterized by very large values of the polarimetric inversion angle $\alpha_{\rm inv}$, most commonly larger than 28°, and $P_{\rm min}$fairly shallow, between the values of -1.4% and -1.6%. This combination of moderate $P_{\rm min}$and large $\alpha_{\rm inv}$characterizes nearly all objects shown in Fig. 7. There are, however, two cases of Barbarians which seem to be characterized by a quite deep value of $P_{\rm min}$, namely (824) Anastasia and (606) Brangäne, shown in Fig. 7.

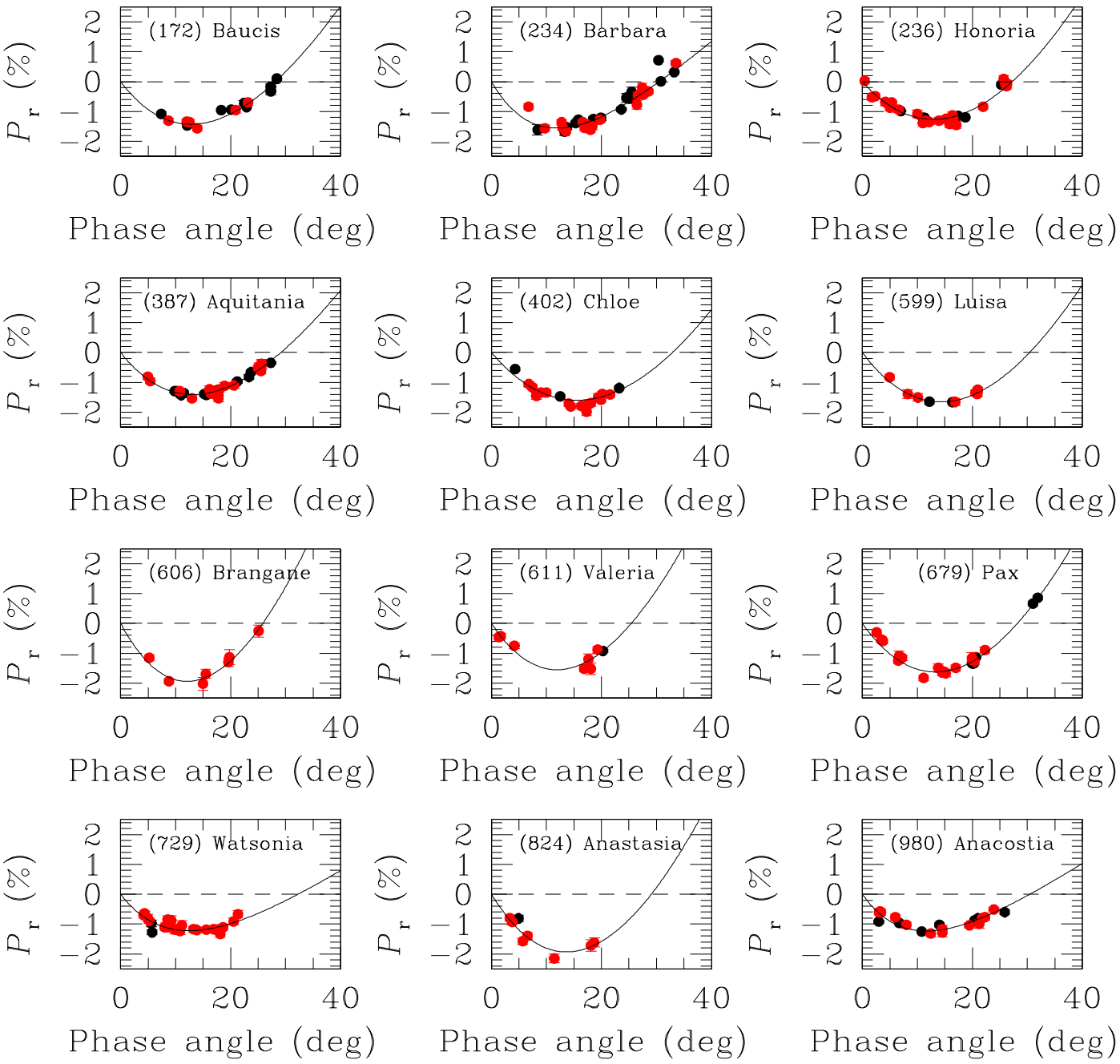

Fig. 7. Phase-polarisation data in *V* for the asteroids currently named "Barbarians", including the prototype of this class, asteroid (234) Barbara, Small members of the dynamical families of (729) Watsonia and (606) Brangane (see text) are not included in this Figure, as well as a couple of measurements of (2085) Henan, another Barbarian candidate for which more data are needed. The meaning of the symbols is the same as in Fig. 1.

Moreover, as mentioned above, a couple of measurements of (2085) Henan, classified as *L*-class in the DeMeo taxonomy, also suggest a fairly deep negative polarisation branch. We note that these three asteroids were considered to be Barbarians by Devogèle et al. (2018) on the basis of a smaller number of measurements obtained at phase angles between 16° and 20°. At these phase angles, negative values of P_r sufficiently deep to suggest a Barbarian polarimetric behaviour are measured. Interestingly enough, the above authors also found that the reflectance spectrum of (824) Anastasia could be hardly reconciled with the kind of surface composition they found to produce the best-fit of the spectra shown by most Barbarians in their adopted sample.

We also note that the Cellino et al. (2019) investigation of the Brangäne family was based on data collected in red light, and no observations were made of Brangäne family members at phase angles smaller than 17°. The transition between the deepest negative values of P_r and the inversion angle was found to be steeper than in the case of (234) Barbara. In the above paper, it was also noted that the α_{inv}value found for the Brangäne family, around 25°, appeared to be unusually low for Barbarians. In Fig. 7 we show four previously unpublished polarisation measurements of Brangäne in the V filter. These measurements were not available at the time of the analyses by Devogèle et al. (2018) and by Cellino et al. (2019), and their analyses made use of two measurements in the R filter at phase angles around 20°, including one having an error bar larger than 0.2% that should be nominally discarded if we apply the quality selection criteria described in this paper.

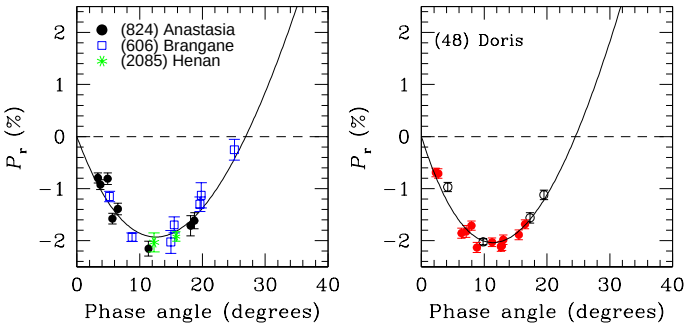

Fig. 8. Left: phase-polarisation curve obtained by merging together all the available V measurements of (824) Anastasia, (606) Brangäne and (2085) Henan. Both literature and CAPS data of these asteroids are shown using the same symbol for each of them. Right: the Phase-polarisation curve of the asteroid (48) Doris, a member of the SMASS and DeMeo *Ch* taxonomic class. The meaning of the symbols in this panel is the same as in Fig. 1.

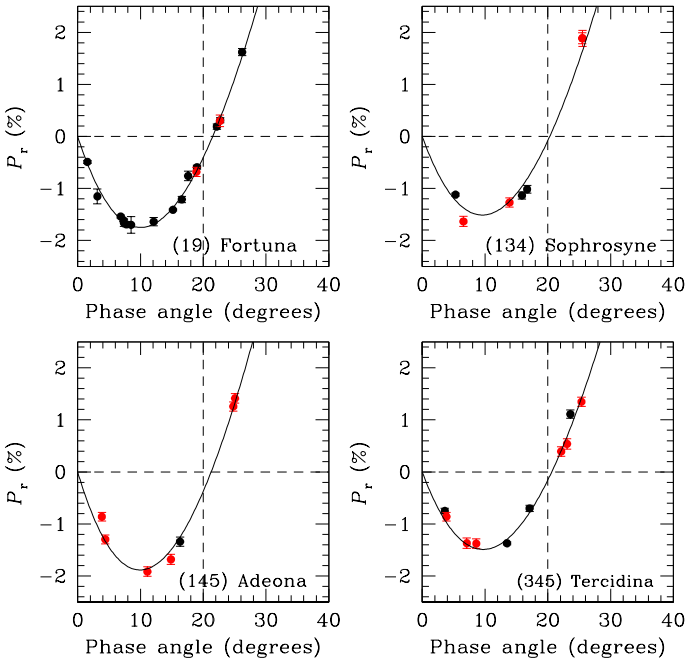

Fig. 9. Phase-polarisation curve of the asteroids (19) Fortuna, (134) Sophrosyne, (145) Adeona and (345) Tercidina. They all belong to the SMASS *Ch* taxonomic class, but they exhibit quite different phase-polarisation curve, with respect to (48) Doris shown in Figure 8. The meaning of the symbols is the same as in Fig. 1.

If one does the exercise of merging together all available polarimetric data of Anastasia, Brangäne and Henan in V light, the resulting best-fit phase-polarisation curve exhibits a deeper $P_{\rm min}$and a slightly smaller value of the inversion angle $\alpha_{\rm inv}$with respect to classical Barbarians. This shown in the left panel of Fig. 8

These results raise clearly some questions. It seems possible that either there are two different subclasses of the objects that we collectively call Barbarians, or we must be more careful when we adopt phenomenological criteria to identify Barbarians, based on the values of $P_{\rm r}$ measured at phase angles between about 18° and 20°. Such simple criterion could lead sometimes to false positives. Some objects can exist, exhibiting deep $P_{\rm min}$and inversion angles well smaller than 28°, but relatively deep negative polarisation branches that could be erroneously interpreted as diagnostic the Barbarian class.

The first interpretation, that there are two main classes of Barbarians, is supported by the classification as members of the DeMeo L taxonomic class of the three above mentioned asteroids whose phase-polarisation data look slightly different with respect to those of the majority of other Barbarians. This means that their reflectance spectra are typical of Barbarians, as shown by Devogèle et al. (2018), apart possibly from the case of (824) Anastasia, as mentioned above.

The alternative possibility, namely that some objects could be erroneously classified as Barbarians based on insufficient polarimetric data, is supported by the phase-polarisation curve of the asteroid (48) Doris, shown in the right panel of Fig. 8. (48) Doris is a *Ch* class asteroid, according to both Bus & Binzel (2002) and DeMeo et al. (2009). Its reflectance spectrum is rather flat, as commonly found among members of the C-complex, and has nothing to do with the strongly reddish spectra of Barbarians. However, its phase polarisation curve, based on currently available data, is characterized by a deep value of $P_{\rm min}$, followed by a steep raise and an inversion angle apparently around 24°, and looks quite similar to the composite phase-polarisation curve of (824) Anastasia, (606) Brangäne and (2085) Henan, shown in the left panel of the same Figure. Of course, we are aware that we should be careful because for (48) Doris there is a lack of data at large phase angles, and in any case this asteroid suggests a rather lower value of the polarimetric inversion angle.

In any case, the existence of asteroids belonging to the C complex, exhibiting a deep $P_{\rm min}$and values of $P_{\rm r}$ not far from -1.0% at phase angles around 20° might be not so unusual. Another example can be that of (238) Hypatia, another asteroid belonging to the *Ch*-class (Bus & Binzel 2002), whose phase-polarisation curve is noisy, but could be similar to that of (48) Doris.

Based on these facts, we conclude that the identification of Barbarians purely based on polarimetric properties, not supported by spectroscopic data, could lead in some cases to false positives. The classification as Barbarians should not be simply based on the measured value of $P_{\rm r}$ at phase angles around 20°, as usually done these days, but it should include measurements taken at higher phase angles. An estimation of $P_{\rm min}$would be also important, because classical Barbarians do not reach $P_{\rm r}$ values more negative than about -1.6. The presence of a deep negative polarisation branch might be diagnostic of non-Barbarian asteroids belonging to the C-taxonomic complex, in some cases displaying $P_{\rm r}$values not very different from those of real Barbarians at relatively high values of phase angle.

Finally, we note that the fact that two asteroids classified as members of the *Ch* taxonomic class of Bus & Binzel (2002), (48) Doris and (238) Hypatia, exhibit phase-polarisation curves that could be erroneously interpreted in terms of a Barbarian nature, should not be over-interpreted. These might be just two unlucky cases, and we cannot conclude that *Ch* asteroids are all "false Barbarians". A few examples are shown in Fig. 9, displaying the cases of (19) Fortuna, (134) Sophrosyne, (145) Adeona and (345) Tercidina. These *Ch* asteroids exhibit "normal" polarimetric inversion angles around 20°, and values of $P_{\rm r}$ of the order of -1% are reached at smaller phase angles, although some care is certainly needed in Barbarian searches. Other examples of unusually steep polarimetric data for asteroids belonging to the *Ch* class, however, will be shown in Subsection 6.6.

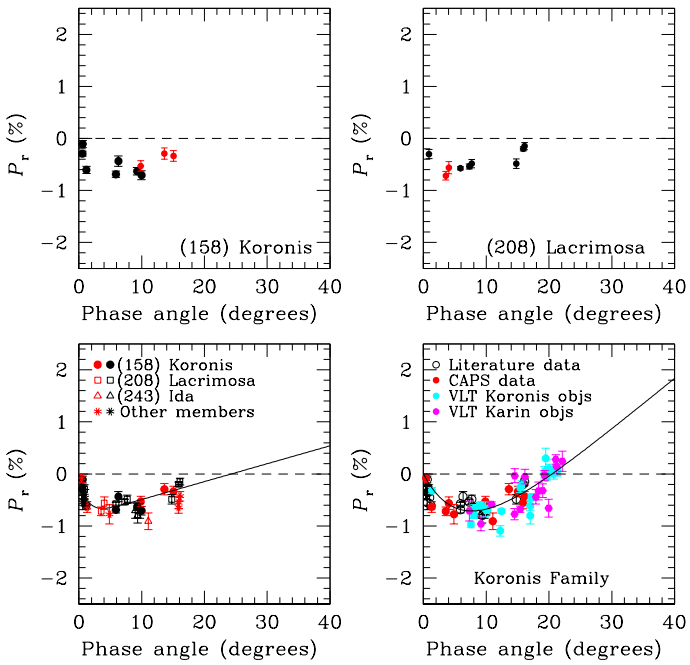

Fig. 10. Top panels: phase-polarisation data for the two asteroids (158) Koronis and (208) Lacrimosa. In both cases, the data do not allow us to compute a phase-polarisation curve according to our criteria explained in Section 3. Bottom-left panel: by merging the polarimetric data for (158) Koronis and (208) Lacrimosa, as well as some data for a small number of additional Koronis family members, we obtain the plotted phase-polarisation curve. Bottom-right panel: a slightly different phase-polarisation curve can be obtained by adding to the measurements used to produce the curve shown in the previous panel a fairly large number of VLT data obtained by Cellino et al. (2010) for a sample of small members of the Koronis and Karin families, the latter being a sub-family of that of Koronis (see text).

6.4. Families

Asteroid dynamical families are sets of objects sharing very similar values of their orbital proper elements (see, for instance, Bendjoya & Zappalà. 2002, and references therein). They are interpreted as the outcomes of energetic collisions having produced a complete shattering and fragmentation of single parent bodies. Since they consist of collisional fragments, most family members are usually fairly small and faint, apart from the largest remnants. Families have been found to be quite homogeneous in terms of spectral reflectance properties (Cellino et al. 2002), apart from the presence of random interlopers which are nearly always present in family member lists (Migliorini et al. 1995). As mentioned above, Cellino et al. (2014) found the first case of a family, that of (729) Watsonia, consisting of Barbarian asteroid members. More recently, the existence of second Barbarian family has been proposed by Cellino et al. (2019), as discussed in Section 6.3.

The Calern telescope is generally too small to allow us to undertake extensive polarimetric studies of large numbers of members of any given family. We are making an effort, however, to observe as many family members as possible, because polarimetric data are important to obtain a better physical characterization of the objects, and to possible identify interlopers, exhibiting properties clearly distinct from those of most members of a given family.

An example is given by the asteroid (194) Prokne. This object is the lowest-numbered and brightest member of the Prokne family identified by Milani et al. (2014). Usually, this should be the largest remnant of the family's parent body, but in this particular case the deep negative polarisation branch and overall morphology of the phase-polarisation curve is typical of a low-albedo asteroid, as also confirmed by neoWISE thermal IR data (Masiero et al. 2014). Most members of the Prokne family, however, turn out to be moderate-albedo objects, according to Masiero et al. (2014) and a few available taxonomic classifications. Polarisation data of (194) Prokne, in agreement with thermal IR data, suggest therefore that it is an interloper in its family, because it is very unlikely that the parent body could have a composition producing a swarm of fragments having mutually inconsistent compositions. The real largest member of the family is most likely the asteroid (686) Gersuind, and the family itself should be accordingly named Gersuind family.

Apart from the identification of likely family interlopers, there are other ways to exploit the general similarity in composition of members of the same family. It can be possible to derive a common phase-polarisation curve of any given family by merging available polarimetric data of its members. This can be then compared with those of non-family objects sharing the same taxonomic classification, based on spectral reflectance data. We plan to develop as much as possible this aspect in forthcoming papers.

Here, we present the particularly favourable case of the Koronis family in Fig. 10. This is a family characterized by a fairly shallow size distribution, suggesting that the family-forming collision was quite energetic, leading to an extensive disruption into many small fragments having similar sizes (Tanga et al. 1999). Some polarimetric data are available for two of the largest members of the family, namely (158) Koronis (10 measurements) and (208) Lacrimosa (9 measurements). As shown in the two top panels of Fig. 10, however, the data are not sufficient to derive for either object an individual phase-polarisation curve, due to insufficient coverage of the phase angle. However, it is fairly evident that these two objects exhibit, as could be expected, a quite similar behaviour, in agreement with their common collisional origin and identical age.

We can, actually, merge together their polarimetric data, as well as those available for a few additional family members, including (243) Ida (four measurements) and five other objects, each having up to a couple of measurements. In this way, we obtain a set of data allowing us to compute a phase-polarisation curve, shown in the bottom-left panel of Fig. 10. This curve is based on data taken at phase angles not exceeding 17°, and shows an extreme value of negative polarisation at a phase angle significantly smaller than 10°.

The Koronis family, however, is really special from the point of view of asteroid polarimetry. Little more than ten years ago, Cellino et al. (2010) carried out a polarimetric project aimed at detecting possible differences in the properties of a sample of very small members of the Koronis family, compared to a similar sample of equal-sized members of the very young Karin family. The latter is believed to be the outcome of a second-generation family-forming event, which caused the disruption of an original member of the Koronis family. The Karin family is supposed to be extremely young, with an estimated age less than 10 Myrs (see Cellino et al. 2010, and references within). The goal of the project was to look for systematic differences in the polarimetric properties of the members of the two families, to be possibly interpreted as indications of different exposures to space weathering mechanisms. The above study did not detect any statistically significant difference between the members of the two families, but what is important for our present purposes is that that project produced a set of little less than forty VLT

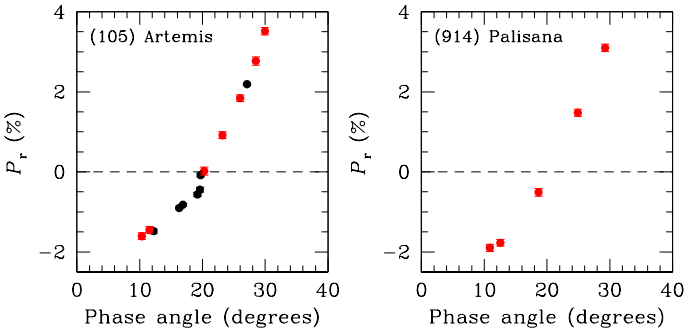

Fig. 11. Phase-polarisation data for the asteroids (105) Artemis, and (914) Palisana. The meaning of the symbols is the same as in Fig. 1.

polarimetric measurements in V light for small members of the Koronis and Karin families, with associated nominal errors below 0.2% (more uncertain data were obtained by Cellino et al. (2010) for some of the observed objects, but we did not make use of them in the current study). If we merge these measurements to those used to produce the phase-polarisation curve shown in the bottom-left panel of Fig. 10, we obtain a new phase-polarisation curve, shown in the bottom-right panel of the same Figure. It is clear that the availability of the additional VLT measurements is extremely important. The range of phase angle covered by the observations increases significantly, and the derived phase-polarisation curve shifts a little toward higher values the phase corresponding to the extreme value of negative polarisation. The resulting curve becomes more similar to those of most asteroids belonging to S taxonomic complex.

Of course, this is just a favourable example, of the application of polarimetric data to the study of asteroid families. We plan to cover this subject of investigation in future papers, as soon as we will have at our disposal a sufficient number of measurements. Currently, we have already data for members of several families, including those of Eos, Themis, Maria, and others. This is work in progress.

6.5. Near-Earth objects

Near-Earth objects (NEO) are generally faint, and most of them are beyond the possibilities of CAPS. Due to their importance, however, we are making a special effort to observe as many NEOs as possible, since they are targets of particular importance. The list of CAPS measurements presented in the Appendix A includes several NEO observations, including those of asteroids (433) Eros, (1036) Ganymede, (1620) Geographos, (1627) Ivar, (1862) Apollo, (3200) Phaethon and several others. Some NEOs that have been observed most recently are not yet included in the Appendix A, because we want to postpone their analysis to some papers in an advanced state of preparation.

6.6. Other cases

Fig. 11 shows available polarisation data for the asteroids (105) Artemis and (914) Palisana. In both cases, the interval of covered phase angles, which does not include measurements at phase angles smaller than 10°, is not sufficient to derive a reliable best-fit curve according to our criteria. However, these two asteroids are interesting and will certainly deserve new measurements in the future.

The cases of (105) Artemis and (914) Palisana are similar, being characterized by a very steep increase of linear polarisation in the positive polarisation branch. Note the different scale for the vertical axis, with respect to the "normal" scale adopted in the other Figures in this paper. In the negative branch available data can only provide a lower limit, but they are already sufficient to indicate a deep $P_{\rm min}$.

(105) Artemis is another *Ch* class asteroid, exhibiting an inversion phase angle of about 20°. (914) Palisana is not classified by either the SMASS or the DeMeo taxonomies, whereas Tholen classified this asteroid as CU, meaning a large uncertainty. It also exhibits a value of $\alpha_{\rm inv}$around 20°. Both objects are remarkable because they show a quite spectacular transition from very negative to very positive values of $P_{\rm r}$ in a limited interval of phase angle.

7. Conclusions and future developments

In this paper we have presented the results of a strong effort to increase the database of asteroid polarimetric data. We have given a general description of the quality and quantity of the CAPS database without entering yet into very specific applications which are postponed to forthcoming papers that we are already preparing.

We think that the interplay between polarimetry and spectroscopy is a major tool in order to significantly improve our knowledge and understanding of the asteroids. So far, the polarimetric side has been under-exploited, as a consequence of a general lack of data. The Calern Asteroid Polarimetric Survey has been designed and managed in order to represent a real change in this field. For this reason, we are still continuing our observing project, and we plan to present in the future periodic updates of the CAPS database.

Acknowledgements. The authors thank the staff of the Calern observing station for their wonderful support to the work of observation, both locally and in remote mode. RGH gratefully acknowledges financial support by CONICET through PIP 112-202001-01227 and San Juan National University by a CICITCA grant for the period 2020-2022.

References

Bagnulo, S., Tozzi, G.P., Boehnhardt, H., et al. 2010, A&A, 514, A99
Bagnulo, S., Cellino, A., & Sterzik, M.F. 2015, MNRAS, 446, L11
Bagnulo, S. Belskaya, I., Stinson, A., Christou, A.A., & Borisov, G. 2016, A&A 575, A122
Belskaya, I.N., Shkuratov, Yu. S., Efimov, N. M., et al. 2005, Icarus, 178, 213
Belskaya, I.N., Levasseur-Regourd, A.-C., Cellino, A., et al. 2010, Belskaya Asteroid Polarimetry V1.0. EAR-A-I0942/I0943-3-BELSKAYAPOL-V1.0. NASA Planetary Data System
Belskaya, I.N., Cellino, A., Gil-Hutton, R., Muinonen, K., et al. 2015, in Asteroids IV, Ed. P. Michel, F. DeMeo, & W.F. Bottke, University of Arizona Press, Tucson, 151
Belskaya, I.N., Fornasier, S., Tozzi, G.P., et al. 2017, Icarus, 284, 30
Benjoya, Ph., & Zappalà, V. 2002, in Asteroids III, Ed. W.F. Bottke, A. Cellino, P. Paolicchi, & R.P. Binzel, University of Arizona Press, Tucson, 613
Borisov, G., Devogéle, M., Cellino, A., et al. 2018, MNRAS, 480, L131–L135
Burbine, T., Gaffey, M, & Bell, J. 1992, Meteorit. Planet. Sci., 27, 424
Bus, S.J. & Binzel R.P. 2002, Icarus, 158, 146
Cañada-Assandri, M., Gil-Hutton, R.& Benavidez, P. 2012, A&A, 542, A11
Cellino, A., Gil-Hutton, R., Tedesco, E.F., et al. 1999, Icarus, 138, 129
Cellino, A., Bus, S.J., Doressoundiram, A., et al. 2002, in Asteroids III, Ed. W.F. Bottke, A. Cellino, P. Paolicchi, & R.P. Binzel, (University of Arizona Press), 633
Cellino, A., Yoshida, F., Anderlucci, E., et al. 2005a, Icarus, 179, 297
Cellino, A., Gil-Hutton, R., Di Martino, M., et al. 2005b, Icarus, 179, 304
Cellino, A., Belskaya, I.N., Bendjoya, Ph., et al. 2006, Icarus, 180, 565
Cellino, A., Delbo, M., Bendjoya, Ph., et al. (2010), Icarus, 209, 556
Cellino, A., Gil-Hutton, R., Dell'Oro, A., et al. 2012, JQSRT, 18, 2552
Cellino, A., Bagnulo, S., Tanga, P., et al. 2014, MNRAS, 439, 75
Cellino, A., Gil-Hutton, R. & Belskaya, I.N., 2015a, in Polarimetry of Stars and Planetary Systems, Ed. L. Kolokolova, J. Hough, & A. Levasseur-Regourd, (Cambridge University Press), 360

Cellino, A., Bagnulo, S., Gil-Hutton, R., et al. 2015b, MNRAS, 451, 3473
Cellino, A., Bagnulo, S., Gil-Hutton, R., et al. 2016a, MNRAS, 455, 2091
Cellino, A., Ammannito, E., Magni, G., et al. 2016b, MNRAS, 456, 248
Cellino, A., Bagnulo, S., Belskaya, I.N., et al. 2018, MNRAS, 481, L49-L53
Cellino, A., Bagnulo, S., Tanga, P., et al. 2019, MNRAS, 485, 570
Collins, K.A., Kielkopf, J.F., Stassun, K.G., Hessman, F.V. 2017, ApJ, 153(2), 77.
DeMeo, F., Binzel, R.P., Slivan, S.M., et al. 2009, Icarus, 202, 160
Devogèle, M., Cellino, A., Bagnulo, S. et al. 2017a, MNRAS, 465, 4335
Devogèle, M. 2017b, "Propriétés des astéroïdes de type L : un lien avec le Système Solaire primordial ?", PhD Thesis, Université Côte d'Azur, October 3rd, 2017.
Devogèle, M., Tanga, P., Cellino, A., et al. 2018, Icarus, 304, 31
Devogéle, M., Cellino, A., Borisov, G. et al. 2018, MNRAS, 479, 3498
Gehrels., T. 1974, University of Arizona Press, Tuscon, pp. 168-169
Gil Hutton, R., Mesa, V., Cellino, A., et al. 2008, A&A, 482, 309
Gil-Hutton, R. and Cañada-Assandri M. 2011, A&A, 529, A86
Gil-Hutton, R. and Cañada-Assandri, M. 2012, A&A, 539, A115
Gil-Hutton, R., Cellino, A., & Bendjoya, Ph., 2014, A&A, 569, A122
Gradie, J. & Tedesco, E.F. 1982, Science, 216, 1405
Hamilton, V. E., Simon, A. A., Christensen, P. R., et al. 2019, Nature Astronomy, 3, 332
Hergenrother, C. W., Maleszewski, C. K., Nolan, M. C., et al. 2019, Nature Comm., 10, 1291
Hsu, J.-C. & Breger, M., 1982, ApJ, 262, 732
Lauretta, D., DellaGiustina, D., Bennett, C., et al. 2019, Nature, 568, 55
Lumme, K & Muinonen, K. 1993, in Proc. IAU Symp. 160, Asteroids, Comets, Meteors, Ed. A. Milani, A. Cellino & M. Di Martino, (LPI Contributioon 810, Lunar and Planetary Institute, Houston, TX), 194
Lupishko, D.F. 2014, Asteroid Polarimetric Data Base (APD) V8.0, EAR-A-3-RDR-APD-POLARIMETRY-V8.0 NASA Planetary Data System
Masiero, J.R. & Cellino, A. 2009, Icarus, 199, 333
Masiero, J.R., Grav, T., Mainzer, A.K. et al. 2014, Ap. J., 791, 121
Migliorini, F., Zappalà, V., Vo, R., et al. 1995, Icarus, 118, 271
in Asteroids III, Ed. W.F. Bottke, A. Cellino, P. Paolicchi, & R.P. Binzel, University of Arizona Press, Tucson, 123
Migliorini, F., Manara, A., Scaltriti, F., et al. 1997, Icarus, 128, 104
Milani, A., Cellino, A., Knežević, Z. et al. 2014, Icarus, 239, 46
Oliva, E. 1997, A&A Sup. Ser., 123, 589
Pernechele, C., Abe, L., Bendjoya, Ph., et al. 2012, Proceedings of SPIE - The International Society for Optical Engineering. 8446. 10.1117/12.925933.
Rosenbush, V.K., Kiselev, N.N., Shevchenko, V.G. et al. 2005, Icarus, 178, 222
Rosenbush, V.K., Shevchenko, V.G., Kiselev, N.N., et al. 2009, Icarus, 201, 655
Sunshine, J.M., Connolly, H.C., Mc Coy, T.J., et al. 2008, Science, 320, 514
Tanga, P., Cellino, A., Michel, P., et al. 1999, Icarus 141, 65
Tholen, D. J., 1984, "Asteroid taxonomy from cluster analysis of Photometry", Ph.D. thesis, Univ. of Arizona
Tholen, D. J. 1989, Asteroid taxonomic classifications, in Asteroids II, ed. R.P. Binzel, T. Gehrels, & M.S. Matthews, (Univ. of Arizona Press, Tucson), 1139
Wiktorowicz, S, & Masiero, J. R. 2017, AAS, DPS Meeting #49, Abstract 110.32

Appendix A: The CAPS catalogue

Table A.1. List of the results obtained by the Calern Asteroid Polarimetric Survey, since the beginning of operations and up to December, 2021. All the observations collected for each object are listed, specifying for each entry the object's identification number, the epoch of observation (expressed as year, month, day and fraction of day), the phase angle, the value of the measured P_r, its error, and the filter used. As for the latter, it is most commonly the standard *V* filter, but in several cases also the *B*, *R* and *I* filters of the Johnson-Cousin system have been used. A few additional measurements in *BRI* colours done since 2018 are not listed because they are still under reduction.

Asteroid Number	Date of observation	Fraction of day	Phase angle (deg)	P_r (%)	Filter
1	2016-08-17	0.073	19.00	0.16 ± 0.09	V
1	2016-08-18	0.071	18.89	0.15 ± 0.09	V
1	2016-08-21	0.018	18.53	0.01 ± 0.09	V
1	2016-08-22	0.108	18.39	0.03 ± 0.09	V
1	2016-12-01	0.867	15.24	−0.83 ± 0.08	V
1	2016-12-05	0.848	16.15	−0.59 ± 0.12	V
1	2017-12-19	0.248	17.02	−0.23 ± 0.09	V
1	2018-01-12	0.034	9.53	−1.40 ± 0.09	V
1	2018-05-08	0.892	23.12	1.40 ± 0.09	V
1	2021-08-22	0.142	20.85	0.69 ± 0.08	V
2	2016-08-17	0.948	7.05	−1.47 ± 0.10	V
2	2016-08-18	0.926	6.99	−1.53 ± 0.09	V
2	2016-12-02	0.721	16.96	−0.34 ± 0.08	V
2	2015-02-18	0.191	18.70	0.05 ± 0.08	V
2	2015-02-18	0.191	18.70	0.08 ± 0.08	R
2	2016-07-19	0.048	12.24	−1.21 ± 0.08	V
2	2019-01-28	0.246	24.05	1.32 ± 0.08	V
2	2019-02-11	0.196	22.17	0.86 ± 0.08	V
2	2019-04-08	0.995	10.61	−1.42 ± 0.08	V
2	2020-02-24	0.228	15.09	−0.67 ± 0.08	V
2	2020-04-06	0.182	17.67	−0.04 ± 0.10	V
2	2020-04-07	0.175	17.69	−0.16 ± 0.09	V
2	2020-05-08	0.132	17.20	−0.43 ± 0.08	V
2	2021-08-13	0.054	10.61	−1.55 ± 0.08	V
2	2021-12-02	0.739	19.23	0.10 ± 0.08	V
3	2015-02-18	0.941	11.91	−0.62 ± 0.08	V
3	2015-02-18	0.941	11.91	−0.66 ± 0.08	R
3	2016-06-01	0.892	12.05	−0.57 ± 0.08	V
3	2017-07-06	0.888	6.08	−0.48 ± 0.08	V
3	2017-07-27	0.842	10.71	−0.69 ± 0.08	V
3	2017-07-29	0.930	11.27	−0.67 ± 0.08	V
3	2017-08-12	0.877	14.77	−0.56 ± 0.09	V
3	2020-02-18	0.144	15.13	−0.45 ± 0.10	V
3	2020-04-10	0.029	4.16	−0.63 ± 0.08	V
3	2021-04-19	0.150	14.35	−0.58 ± 0.09	V
4	2016-12-01	0.116	18.90	−0.20 ± 0.09	V
4	2018-03-19	0.212	27.43	0.36 ± 0.10	V
4	2018-03-21	0.189	27.41	0.17 ± 0.08	V
4	2018-03-22	0.185	27.39	0.26 ± 0.08	V
4	2018-05-23	0.057	14.21	−0.48 ± 0.08	V
4	2019-10-07	0.127	15.70	−0.43 ± 0.08	V
4	2019-10-09	0.088	15.05	−0.43 ± 0.08	V
4	2020-01-07	0.888	20.29	−0.20 ± 0.08	V
4	2021-01-11	0.136	20.68	−0.14 ± 0.08	V
4	2021-03-01	0.005	4.69	−0.61 ± 0.08	V
5	2016-06-08	0.883	27.22	0.79 ± 0.10	V
5	2017-07-09	0.937	3.71	−0.55 ± 0.09	V
5	2017-07-11	0.935	4.41	−0.68 ± 0.10	V

Table A.1. continued.

Asteroid Number	Date of observation	Fraction of day	Phase angle (deg)	P_r (%)	Filter
5	2017-07-18	0.910	6.94	−0.75 ± 0.10	V
5	2017-07-05	0.883	2.45	−0.38 ± 0.09	V
5	2020-02-18	0.899	15.55	−0.36 ± 0.08	V
5	2020-04-08	0.842	28.12	1.02 ± 0.08	V
6	2015-02-19	0.783	27.14	0.53 ± 0.08	V
6	2015-02-19	0.783	27.14	0.45 ± 0.08	R
6	2016-06-08	0.908	20.37	−0.13 ± 0.10	V
6	2017-07-05	0.917	11.29	−0.59 ± 0.08	V
6	2017-07-18	0.846	15.48	−0.47 ± 0.11	V
6	2017-07-20	0.934	16.14	−0.47 ± 0.08	V
6	2017-08-02	0.952	19.85	−0.28 ± 0.09	V
6	2020-02-18	0.156	16.08	−0.45 ± 0.08	V
6	2020-04-09	0.076	6.76	−0.81 ± 0.09	V
6	2020-04-22	0.020	9.70	−0.57 ± 0.08	V
6	2021-08-11	0.939	13.64	−0.57 ± 0.08	V
7	2017-07-07	0.076	30.53	0.95 ± 0.11	V
7	2015-02-18	0.014	8.24	−0.75 ± 0.08	V
7	2015-02-18	0.014	8.24	−0.67 ± 0.08	R
7	2017-08-13	0.059	30.29	0.97 ± 0.12	V
7	2021-08-22	0.154	29.29	0.79 ± 0.08	V
8	2015-02-18	0.004	3.33	−0.55 ± 0.08	V
8	2015-02-18	0.004	3.33	−0.46 ± 0.08	R
8	2015-03-10	0.989	12.40	−0.32 ± 0.08	V
8	2017-12-21	0.050	7.49	−0.61 ± 0.24	V
8	2017-12-22	0.030	6.89	−0.70 ± 0.09	V
8	2018-05-08	0.861	24.88	0.43 ± 0.09	V
8	2019-02-11	0.249	22.83	0.20 ± 0.15	V
8	2019-02-12	0.206	22.83	0.20 ± 0.08	V
8	2019-04-04	0.096	15.85	−0.36 ± 0.08	V
8	2019-04-13	0.089	12.86	−0.69 ± 0.08	V
8	2019-05-29	0.921	9.10	−0.48 ± 0.08	V
9	2015-12-11	0.739	26.1	0.31 ± 0.10	V
9	2019-10-02	0.118	12.55	−0.82 ± 0.08	V
9	2019-10-03	0.052	12.12	−0.82 ± 0.08	V
9	2019-10-09	0.065	9.26	−0.82 ± 0.08	V
9	2020-01-07	0.879	27.12	0.47 ± 0.08	V
9	2021-01-17	0.193	23.90	0.32 ± 0.08	V
9	2021-02-23	0.980	17.25	−0.53 ± 0.09	V
9	2021-02-26	0.119	16.25	−0.55 ± 0.09	V
9	2021-05-07	0.919	14.69	−0.67 ± 0.08	V
10	2015-02-18	0.821	14.45	−0.74 ± 0.08	V
10	2015-02-18	0.821	14.45	−0.82 ± 0.09	R
10	2017-07-11	0.948	4.89	−1.36 ± 0.09	V
10	2019-10-07	0.149	13.73	−1.02 ± 0.09	V
10	2019-11-08	0.077	5.87	−1.45 ± 0.08	V
10	2020-01-07	0.900	12.41	−1.17 ± 0.08	V
10	2021-01-06	0.033	7.76	−1.44 ± 0.08	V
10	2021-02-10	0.035	4.97	−1.33 ± 0.08	V
10	2021-04-24	0.849	18.84	0.22 ± 0.08	V
11	2016-07-19	0.057	26.07	0.79 ± 0.09	V
11	2016-12-12	0.763	24.26	0.41 ± 0.10	V
11	2017-12-19	0.084	15.19	−0.43 ± 0.10	V
11	2015-02-18	0.149	21.08	0.33 ± 0.08	V
11	2015-02-18	0.149	21.08	0.23 ± 0.08	R
11	2015-05-20	0.852	12.75	−0.62 ± 0.08	V
11	2018-05-08	0.885	21.51	0.35 ± 0.09	V
11	2019-02-12	0.216	23.09	0.34 ± 0.09	V
11	2019-04-08	0.073	15.57	−0.49 ± 0.09	V
11	2019-05-31	0.976	9.12	−0.60 ± 0.08	V

Table A.1. continued.

Asteroid Number	Date of observation	Fraction of day	Phase angle (deg)	P_r (%)	Filter
12	2016-02-04	0.852	9.83	−0.89 ± 0.09	V
12	2020-02-20	0.014	4.73	−0.47 ± 0.08	V
12	2020-02-21	0.055	4.87	−0.64 ± 0.09	V
12	2020-04-07	0.923	18.35	−0.21 ± 0.08	V
12	2021-08-11	0.945	12.41	−0.71 ± 0.08	V
12	2021-08-17	0.825	14.62	−0.57 ± 0.08	V
12	2021-09-19	0.789	26.05	0.44 ± 0.08	V
12	2021-11-16	0.723	30.67	1.10 ± 0.08	V
13	2016-12-07	0.119	16.81	−1.28 ± 0.08	V
13	2016-12-12	0.083	15.16	−1.64 ± 0.10	V
13	2017-01-16	0.950	11.08	−2.10 ± 0.08	V
13	2015-12-11	0.705	21.79	−0.07 ± 0.09	V
13	2016-12-01	0.124	18.38	−0.93 ± 0.09	V
14	2015-12-10	0.811	15.18	−0.62 ± 0.09	V
14	2016-12-01	0.160	24.96	0.47 ± 0.09	V
14	2019-10-02	0.096	6.89	−0.92 ± 0.09	V
14	2019-10-03	0.029	6.61	−0.85 ± 0.08	V
14	2019-10-08	0.001	5.23	−0.77 ± 0.09	V
14	2019-12-27	0.797	19.23	−0.38 ± 0.08	V
14	2021-02-10	0.045	10.13	−0.73 ± 0.08	V
15	2015-07-15	0.066	26.05	0.38 ± 0.08	V
15	2016-12-13	0.109	20.73	−0.01 ± 0.08	V
15	2019-07-24	0.027	9.60	−0.79 ± 0.08	V
15	2019-07-29	0.064	7.60	−0.79 ± 0.08	V
15	2019-08-06	0.041	4.77	−0.71 ± 0.09	V
15	2019-10-02	0.781	21.21	0.01 ± 0.08	V
15	2019-10-07	0.852	22.36	0.09 ± 0.08	V
15	2019-10-10	0.792	22.94	0.13 ± 0.08	V
15	2021-01-06	0.026	7.19	−0.69 ± 0.08	V
15	2021-01-19	0.971	1.40	−0.34 ± 0.08	V
16	2015-12-09	0.071	1.73	−0.51 ± 0.08	V
16	2018-03-19	0.205	14.74	−0.92 ± 0.08	V
16	2018-05-12	0.001	1.68	−0.30 ± 0.08	V
16	2018-05-25	0.964	5.75	−1.04 ± 0.09	V
16	2019-07-23	0.048	6.03	−0.99 ± 0.09	V
16	2019-07-29	0.016	3.56	−0.81 ± 0.08	V
16	2019-07-30	0.009	3.15	−0.80 ± 0.08	V
16	2019-07-31	0.013	2.72	−0.70 ± 0.08	V
16	2019-08-06	0.002	0.51	−0.08 ± 0.08	V
16	2021-01-17	0.870	15.58	−0.71 ± 0.08	V
17	2016-07-19	0.015	16.78	−0.40 ± 0.09	V
17	2016-07-27	0.051	13.50	−0.78 ± 0.09	V
17	2016-08-21	0.041	2.11	−0.32 ± 0.09	V
17	2015-02-18	0.045	8.14	−0.80 ± 0.08	V
17	2015-02-18	0.045	8.14	−0.75 ± 0.08	R
17	2021-11-19	0.026	12.93	−0.57 ± 0.08	V
18	2015-02-19	0.193	20.25	−0.12 ± 0.09	V
18	2015-02-19	0.193	20.25	0.21 ± 0.09	R
18	2016-12-13	0.921	26.34	0.45 ± 0.08	V
18	2017-01-17	0.820	30.53	0.96 ± 0.08	V
18	2018-05-06	0.901	17.13	−0.44 ± 0.09	V
18	2018-05-11	0.900	18.15	−0.36 ± 0.09	V
18	2019-08-01	0.883	16.58	−0.52 ± 0.09	V
19	2017-12-20	0.109	18.90	−0.68 ± 0.09	V
19	2018-05-10	0.884	22.66	0.30 ± 0.11	V
20	2015-02-19	0.172	22.38	0.32 ± 0.09	V
20	2015-02-19	0.172	22.38	0.22 ± 0.08	R
20	2017-12-21	0.916	2.60	−0.47 ± 0.13	V
20	2017-12-21	0.916	2.60	0.22 ± 0.08	R

Table A.1. continued.

Asteroid Number	Date of observation	Fraction of day	Phase angle (deg)	P_r (%)	Filter
20	2018-05-08	0.841	25.13	0.57 ± 0.09	V
21	2016-12-01	0.141	16.57	−0.93 ± 0.09	V
21	2017-01-16	0.969	2.51	−0.73 ± 0.08	V
21	2017-12-19	0.231	19.57	−0.67 ± 0.11	V
21	2018-03-08	0.065	13.49	−1.29 ± 0.09	V
21	2018-05-06	0.953	11.59	−1.42 ± 0.09	V
21	2019-10-02	0.017	3.89	−0.71 ± 0.08	V
21	2019-10-09	0.957	7.18	−1.36 ± 0.08	V
21	2021-01-06	0.066	9.66	−1.39 ± 0.09	V
22	2016-12-12	0.006	7.18	−1.03 ± 0.10	V
22	2018-03-24	0.094	6.04	−0.93 ± 0.08	V
22	2018-05-06	0.944	12.79	−0.92 ± 0.09	V
22	2021-11-19	0.938	16.02	−0.52 ± 0.09	V
23	2015-02-19	0.837	28.37	0.76 ± 0.08	V
23	2015-02-19	0.837	28.37	0.36 ± 0.09	R
23	2020-02-18	0.218	24.20	0.41 ± 0.08	V
23	2020-04-06	0.002	9.44	−0.80 ± 0.08	V
23	2020-05-19	0.922	11.97	−0.47 ± 0.09	V
24	2016-07-28	0.996	5.83	−1.69 ± 0.10	V
24	2017-12-21	0.818	16.78	−1.22 ± 0.26	V
24	2019-01-28	0.967	6.36	−1.50 ± 0.08	V
24	2019-02-04	0.884	9.09	−1.61 ± 0.08	V
24	2019-04-08	0.845	21.32	0.24 ± 0.10	V
25	2017-08-12	0.963	22.96	0.35 ± 0.09	V
25	2015-02-22	0.805	20.15	0.19 ± 0.09	R
25	2017-07-03	0.039	27.87	0.76 ± 0.14	V
25	2017-07-09	0.916	26.99	0.63 ± 0.09	V
25	2017-07-22	0.058	25.09	0.60 ± 0.11	V
25	2017-07-30	0.982	24.03	0.50 ± 0.09	V
25	2019-01-28	0.927	13.61	−0.05 ± 0.11	V
25	2019-02-05	0.869	15.14	−0.47 ± 0.09	V
25	2020-04-06	0.899	10.44	−0.75 ± 0.09	V
25	2021-08-22	0.164	27.80	0.79 ± 0.08	V
25	2021-11-16	0.921	14.74	−0.40 ± 0.16	V
26	2016-12-13	0.122	20.91	0.13 ± 0.09	V
26	2015-10-15	0.078	14.00	−0.52 ± 0.08	V
26	2015-12-10	0.937	7.50	−0.71 ± 0.09	V
26	2016-02-05	0.823	19.76	−0.13 ± 0.08	V
26	2019-10-05	0.081	8.03	−1.12 ± 0.09	V
26	2020-01-07	0.826	19.63	−0.01 ± 0.10	V
27	2016-02-04	0.862	22.02	0.06 ± 0.09	V
27	2016-04-13	0.831	29.34	0.75 ± 0.09	V
27	2020-01-06	0.181	26.63	0.51 ± 0.08	V
27	2020-02-18	0.139	13.30	−0.52 ± 0.09	V
28	2017-07-09	0.926	7.51	−0.74 ± 0.10	V
28	2017-08-11	0.840	15.65	−0.52 ± 0.09	V
28	2017-08-13	0.842	15.98	−0.57 ± 0.13	V
28	2017-08-14	0.881	16.15	−0.58 ± 0.09	V
28	2016-06-08	0.892	23.55	0.29 ± 0.13	V
28	2017-07-04	0.885	6.05	−0.60 ± 0.10	V
28	2019-12-26	0.925	9.35	−0.71 ± 0.08	V
28	2019-12-29	0.927	10.45	−0.69 ± 0.09	V
28	2020-02-20	0.889	23.71	0.23 ± 0.08	V
28	2020-04-09	0.806	23.21	0.30 ± 0.08	V
28	2021-04-23	0.992	5.23	−0.69 ± 0.09	V
29	2015-10-15	0.063	5.33	−0.80 ± 0.08	V
29	2015-12-10	0.835	19.49	−0.27 ± 0.09	V
29	2016-12-13	0.136	22.82	0.15 ± 0.08	V
29	2019-10-02	0.084	5.47	−0.79 ± 0.08	V

Table A.1. continued.

Asteroid Number	Date of observation	Fraction of day	Phase angle (deg)	P_r (%)	Filter
29	2019-10-03	0.019	5.03	−0.72 ± 0.08	V
29	2019-10-09	0.005	2.44	−0.57 ± 0.08	V
29	2021-05-04	0.861	22.03	−0.00 ± 0.08	V
30	2020-01-03	0.156	21.37	−0.06 ± 0.08	V
30	2020-02-22	0.085	3.31	−0.63 ± 0.09	V
30	2020-04-07	0.932	16.19	−0.40 ± 0.12	V
30	2020-04-30	0.828	21.16	0.23 ± 0.08	V
31	2016-12-12	0.776	19.05	−0.31 ± 0.11	V
31	2018-05-08	0.850	20.85	0.38 ± 0.09	V
31	2019-02-05	0.185	17.84	−0.51 ± 0.08	V
31	2019-04-08	0.987	2.60	−0.79 ± 0.10	V
32	2017-12-19	0.140	10.62	−0.72 ± 0.10	V
32	2017-12-19	0.140	10.62	−0.72 ± 0.10	R
32	2016-08-14	0.093	17.84	−0.27 ± 0.09	V
32	2017-12-22	0.080	9.49	−0.78 ± 0.10	V
32	2021-11-19	0.048	14.77	−0.59 ± 0.09	V
33	2016-02-10	0.903	7.00	−0.68 ± 0.09	V
33	2018-05-23	0.877	8.40	−0.72 ± 0.14	V
33	2019-08-08	0.126	28.82	0.82 ± 0.09	V
33	2019-10-02	0.107	6.87	−0.66 ± 0.08	V
33	2019-10-03	0.043	6.32	−0.59 ± 0.08	V
33	2019-10-08	0.007	3.39	−0.66 ± 0.08	V
33	2020-01-07	0.859	25.8	0.56 ± 0.09	V
33	2020-02-25	0.777	22.27	0.26 ± 0.10	V
34	2016-12-08	0.033	3.26	−0.19 ± 0.13	V
34	2018-05-12	0.955	11.67	−1.62 ± 0.08	V
34	2019-08-02	0.966	2.39	−0.56 ± 0.11	V
34	2019-08-05	0.990	2.82	−0.61 ± 0.09	V
34	2019-10-08	0.850	18.71	−0.85 ± 0.10	V
35	2015-02-18	0.843	16.96	−0.95 ± 0.11	V
35	2015-02-18	0.843	16.96	−0.67 ± 0.08	R
35	2019-12-30	0.937	6.48	−1.21 ± 0.10	V
35	2021-02-26	0.093	14.13	−1.34 ± 0.10	V
35	2021-05-08	0.883	17.93	−0.72 ± 0.09	V
36	2016-02-10	0.951	13.56	−1.63 ± 0.09	V
36	2019-10-02	0.920	10.23	−1.71 ± 0.08	V
36	2019-10-07	0.958	12.97	−1.75 ± 0.08	V
36	2019-10-10	0.926	14.51	−1.50 ± 0.09	V
36	2019-12-31	0.809	30.44	3.15 ± 0.10	V
36	2021-01-18	0.103	17.16	−1.26 ± 0.09	V
37	2020-01-06	0.117	13.35	−0.73 ± 0.08	V
37	2020-02-20	0.999	9.08	−0.94 ± 0.08	V
37	2020-05-04	0.843	23.40	0.39 ± 0.08	V
37	2020-05-20	0.833	22.70	0.29 ± 0.09	V
38	2017-07-17	0.047	10.52	−2.12 ± 0.10	V
38	2017-08-02	0.085	5.20	−1.52 ± 0.11	V
38	2015-02-18	0.982	2.74	−0.93 ± 0.08	V
38	2015-02-18	0.982	2.74	−1.00 ± 0.08	R
38	2017-07-25	0.068	7.97	−1.90 ± 0.15	V
38	2017-08-01	0.024	5.58	−2.03 ± 0.14	V
38	2019-02-09	0.855	24.25	1.17 ± 0.09	V
38	2020-05-06	0.920	9.96	−1.97 ± 0.09	V
39	2016-12-12	0.134	18.50	−0.20 ± 0.10	V
39	2017-12-20	0.248	15.27	−0.52 ± 0.11	V
39	2018-05-12	0.989	6.10	−0.55 ± 0.08	V
39	2019-10-02	0.789	18.38	−0.24 ± 0.08	V
39	2019-10-07	0.860	19.58	−0.24 ± 0.08	V
39	2019-10-10	0.801	20.20	−0.18 ± 0.08	V
40	2020-02-18	0.209	23.04	0.17 ± 0.08	V

Table A.1. continued.

Asteroid Number	Date of observation	Fraction of day	Phase angle (deg)	P_r (%)	Filter
40	2020-04-24	0.010	2.87	−0.46 ± 0.09	V
40	2021-11-18	0.820	21.83	0.03 ± 0.09	V
42	2015-02-18	0.878	8.09	−0.63 ± 0.08	V
42	2015-02-18	0.878	8.09	−0.59 ± 0.08	R
42	2016-06-09	0.930	19.53	0.05 ± 0.09	V
42	2019-02-12	0.072	3.63	−0.59 ± 0.09	V
42	2020-02-24	0.181	23.79	0.59 ± 0.08	V
42	2020-04-06	0.094	19.54	0.17 ± 0.09	V
42	2020-05-05	0.035	9.41	−0.68 ± 0.08	V
43	2015-12-09	0.951	10.44	−0.58 ± 0.08	V
43	2016-12-08	0.149	23.73	0.30 ± 0.14	V
43	2015-10-15	0.106	16.10	−0.27 ± 0.08	V
43	2020-02-18	0.980	8.57	−0.63 ± 0.08	V
43	2021-08-20	0.945	3.57	−0.35 ± 0.08	V
43	2021-09-19	0.890	17.69	−0.29 ± 0.08	V
43	2021-11-16	0.792	28.38	0.74 ± 0.08	V
44	2015-02-18	0.068	17.17	−0.07 ± 0.08	V
44	2015-02-18	0.068	17.17	−0.10 ± 0.08	R
44	2015-05-13	0.862	21.53	0.09 ± 0.08	V
44	2016-07-19	0.001	2.18	−0.14 ± 0.09	V
44	2016-08-10	0.905	10.88	−0.24 ± 0.13	V
44	2017-12-21	0.882	21.85	0.50 ± 0.29	V
44	2019-01-28	0.234	25.48	0.28 ± 0.08	V
44	2019-02-06	0.145	25.00	0.33 ± 0.08	V
44	2019-02-11	0.202	24.53	0.14 ± 0.08	V
44	2019-04-08	0.034	8.20	−0.25 ± 0.09	V
44	2021-11-19	0.004	12.16	−0.17 ± 0.09	V
45	2017-01-17	0.940	13.84	−0.55 ± 0.09	V
45	2015-07-15	0.072	19.84	0.99 ± 0.08	V
45	2015-07-17	0.072	19.54	0.99 ± 0.09	V
45	2016-12-09	0.962	3.18	−0.68 ± 0.08	V
45	2017-12-19	0.158	21.70	1.72 ± 0.09	V
45	2018-03-08	0.998	4.58	−0.98 ± 0.08	V
45	2018-05-10	0.918	20.01	0.85 ± 0.40	V
45	2019-05-30	0.097	20.05	1.11 ± 0.08	V
45	2019-07-22	0.012	2.36	−0.68 ± 0.09	V
45	2019-07-30	1.000	2.70	−0.70 ± 0.08	V
45	2019-07-31	0.961	3.05	−0.70 ± 0.08	V
45	2019-08-06	0.914	5.41	−1.05 ± 0.09	V
45	2021-01-17	0.834	19.38	0.86 ± 0.08	V
46	2020-02-22	0.064	0.86	−0.36 ± 0.09	V
46	2020-04-09	0.983	16.42	−0.12 ± 0.11	V
47	2016-02-04	0.960	1.71	−0.51 ± 0.09	V
47	2019-11-06	0.092	9.63	−1.36 ± 0.09	V
47	2019-12-30	0.902	11.18	−1.24 ± 0.08	V
47	2021-01-06	0.132	11.36	−1.12 ± 0.09	V
47	2021-02-10	0.061	1.49	−0.53 ± 0.09	V
48	2015-07-13	0.883	12.83	−2.10 ± 0.09	V
48	2015-07-14	0.883	13.04	−1.98 ± 0.09	V
48	2016-07-19	0.035	8.84	−2.13 ± 0.10	V
48	2016-07-27	0.036	6.38	−1.86 ± 0.10	V
48	2016-08-18	0.964	2.69	−0.71 ± 0.09	V
48	2017-12-22	0.932	15.52	−1.89 ± 0.10	V
48	2019-02-09	0.999	2.27	−0.69 ± 0.08	V
48	2020-02-23	0.173	16.50	−1.68 ± 0.09	V
48	2020-04-06	0.011	7.14	−1.82 ± 0.12	V
48	2020-05-19	0.960	7.96	−1.71 ± 0.09	V
48	2021-08-11	0.891	11.25	−2.03 ± 0.08	V
48	2021-08-17	0.835	12.65	−2.11 ± 0.09	V

Table A.1. continued.

Asteroid Number	Date of observation	Fraction of day	Phase angle (deg)	P_r (%)	Filter
49	2016-12-12	0.194	17.82	−0.78 ± 0.10	V
49	2016-02-05	0.870	22.13	0.21 ± 0.08	V
49	2018-03-22	0.086	9.14	−1.95 ± 0.12	V
50	2015-02-18	0.108	12.96	−1.64 ± 0.10	V
50	2015-02-18	0.108	12.96	−0.67 ± 0.08	R
50	2015-04-01	0.920	0.66	0.82 ± 0.48	V
50	2021-11-18	0.923	18.33	−0.76 ± 0.10	V
51	2015-07-14	0.966	17.12	−0.67 ± 0.10	V
51	2015-10-14	0.767	22.64	0.44 ± 0.10	V
51	2016-12-13	0.905	21.64	0.28 ± 0.09	V
51	2015-05-12	0.984	14.72	−1.34 ± 0.08	V
51	2017-01-17	0.782	23.28	0.74 ± 0.09	V
51	2017-12-20	0.118	24.76	1.30 ± 0.09	V
51	2019-05-30	0.111	22.45	0.49 ± 0.08	V
51	2019-07-22	0.001	6.58	−1.86 ± 0.08	V
51	2019-07-24	0.991	6.05	−1.79 ± 0.08	V
51	2019-08-05	0.950	5.93	−1.61 ± 0.08	V
51	2019-10-07	0.761	22.49	0.55 ± 0.09	V
52	2019-08-08	0.135	15.12	−1.26 ± 0.09	V
52	2019-10-02	0.074	3.37	−0.64 ± 0.09	V
52	2019-10-08	0.973	4.85	−0.99 ± 0.09	V
53	2016-07-05	0.980	2.27	−0.48 ± 0.15	V
53	2016-08-10	0.847	13.23	−1.09 ± 0.15	V
53	2015-02-19	0.133	19.32	−0.36 ± 0.09	V
53	2015-02-19	0.133	19.32	−0.40 ± 0.09	R
53	2016-07-28	0.871	9.68	−1.96 ± 0.13	V
53	2019-02-07	0.101	16.07	−1.11 ± 0.08	V
53	2019-04-14	0.027	14.58	−1.16 ± 0.09	V
53	2021-08-22	0.001	4.36	−1.24 ± 0.12	V
53	2021-08-27	0.032	2.30	−0.60 ± 0.08	V
54	2016-12-06	0.166	15.73	−1.43 ± 0.09	V
54	2017-01-17	0.055	4.74	−1.33 ± 0.09	V
54	2019-08-10	0.108	22.33	0.12 ± 0.09	V
54	2019-10-07	0.985	6.79	−1.72 ± 0.08	V
55	2020-02-21	0.781	21.30	0.07 ± 0.09	V
55	2020-04-07	0.840	20.18	0.14 ± 0.08	V
55	2021-01-18	0.141	16.12	−0.59 ± 0.08	V
55	2021-04-12	0.954	11.20	−0.83 ± 0.09	V
56	2015-02-19	0.075	6.39	−1.21 ± 0.09	V
56	2015-02-19	0.075	6.39	−1.13 ± 0.09	R
56	2016-07-19	0.024	15.66	−1.01 ± 0.09	V
56	2016-07-27	0.045	12.08	−1.45 ± 0.09	V
56	2016-08-01	0.066	9.88	−1.60 ± 0.09	V
56	2020-05-08	0.090	23.12	0.91 ± 0.09	V
56	2020-05-27	0.050	17.57	−0.54 ± 0.08	V
56	2021-11-14	0.043	8.52	−1.71 ± 0.09	V
57	2017-12-20	0.100	13.80	−0.55 ± 0.09	V
57	2015-07-14	0.980	7.01	−0.81 ± 0.09	V
57	2015-07-15	1.000	6.90	−0.74 ± 0.09	V
57	2016-12-12	0.846	18.05	−0.29 ± 0.10	V
57	2017-01-16	0.782	20.60	0.04 ± 0.08	V
57	2017-12-22	0.089	13.34	−0.62 ± 0.09	V
57	2020-04-06	0.168	15.36	−0.42 ± 0.09	V
57	2020-05-05	0.109	10.79	−0.67 ± 0.09	V
57	2020-05-21	0.033	7.36	−0.92 ± 0.08	V
57	2021-08-20	0.953	5.72	−0.67 ± 0.08	V
57	2021-12-03	0.746	19.18	−0.20 ± 0.09	V
58	2015-02-22	0.981	6.05	−0.81 ± 0.09	V
58	2020-02-24	0.148	19.88	−0.53 ± 0.09	V

Table A.1. continued.

Asteroid Number	Date of observation	Fraction of day	Phase angle (deg)	P_r (%)	Filter
58	2020-04-10	0.106	5.56	−1.32 ± 0.09	V
58	2020-04-15	0.050	3.70	−1.13 ± 0.12	V
58	2020-05-17	0.970	11.52	−1.65 ± 0.10	V
58	2021-08-12	0.024	1.29	−0.45 ± 0.08	V
58	2021-08-13	0.000	1.08	−0.22 ± 0.09	V
59	2015-05-12	0.863	7.67	−1.16 ± 0.08	V
59	2016-07-28	0.986	3.82	−0.53 ± 0.11	V
59	2016-08-22	0.904	11.06	−1.20 ± 0.10	V
59	2016-06-07	0.073	18.55	−0.12 ± 0.08	V
59	2016-07-18	0.030	6.22	−1.00 ± 0.09	V
59	2016-07-27	0.991	3.90	−0.74 ± 0.08	V
59	2018-03-06	0.853	22.19	0.69 ± 0.09	V
59	2019-04-08	0.908	8.28	−1.06 ± 0.09	V
59	2020-04-07	0.139	18.4	−0.02 ± 0.10	V
59	2020-05-11	0.071	11.41	−1.26 ± 0.08	V
59	2021-11-16	0.899	16.64	−0.46 ± 0.09	V
60	2016-08-17	0.115	27.53	0.81 ± 0.10	V
60	2016-08-18	0.067	27.56	0.89 ± 0.12	V
60	2016-12-08	0.050	7.67	−0.82 ± 0.14	V
60	2018-03-21	0.123	20.32	−0.19 ± 0.09	V
60	2018-05-23	0.968	3.40	−0.52 ± 0.08	V
60	2019-10-02	0.801	17.45	−0.21 ± 0.10	V
60	2019-10-07	0.878	18.70	−0.11 ± 0.10	V
60	2019-10-10	0.817	19.35	−0.10 ± 0.09	V
61	2015-07-22	0.104	23.83	0.32 ± 0.13	V
61	2015-12-10	0.778	20.17	0.09 ± 0.09	V
61	2016-12-05	0.157	14.13	−0.59 ± 0.10	V
61	2017-01-17	0.986	4.77	−0.65 ± 0.09	V
62	2015-12-09	0.012	3.40	−1.17 ± 0.09	V
62	2016-02-10	0.852	20.51	0.10 ± 0.09	V
62	2016-12-07	0.184	17.97	−0.51 ± 0.10	V
62	2017-01-18	0.132	12.84	−1.46 ± 0.10	V
63	2015-12-10	0.066	5.89	−0.73 ± 0.09	V
63	2017-01-18	0.222	24.22	0.37 ± 0.09	V
63	2020-01-06	0.035	5.84	−0.74 ± 0.08	V
63	2020-02-18	0.885	13.46	−0.50 ± 0.09	V
64	2017-12-22	0.832	20.60	−0.07 ± 0.10	V
64	2019-02-07	0.040	11.10	−0.29 ± 0.08	V
64	2019-02-09	0.041	10.21	−0.21 ± 0.08	V
64	2021-08-17	0.071	10.79	−0.32 ± 0.08	V
64	2021-08-20	0.994	9.49	−0.32 ± 0.09	V
64	2021-11-18	0.768	19.21	0.12 ± 0.09	V
64	2021-12-02	0.761	20.25	−0.07 ± 0.08	V
65	2016-08-11	0.079	15.75	−0.90 ± 0.09	V
65	2016-08-17	0.070	15.18	−0.99 ± 0.10	V
65	2016-12-12	0.904	13.43	−1.28 ± 0.10	V
65	2016-08-18	0.034	15.07	−0.94 ± 0.10	V
65	2016-12-01	0.875	11.66	−1.38 ± 0.09	V
65	2019-02-09	0.934	1.75	−0.46 ± 0.08	V
65	2020-02-24	0.119	14.48	−1.04 ± 0.08	V
65	2020-04-09	0.084	1.87	−0.50 ± 0.08	V
67	2016-07-31	0.094	21.90	−0.43 ± 0.20	V
67	2016-12-12	0.797	26.43	0.56 ± 0.10	V
67	2019-02-12	0.182	20.47	0.13 ± 0.08	V
67	2019-04-01	0.016	5.84	−0.65 ± 0.09	V
67	2015-05-21	0.877	21.95	0.26 ± 0.09	V
68	2017-12-20	0.196	17.29	−0.24 ± 0.09	V
68	2018-05-08	0.904	16.87	−0.29 ± 0.08	V
68	2021-11-30	0.166	16.63	−0.30 ± 0.08	V

Table A.1. continued.

Asteroid Number	Date of observation	Fraction of day	Phase angle (deg)	P_r (%)	Filter
69	2015-02-19	0.861	15.64	−0.68 ± 0.08	V
69	2015-02-19	0.861	15.64	−0.73 ± 0.08	R
69	2016-06-09	0.939	12.16	−0.90 ± 0.09	V
69	2017-07-05	0.036	4.25	−0.56 ± 0.09	V
69	2017-07-13	0.974	3.37	−0.62 ± 0.12	V
69	2017-07-29	0.944	6.13	−1.05 ± 0.09	V
69	2019-12-29	0.990	5.54	−0.83 ± 0.08	V
69	2020-02-18	0.832	19.86	−0.22 ± 0.08	V
69	2021-02-26	0.146	17.77	−0.50 ± 0.09	V
69	2021-04-23	0.984	2.15	−0.69 ± 0.08	V
70	2016-12-13	0.159	19.26	−0.23 ± 0.10	V
70	2019-12-30	0.958	7.47	−1.70 ± 0.09	V
70	2020-04-09	0.828	17.34	−0.91 ± 0.10	V
71	2017-07-09	0.098	19.35	0.11 ± 0.09	V
71	2017-07-10	0.083	19.35	−0.01 ± 0.09	V
71	2015-02-19	0.983	7.64	−0.48 ± 0.08	V
71	2015-02-19	0.983	7.64	−0.46 ± 0.08	R
71	2019-02-09	0.894	17.09	−0.01 ± 0.08	V
71	2021-08-13	0.028	4.43	−0.76 ± 0.08	V
71	2021-08-20	0.981	2.90	−0.47 ± 0.08	V
71	2021-09-19	0.837	11.94	−0.33 ± 0.08	V
72	2018-05-06	0.920	16.51	−1.74 ± 0.08	V
72	2019-08-10	0.130	26.86	0.16 ± 0.10	V
72	2019-10-05	0.040	3.98	−1.03 ± 0.09	V
75	2018-03-24	0.066	2.19	−0.58 ± 0.09	V
76	2015-02-19	0.025	3.23	−0.45 ± 0.08	V
76	2015-02-19	0.025	3.23	−0.49 ± 0.08	R
76	2019-10-05	0.064	7.82	−1.27 ± 0.11	V
76	2019-11-06	0.932	3.98	−0.78 ± 0.09	V
76	2019-12-27	0.829	17.61	−0.57 ± 0.08	V
76	2021-01-11	0.098	7.78	−1.07 ± 0.08	V
77	2015-12-09	0.991	6.04	−1.29 ± 0.08	V
77	2016-02-05	0.921	23.82	0.14 ± 0.09	V
77	2019-08-10	0.162	20.62	0.09 ± 0.49	V
77	2021-04-19	0.856	19.57	−0.44 ± 0.09	V
78	2015-03-07	0.815	24.84	0.94 ± 0.10	V
78	2020-01-03	0.176	26.85	1.65 ± 0.08	V
78	2020-02-23	0.059	11.72	−1.74 ± 0.08	V
78	2020-04-11	0.989	13.60	−1.54 ± 0.09	V
80	2020-03-04	0.085	9.96	−0.57 ± 0.08	V
80	2021-08-12	0.987	9.50	−0.41 ± 0.09	V
80	2021-08-21	0.897	10.29	−0.50 ± 0.08	V
80	2021-09-19	0.796	21.45	0.04 ± 0.08	V
80	2021-11-20	0.801	32.48	1.28 ± 0.08	V
81	2019-12-27	0.066	9.44	−1.51 ± 0.09	V
81	2020-01-07	0.951	5.62	−1.09 ± 0.08	V
81	2020-02-21	0.871	16.36	−0.58 ± 0.13	V
83	2020-01-06	0.100	12.18	−1.27 ± 0.08	V
84	2016-02-10	0.997	0.95	−0.34 ± 0.09	V
85	2016-07-17	0.016	15.49	−0.84 ± 0.11	V
85	2016-07-18	0.052	15.13	−0.88 ± 0.08	V
85	2016-07-28	0.980	11.95	−0.94 ± 0.10	V
85	2016-12-02	0.809	26.37	2.20 ± 0.08	V
85	2019-01-28	0.128	13.11	−0.99 ± 0.08	V
85	2019-02-06	0.117	10.81	−1.19 ± 0.09	V
85	2020-04-07	0.160	21.99	0.95 ± 0.09	V
85	2020-05-11	0.109	15.03	−0.91 ± 0.08	V
85	2020-05-27	0.041	10.13	−1.27 ± 0.08	V
85	2021-11-14	0.034	7.26	−1.39 ± 0.08	V

Table A.1. continued.

Asteroid Number	Date of observation	Fraction of day	Phase angle (deg)	P_r (%)	Filter
86	2015-02-19	0.910	6.27	−1.17 ± 0.33	V
86	2015-02-19	0.910	6.27	−1.24 ± 0.09	R
86	2019-12-26	0.991	3.43	−0.82 ± 0.09	V
86	2019-12-29	0.955	4.75	−1.20 ± 0.08	V
87	2017-07-17	0.120	14.27	−1.10 ± 0.11	V
87	2019-12-27	0.086	6.65	−1.13 ± 0.09	V
87	2020-01-07	0.974	3.92	−0.69 ± 0.09	V
87	2020-02-22	0.939	10.55	−1.08 ± 0.09	V
87	2021-02-26	0.079	5.19	−0.93 ± 0.09	V
88	2016-12-10	0.235	17.83	−0.23 ± 0.13	V
88	2015-12-09	0.140	11.92	−1.33 ± 0.09	V
88	2019-12-26	0.895	10.92	−1.31 ± 0.08	V
88	2019-12-29	0.883	11.84	−1.28 ± 0.08	V
88	2020-01-06	0.835	14.02	−1.06 ± 0.08	V
88	2020-02-18	0.781	19.22	0.01 ± 0.09	V
89	2017-08-11	0.067	15.78	−0.67 ± 0.08	V
89	2017-08-14	0.020	14.66	−0.76 ± 0.08	V
89	2015-02-19	0.958	6.09	−0.78 ± 0.08	V
89	2015-02-19	0.958	6.09	−0.81 ± 0.08	R
89	2017-07-09	0.013	25.21	0.15 ± 0.09	V
89	2017-07-15	0.050	24.03	0.21 ± 0.11	V
89	2021-08-13	0.046	8.13	−1.15 ± 0.08	V
89	2021-08-21	0.903	5.40	−0.77 ± 0.08	V
89	2021-11-20	0.783	28.19	0.58 ± 0.08	V
90	2017-08-03	0.118	20.30	0.02 ± 0.09	V
90	2017-08-14	0.079	18.58	−0.38 ± 0.10	V
90	2019-12-31	0.164	12.55	−1.51 ± 0.10	V
90	2020-02-19	0.995	1.27	−0.35 ± 0.11	V
90	2021-02-26	0.162	14.53	−1.00 ± 0.14	V
91	2016-08-12	0.032	22.26	0.22 ± 0.10	V
91	2016-12-21	0.923	23.21	0.48 ± 0.11	V
91	2018-03-24	0.000	8.94	−1.36 ± 0.09	V
92	2016-08-08	0.082	15.91	−0.64 ± 0.09	V
92	2016-12-13	0.844	19.68	−0.19 ± 0.09	V
92	2019-02-09	0.063	4.34	−0.69 ± 0.09	V
92	2020-02-18	0.231	15.83	−0.47 ± 0.09	V
92	2020-02-21	0.154	15.56	−0.51 ± 0.09	V
92	2020-04-06	0.991	6.71	−1.00 ± 0.09	V
92	2020-05-04	0.942	5.45	−0.66 ± 0.08	V
93	2020-01-06	0.929	6.85	−1.27 ± 0.10	V
93	2020-01-06	0.929	6.85	−1.27 ± 0.09	V
93	2020-02-23	0.893	17.39	−0.34 ± 0.08	V
93	2020-04-07	0.869	17.70	−0.23 ± 0.12	V
93	2021-01-11	0.149	17.39	−0.42 ± 0.08	V
93	2021-02-23	0.899	5.33	−1.01 ± 0.12	V
93	2021-03-01	0.015	2.95	−0.88 ± 0.08	V
93	2021-04-08	0.899	12.63	−1.08 ± 0.08	V
93	2021-04-24	0.887	17.14	−0.44 ± 0.09	V
94	2015-02-22	0.841	16.63	−0.35 ± 0.09	V
94	2019-11-08	0.007	3.22	−0.79 ± 0.08	V
94	2021-01-13	0.072	8.88	−1.28 ± 0.08	V
95	2017-07-20	0.058	18.66	−0.70 ± 0.20	V
95	2017-07-16	0.080	19.22	−0.40 ± 0.10	V
95	2017-08-10	0.962	14.47	−1.50 ± 0.11	V
96	2015-07-21	0.096	17.22	−0.95 ± 0.09	V
96	2015-07-23	0.078	17.22	−0.90 ± 0.09	V
96	2016-12-05	0.139	12.88	−1.51 ± 0.09	V
96	2016-12-10	0.002	11.50	−1.55 ± 0.11	V
96	2021-11-18	0.965	9.74	−1.54 ± 0.09	V

Table A.1. continued.

Asteroid Number	Date of observation	Fraction of day	Phase angle (deg)	P_r (%)	Filter
97	2020-02-18	0.819	28.23	0.67 ± 0.09	V
97	2020-04-09	0.852	26.46	0.36 ± 0.09	V
98	2016-12-05	0.937	10.92	−1.55 ± 0.12	V
98	2016-12-09	0.927	12.05	−1.45 ± 0.09	V
98	2016-12-11	0.007	12.63	−1.47 ± 0.09	V
98	2016-12-28	0.989	17.40	−1.09 ± 0.09	V
99	2020-03-03	0.155	10.21	−2.10 ± 0.09	V
99	2020-05-25	0.929	25.59	0.71 ± 0.09	V
100	2016-08-18	0.108	19.85	0.18 ± 0.11	V
100	2016-12-12	0.928	9.16	−0.95 ± 0.11	V
100	2017-01-17	0.803	16.45	−0.37 ± 0.09	V
100	2019-04-08	0.927	7.97	−0.73 ± 0.09	V
100	2020-04-06	0.128	18.93	−0.07 ± 0.09	V
100	2020-05-08	0.073	12.18	−0.76 ± 0.09	V
100	2020-05-27	0.025	5.74	−0.85 ± 0.08	V
100	2021-11-18	0.901	14.03	−0.55 ± 0.08	V
101	2020-02-18	0.119	2.78	−0.51 ± 0.09	V
102	2018-03-25	0.953	7.80	−1.37 ± 0.17	V
103	2015-10-10	0.051	13.70	−0.49 ± 0.08	V
103	2018-03-15	0.129	19.16	−0.04 ± 0.08	V
103	2018-03-21	0.107	18.22	−0.14 ± 0.08	V
103	2018-05-12	0.009	3.29	−0.54 ± 0.08	V
103	2019-08-09	0.079	17.05	−0.40 ± 0.08	V
103	2019-10-05	0.964	7.75	−0.74 ± 0.08	V
104	2019-08-08	0.049	15.54	−1.52 ± 0.08	V
104	2019-10-07	0.971	5.09	−1.08 ± 0.08	V
104	2019-11-06	0.861	15.00	−1.50 ± 0.10	V
104	2021-02-15	0.898	13.02	−1.91 ± 0.11	V
105	2015-12-10	0.965	10.34	−1.61 ± 0.09	V
105	2019-11-06	0.192	20.27	0.02 ± 0.10	V
105	2020-01-06	1.000	11.57	−1.45 ± 0.09	V
105	2021-02-26	0.190	29.95	3.51 ± 0.10	V
105	2021-04-19	0.158	28.51	2.77 ± 0.10	V
105	2021-07-28	0.913	23.19	0.92 ± 0.08	V
105	2021-08-17	0.849	25.99	1.84 ± 0.08	V
106	2015-12-09	0.842	15.29	−1.44 ± 0.08	V
106	2016-12-06	0.197	16.89	−1.19 ± 0.10	V
106	2016-12-10	0.096	16.30	−1.18 ± 0.12	V
106	2018-03-15	0.100	6.71	−1.73 ± 0.09	V
106	2018-05-12	0.934	10.42	−1.80 ± 0.10	V
107	2020-01-06	0.054	8.46	−1.23 ± 0.08	V
107	2020-02-22	0.981	8.60	−1.37 ± 0.08	V
107	2021-02-26	0.133	12.48	−1.29 ± 0.12	V
107	2021-05-08	0.927	9.14	−1.27 ± 0.09	V
108	2016-12-21	0.786	16.58	−0.50 ± 0.11	V
108	2019-02-05	0.097	7.23	−0.79 ± 0.08	V
109	2016-12-13	0.197	22.84	0.70 ± 0.11	V
109	2015-12-09	0.792	29.40	2.77 ± 0.09	V
109	2021-01-19	0.982	5.95	−1.53 ± 0.08	V
110	2019-02-05	0.157	13.84	−0.81 ± 0.08	V
110	2019-02-11	0.121	12.22	−0.98 ± 0.08	V
110	2019-04-04	0.027	8.11	−1.02 ± 0.08	V
110	2019-06-15	0.870	20.39	−0.11 ± 0.14	V
111	2021-11-16	0.879	15.25	−1.32 ± 0.09	V
113	2019-10-05	0.053	6.66	−0.49 ± 0.11	V
113	2021-01-13	0.103	16.62	−0.15 ± 0.09	V
114	2016-08-03	0.096	15.77	−1.01 ± 0.09	V
114	2019-04-08	0.132	16.86	−0.78 ± 0.08	V
114	2019-05-31	0.034	6.17	−0.85 ± 0.08	V

Table A.1. continued.

Asteroid Number	Date of observation	Fraction of day	Phase angle (deg)	P_r (%)	Filter
114	2021-11-13	0.942	2.65	−0.61 ± 0.08	V
115	2020-01-06	0.168	22.21	0.20 ± 0.09	V
115	2020-02-22	0.095	7.73	−0.71 ± 0.09	V
115	2020-04-07	0.951	14.20	−0.35 ± 0.09	V
116	2019-12-31	0.892	17.78	−0.20 ± 0.08	V
116	2021-01-13	0.129	21.34	−0.12 ± 0.09	V
116	2021-01-17	0.162	20.50	0.10 ± 0.08	V
116	2021-02-23	0.942	7.63	−0.82 ± 0.09	V
117	2016-07-27	0.103	18.92	−0.51 ± 0.10	V
117	2016-08-13	0.118	16.19	−0.98 ± 0.14	V
117	2019-02-12	0.138	13.74	−1.01 ± 0.08	V
117	2021-08-12	0.098	12.75	−1.04 ± 0.09	V
117	2021-08-22	0.024	9.63	−1.27 ± 0.09	V
117	2021-09-19	0.959	1.73	−0.39 ± 0.09	V
118	2020-01-03	0.051	5.76	−0.63 ± 0.08	V
119	2019-10-07	0.138	20.11	0.03 ± 0.08	V
119	2019-12-27	0.876	14.57	−0.52 ± 0.08	V
119	2020-02-23	0.859	23.29	0.21 ± 0.10	V
119	2021-05-03	0.824	17.82	−0.06 ± 0.10	V
120	2020-04-08	0.944	18.11	−0.15 ± 0.10	V
121	2015-12-10	0.844	12.44	−1.82 ± 0.09	V
121	2018-03-25	0.060	4.52	−0.91 ± 0.09	V
121	2018-05-06	0.871	13.02	−1.56 ± 0.09	V
121	2019-06-12	0.928	10.85	−1.91 ± 0.09	V
121	2021-11-16	0.834	15.87	−1.39 ± 0.09	V
122	2016-07-04	0.025	7.24	−0.80 ± 0.09	V
122	2016-07-26	0.986	0.61	−0.02 ± 0.09	V
122	2015-05-20	0.894	3.07	−0.47 ± 0.08	V
122	2015-05-22	0.928	3.45	−0.55 ± 0.09	V
122	2016-08-18	0.943	7.79	−0.64 ± 0.15	V
122	2020-01-07	0.183	16.97	−0.47 ± 0.10	V
122	2020-01-07	0.183	16.97	−0.54 ± 0.09	V
122	2020-02-21	0.091	6.16	−0.62 ± 0.09	V
122	2020-04-11	1.000	11.43	−0.59 ± 0.12	V
123	2020-01-03	0.028	6.46	−0.77 ± 0.09	V
123	2020-01-03	0.028	6.46	−0.80 ± 0.09	V
124	2017-07-09	0.080	18.05	−0.48 ± 0.09	V
124	2017-07-27	0.088	12.29	−0.81 ± 0.08	V
124	2017-07-29	0.079	11.53	−0.84 ± 0.09	V
124	2017-08-03	0.060	9.54	−0.84 ± 0.08	V
124	2017-08-12	0.031	5.69	−0.70 ± 0.10	V
124	2020-01-01	0.112	20.93	0.06 ± 0.09	V
124	2020-02-22	0.109	7.10	−0.92 ± 0.08	V
124	2020-04-11	0.976	14.45	−0.50 ± 0.09	V
124	2020-04-30	0.862	19.77	0.06 ± 0.09	V
124	2020-05-04	0.864	20.59	0.14 ± 0.08	V
125	2017-08-03	0.995	1.93	−0.58 ± 0.08	V
125	2017-08-12	0.973	4.87	−0.99 ± 0.12	V
125	2020-01-07	0.102	12.20	−0.63 ± 0.09	V
125	2020-02-22	0.022	5.85	−0.91 ± 0.11	V
125	2020-04-07	0.902	18.59	−0.32 ± 0.16	V
125	2021-04-23	0.065	12.64	−0.80 ± 0.09	V
126	2015-02-22	0.019	4.20	−0.59 ± 0.09	V
126	2021-11-19	0.952	17.34	−0.11 ± 0.09	V
127	2020-01-06	0.966	5.54	−1.18 ± 0.08	V
127	2021-02-28	0.155	18.48	−0.98 ± 0.12	V
127	2021-04-23	0.971	0.23	−0.36 ± 0.10	V
128	2015-02-22	0.947	9.27	−1.49 ± 0.09	R
128	2020-01-06	0.198	18.01	−0.45 ± 0.08	V

Table A.1. continued.

Asteroid Number	Date of observation	Fraction of day	Phase angle (deg)	P_r (%)	Filter
128	2020-02-21	0.109	6.90	−1.47 ± 0.10	V
128	2020-05-05	0.924	17.21	−0.49 ± 0.09	V
129	2017-01-18	0.745	16.79	−0.58 ± 0.09	V
129	2019-02-09	0.025	3.44	−0.76 ± 0.08	V
129	2021-11-19	0.908	10.60	−1.04 ± 0.10	V
130	2018-03-08	0.144	16.02	−1.36 ± 0.08	V
130	2018-05-17	0.995	9.44	−1.97 ± 0.09	V
130	2019-07-30	0.096	11.41	−1.83 ± 0.10	V
130	2019-07-31	0.084	11.06	−1.88 ± 0.08	V
131	2019-12-31	0.054	8.54	−0.89 ± 0.10	V
132	2017-07-29	0.046	7.62	−0.93 ± 0.10	V
132	2017-08-02	0.009	8.01	−0.72 ± 0.13	V
132	2017-07-09	0.987	8.71	−0.79 ± 0.10	V
132	2019-11-08	0.124	18.87	−0.21 ± 0.10	V
132	2019-12-26	0.963	9.19	−0.79 ± 0.08	V
132	2020-01-03	0.982	14.6	−0.50 ± 0.08	V
132	2020-02-18	0.805	33.99	2.21 ± 0.08	V
132	2021-08-12	0.907	12.20	−0.65 ± 0.11	V
132	2021-08-17	0.878	13.20	−0.45 ± 0.11	V
133	2015-02-22	0.876	15.78	−0.25 ± 0.09	R
133	2020-01-06	0.862	11.17	−0.63 ± 0.10	V
134	2017-08-14	0.128	25.49	1.89 ± 0.11	V
134	2017-08-11	0.111	25.53	1.88 ± 0.15	V
134	2019-04-08	0.972	6.56	−1.63 ± 0.10	V
134	2021-11-18	0.914	13.89	−1.27 ± 0.09	V
135	2016-12-09	0.084	9.53	−1.08 ± 0.09	V
135	2016-12-10	0.978	9.17	−0.93 ± 0.10	V
135	2018-05-10	0.908	18.30	−0.45 ± 0.09	V
135	2019-07-24	0.076	22.61	0.14 ± 0.09	V
135	2019-07-29	0.084	20.70	−0.10 ± 0.08	V
135	2019-07-31	0.097	19.87	−0.22 ± 0.08	V
135	2019-08-05	0.040	17.68	−0.66 ± 0.09	V
135	2019-10-02	0.901	14.94	−0.76 ± 0.08	V
135	2019-10-05	0.906	16.31	−0.85 ± 0.08	V
135	2019-10-10	0.917	18.42	−0.49 ± 0.08	V
135	2019-11-08	0.817	26.26	0.62 ± 0.08	V
135	2019-12-29	0.757	27.28	0.82 ± 0.09	V
135	2021-01-06	0.016	5.09	−0.99 ± 0.09	V
136	2021-11-30	0.074	16.48	−0.90 ± 0.09	V
137	2018-05-23	0.084	19.17	−0.43 ± 0.08	V
137	2019-11-08	0.047	2.83	−0.80 ± 0.09	V
137	2019-12-31	0.930	15.31	−1.26 ± 0.09	V
138	2019-04-08	0.941	9.57	−0.56 ± 0.09	V
138	2021-11-20	0.057	17.32	0.02 ± 0.10	V
139	2015-03-28	0.814	23.05	0.79 ± 0.08	V
139	2020-01-03	0.100	12.82	−1.31 ± 0.08	V
139	2020-02-20	0.985	12.68	−1.30 ± 0.08	V
139	2020-04-08	0.859	24.76	1.34 ± 0.09	V
139	2020-05-25	0.868	24.94	1.40 ± 0.08	V
140	2017-01-18	0.170	16.03	−1.18 ± 0.10	V
140	2020-01-01	0.868	10.34	−1.71 ± 0.08	V
141	2019-02-07	0.066	12.68	−1.70 ± 0.09	V
141	2021-08-22	0.048	24.14	0.92 ± 0.09	V
141	2021-08-27	0.105	22.96	0.52 ± 0.08	V
141	2021-11-16	0.858	18.25	−0.68 ± 0.08	V
142	2018-03-08	0.022	16.61	−0.00 ± 0.09	V
144	2019-12-31	0.018	1.74	−0.55 ± 0.09	V
144	2021-01-18	0.188	16.68	−1.05 ± 0.10	V
144	2021-05-07	0.892	14.27	−1.48 ± 0.09	V

Table A.1. continued.

Asteroid Number	Date of observation	Fraction of day	Phase angle (deg)	P_r (%)	Filter
145	2017-12-22	0.106	11.09	−1.91 ± 0.09	V
145	2018-03-25	0.979	25.06	1.41 ± 0.09	V
145	2018-05-08	0.872	24.78	1.26 ± 0.09	V
145	2019-04-14	0.100	14.85	−1.68 ± 0.10	V
145	2019-05-31	0.014	3.85	−0.86 ± 0.09	V
145	2021-11-14	0.026	4.40	−1.30 ± 0.09	V
148	2017-08-02	0.891	18.29	−0.26 ± 0.11	V
148	2017-07-19	0.889	17.15	−0.17 ± 0.14	V
148	2017-07-27	0.861	17.88	−0.27 ± 0.09	V
148	2017-07-30	0.885	18.10	−0.09 ± 0.10	V
148	2019-12-31	0.090	12.30	−0.61 ± 0.09	V
148	2020-01-03	0.071	11.25	−0.58 ± 0.08	V
148	2020-02-20	0.965	12.75	−0.81 ± 0.08	V
148	2020-04-09	0.874	21.06	0.20 ± 0.09	V
148	2021-01-17	0.210	17.89	0.03 ± 0.09	V
148	2021-02-23	0.996	14.50	−0.25 ± 0.13	V
148	2021-04-24	1.000	10.31	−0.62 ± 0.10	V
150	2019-12-29	0.788	21.54	0.80 ± 0.18	V
151	2021-11-30	0.916	11.26	−0.81 ± 0.09	V
152	2021-01-06	0.858	14.08	−0.44 ± 0.09	V
153	2016-07-28	0.014	9.46	−1.21 ± 0.09	V
154	2020-01-07	0.226	19.37	−0.10 ± 0.09	V
154	2020-02-19	0.146	15.14	−0.78 ± 0.09	V
156	2019-11-05	0.013	5.72	−1.44 ± 0.10	V
156	2021-01-18	0.850	10.64	−2.93 ± 0.37	V
158	2016-12-05	0.110	15.06	−0.34 ± 0.10	V
158	2016-12-10	0.024	13.62	−0.29 ± 0.11	V
158	2016-12-21	0.065	9.85	−0.53 ± 0.10	V
159	2019-02-07	0.990	3.29	−0.86 ± 0.08	V
159	2019-02-12	0.042	5.40	−1.29 ± 0.08	V
159	2020-05-04	0.961	3.29	−0.80 ± 0.10	V
159	2020-05-08	0.988	4.23	−0.92 ± 0.10	V
159	2020-05-21	0.963	8.05	−1.57 ± 0.10	V
161	2019-04-13	0.010	6.73	−0.78 ± 0.08	V
161	2021-11-30	0.190	19.38	0.20 ± 0.09	V
163	2016-08-11	0.046	22.72	0.45 ± 0.10	V
163	2016-08-17	0.031	21.45	0.02 ± 0.13	V
163	2016-12-21	0.865	27.64	2.33 ± 0.12	V
163	2019-07-22	0.030	2.36	−0.79 ± 0.19	V
163	2019-07-23	0.018	2.08	−0.34 ± 0.18	V
163	2019-07-29	0.000	2.19	−0.59 ± 0.10	V
163	2021-01-17	0.895	16.88	−1.01 ± 0.08	V
164	2021-05-05	0.028	6.05	−1.17 ± 0.09	V
165	2015-07-16	0.991	19.59	0.03 ± 0.10	V
165	2017-12-20	0.175	15.74	−0.66 ± 0.10	V
165	2021-11-27	0.896	7.34	−1.22 ± 0.10	V
167	2021-09-19	0.990	4.17	−0.59 ± 0.10	V
168	2015-02-22	0.913	12.94	−1.63 ± 0.11	R
168	2019-10-05	0.025	1.54	−0.60 ± 0.09	V
169	2021-11-19	0.900	13.13	−0.66 ± 0.10	V
170	2019-12-31	0.118	19.02	−0.06 ± 0.09	V
170	2020-02-22	0.046	5.89	−0.71 ± 0.09	V
172	2015-10-10	0.090	23.17	−0.70 ± 0.09	V
172	2015-12-09	0.102	12.00	−1.34 ± 0.09	V
172	2020-01-03	0.126	13.92	−1.56 ± 0.09	V
172	2020-01-07	0.144	12.50	−1.36 ± 0.08	V
172	2020-02-23	0.027	8.70	−1.30 ± 0.08	V
172	2020-04-08	0.916	20.93	−0.95 ± 0.09	V
173	2019-12-30	0.126	14.05	−0.89 ± 0.09	V

Table A.1. continued.

Asteroid Number	Date of observation	Fraction of day	Phase angle (deg)	P_r (%)	Filter
173	2020-02-22	0.998	7.22	−1.39 ± 0.09	V
174	2017-07-13	0.072	11.86	−0.61 ± 0.12	V
175	2016-12-13	0.023	7.42	−1.41 ± 0.09	V
175	2021-09-19	0.905	8.54	−1.63 ± 0.09	V
175	2021-11-29	0.752	23.37	1.09 ± 0.09	V
179	2021-11-30	0.134	13.91	−0.48 ± 0.10	V
181	2015-12-10	0.094	11.47	−1.20 ± 0.09	V
181	2019-08-02	0.068	2.31	−0.61 ± 0.09	V
182	2019-10-05	0.975	4.55	−0.70 ± 0.09	V
182	2019-11-06	0.918	20.23	0.01 ± 0.08	V
182	2021-05-07	0.850	17.49	0.07 ± 0.10	V
183	2017-12-20	0.151	21.79	0.20 ± 0.09	V
183	2019-04-12	0.052	8.39	−0.43 ± 0.11	V
185	2015-07-16	0.869	18.56	−0.08 ± 0.10	V
185	2016-07-27	0.061	17.86	−0.44 ± 0.09	V
185	2016-08-17	0.973	10.49	−1.38 ± 0.10	V
185	2020-04-08	0.174	20.69	0.57 ± 0.20	V
185	2020-05-08	0.120	19.42	−0.06 ± 0.09	V
185	2020-05-25	0.121	17.11	−0.57 ± 0.09	V
186	2019-01-30	0.192	7.53	−0.55 ± 0.09	V
186	2019-02-04	0.040	6.49	−0.51 ± 0.08	V
186	2019-02-05	0.990	6.35	−0.55 ± 0.09	V
186	2021-11-18	0.933	10.74	−1.25 ± 0.09	V
187	2019-10-05	0.935	8.84	−1.53 ± 0.10	V
188	2016-07-26	0.011	12.49	−0.58 ± 0.10	V
188	2016-08-01	0.906	14.67	−0.64 ± 0.10	V
188	2016-08-08	0.877	17.07	−0.41 ± 0.10	V
188	2016-08-08	0.877	17.72	−0.28 ± 0.13	V
188	2021-08-27	0.057	12.33	−0.70 ± 0.09	V
188	2021-09-19	0.932	8.06	−0.88 ± 0.09	V
189	2016-08-07	0.094	20.18	−0.50 ± 0.12	V
190	2017-07-04	0.924	5.18	−0.94 ± 0.12	V
190	2017-07-10	0.961	6.38	−1.26 ± 0.14	V
190	2019-08-05	0.073	8.16	−1.34 ± 0.10	V
191	2015-07-16	0.924	12.89	−0.97 ± 0.10	V
191	2016-08-08	0.063	16.28	−0.67 ± 0.10	V
191	2020-04-14	0.148	17.89	−0.31 ± 0.17	V
191	2020-05-17	0.087	12.06	−1.23 ± 10.00	V
191	2020-05-20	0.086	11.30	−1.22 ± 0.10	V
191	2020-05-21	0.069	11.05	−1.24 ± 0.08	V
192	2015-07-16	0.084	33.18	1.02 ± 0.10	V
192	2019-12-29	0.039	7.17	−0.71 ± 0.09	V
192	2019-12-30	0.047	6.73	−0.85 ± 0.08	V
192	2020-02-19	0.867	18.08	−0.26 ± 0.09	V
192	2021-02-26	0.107	13.96	−0.43 ± 0.09	V
194	2015-05-21	0.062	12.40	−1.67 ± 0.08	V
194	2016-12-10	0.819	13.50	−1.74 ± 0.27	V
194	2017-01-16	0.807	19.91	−0.35 ± 0.09	V
194	2017-12-20	0.132	15.06	−1.44 ± 0.10	V
194	2015-07-17	0.859	24.72	1.27 ± 0.09	V
194	2016-12-05	0.895	12.54	−1.66 ± 0.11	V
194	2019-04-08	0.002	8.47	−1.91 ± 0.09	V
194	2019-05-30	0.011	18.12	−0.68 ± 0.08	V
194	2019-06-15	0.896	21.29	0.13 ± 0.11	V
194	2021-01-19	0.810	23.44	0.74 ± 0.08	V
196	2019-10-09	0.076	8.72	−0.78 ± 0.08	V
196	2019-12-31	0.867	16.61	−0.41 ± 0.08	V
196	2020-02-23	0.791	16.91	−0.40 ± 0.09	V
196	2021-01-13	0.033	2.39	−0.49 ± 0.08	V

Table A.1. continued.

Asteroid Number	Date of observation	Fraction of day	Phase angle (deg)	P_r (%)	Filter
198	2020-01-01	0.044	7.26	−0.73 ± 0.09	V
199	2020-04-06	0.019	11.82	−1.08 ± 0.11	V
199	2020-05-08	0.954	6.87	−0.91 ± 0.09	V
200	2015-07-22	0.980	13.40	−1.71 ± 0.11	V
200	2015-10-15	0.844	19.25	−0.60 ± 0.08	V
201	2015-07-14	0.092	23.55	0.19 ± 0.10	V
201	2015-07-15	0.026	23.35	0.15 ± 0.09	V
201	2019-05-29	0.070	15.63	−0.90 ± 0.08	V
201	2019-06-15	0.028	9.43	−1.05 ± 0.09	V
203	2018-03-23	0.145	16.84	−0.44 ± 0.09	V
203	2019-10-10	0.878	17.72	−0.12 ± 0.20	V
204	2015-12-10	0.002	3.05	−0.52 ± 0.24	V
204	2021-01-11	0.073	6.81	−0.89 ± 0.08	V
205	2017-07-05	0.941	8.76	−1.68 ± 0.11	V
205	2017-07-11	0.974	7.26	−1.18 ± 0.11	V
205	2021-04-19	0.065	11.37	−1.63 ± 0.09	V
207	2021-11-19	0.979	18.76	−0.73 ± 0.10	V
208	2016-08-07	0.038	4.04	−0.56 ± 0.12	V
208	2021-08-17	0.038	3.56	−0.72 ± 0.08	V
210	2016-06-09	0.870	19.54	0.92 ± 0.14	V
210	2019-12-30	0.149	15.56	−0.15 ± 0.11	V
210	2020-02-19	0.961	6.39	−1.06 ± 0.08	V
211	2016-07-15	0.059	10.21	−1.74 ± 0.14	V
211	2016-07-26	0.030	6.91	−1.65 ± 0.11	V
213	2015-10-16	0.083	17.30	−0.35 ± 0.08	V
213	2015-12-09	0.043	2.67	−1.27 ± 0.09	V
213	2016-12-12	0.109	18.51	0.38 ± 0.11	V
213	2019-11-08	0.994	5.50	−2.03 ± 0.11	V
213	2019-12-29	0.818	18.17	−0.13 ± 0.11	V
213	2021-01-11	0.008	0.58	−0.46 ± 0.08	V
214	2017-12-21	0.794	21.58	0.22 ± 0.14	V
214	2017-07-28	0.086	22.12	0.18 ± 0.12	V
214	2021-08-21	0.016	12.04	−0.10 ± 0.09	V
216	2016-06-09	0.956	9.89	−0.97 ± 0.09	V
216	2017-07-06	0.935	10.46	−1.08 ± 0.09	V
216	2017-07-26	0.972	7.92	−0.99 ± 0.09	V
216	2020-02-24	0.096	11.84	−0.94 ± 0.08	V
216	2021-04-12	0.144	13.61	−0.87 ± 0.08	V
217	2016-07-29	0.985	12.24	−0.82 ± 0.10	V
217	2016-07-27	0.905	11.46	−0.81 ± 0.09	V
217	2016-08-08	0.848	16.18	−0.31 ± 0.10	V
217	2021-08-21	0.914	3.48	−0.57 ± 0.09	V
218	2019-05-30	0.080	21.59	0.17 ± 0.09	V
218	2019-07-19	0.014	8.30	−0.71 ± 0.10	V
218	2019-07-31	0.921	7.42	−0.70 ± 0.09	V
218	2019-08-05	0.959	8.13	−0.54 ± 0.10	V
218	2019-11-06	0.802	21.75	0.25 ± 0.16	V
219	2017-07-03	0.055	18.59	−0.13 ± 0.16	V
219	2017-07-26	0.005	11.98	−0.59 ± 0.09	V
219	2017-07-29	0.977	11.63	−0.58 ± 0.09	V
219	2020-04-07	0.107	6.11	−0.88 ± 0.13	V
221	2017-01-18	0.955	13.47	−0.78 ± 0.10	V
221	2015-07-14	0.070	17.78	−0.58 ± 0.09	V
221	2016-12-10	0.903	4.55	−0.83 ± 0.10	V
221	2019-02-11	0.226	17.89	−0.28 ± 0.10	V
221	2019-04-08	0.056	9.01	−1.12 ± 0.09	V
221	2019-04-13	0.066	7.72	−1.13 ± 0.09	V
221	2019-06-10	0.926	14.16	−0.74 ± 0.10	V
221	2019-06-15	0.908	15.22	−0.77 ± 0.13	V

Table A.1. continued.

Asteroid Number	Date of observation	Fraction of day	Phase angle (deg)	P_r (%)	Filter
222	2017-07-30	0.084	10.16	−1.92 ± 0.11	V
222	2017-08-11	0.049	5.91	−1.58 ± 0.12	V
222	2017-08-14	0.000	4.81	−1.39 ± 0.11	V
222	2016-06-01	0.902	9.90	−1.80 ± 0.09	V
222	2017-07-27	0.115	11.13	−1.69 ± 0.10	V
222	2021-04-24	0.914	14.14	−1.43 ± 0.23	V
223	2016-12-10	0.928	1.50	−0.20 ± 0.12	V
223	2017-01-18	0.914	15.65	−0.78 ± 0.14	V
224	2021-08-13	0.071	13.99	−1.15 ± 0.09	V
225	2015-10-16	0.130	13.83	−0.73 ± 0.08	V
225	2019-04-08	0.096	13.74	−0.84 ± 0.08	V
225	2019-04-13	0.108	12.59	−1.12 ± 0.09	V
225	2019-05-30	0.033	9.59	−1.01 ± 0.08	V
225	2019-05-31	0.992	9.84	−0.92 ± 0.09	V
225	2019-06-15	0.928	13.93	−0.87 ± 0.11	V
225	2019-07-23	0.876	21.22	0.74 ± 0.13	V
225	2019-07-24	0.873	21.32	0.91 ± 0.09	V
225	2019-07-30	0.861	21.84	1.03 ± 0.09	V
225	2019-07-31	0.874	21.91	0.96 ± 0.14	V
225	2019-08-09	0.845	22.37	1.33 ± 0.10	V
226	2016-07-15	0.018	11.36	−0.72 ± 0.09	V
226	2016-07-26	0.903	5.72	−1.03 ± 0.09	V
226	2016-07-27	0.002	5.12	−0.94 ± 0.09	V
226	2020-04-06	0.069	16.83	−0.52 ± 0.10	V
226	2020-05-19	0.004	12.21	−0.53 ± 0.10	V
226	2020-05-21	0.985	12.56	−0.48 ± 0.12	V
227	2016-08-06	0.063	6.14	−1.42 ± 0.10	V
227	2016-08-14	0.055	3.20	−0.90 ± 0.09	V
227	2016-08-16	0.078	2.44	−0.67 ± 0.11	V
227	2019-01-30	0.915	12.70	−1.44 ± 0.18	V
227	2019-02-04	0.839	13.53	−1.30 ± 0.12	V
230	2015-12-09	0.088	2.26	−0.43 ± 0.08	V
230	2020-02-18	0.893	13.64	−0.79 ± 0.09	V
233	2019-12-29	0.851	18.87	−0.44 ± 0.09	V
233	2021-01-18	0.071	11.49	−1.16 ± 0.09	V
234	2015-02-25	0.165	16.95	−1.54 ± 0.11	V
234	2015-05-22	0.876	17.38	−1.43 ± 0.08	V
234	2016-07-19	0.069	33.54	0.62 ± 0.09	V
234	2016-12-04	0.945	18.34	−1.49 ± 0.12	V
234	2018-03-06	0.882	6.74	−0.84 ± 0.09	V
234	2019-04-04	0.121	19.71	−1.28 ± 0.09	V
234	2019-04-13	0.129	17.95	−1.62 ± 0.09	V
234	2019-06-01	0.035	12.76	−1.36 ± 0.09	V
234	2019-06-15	0.941	16.58	−1.36 ± 0.09	V
234	2019-07-23	0.857	26.45	−0.78 ± 0.14	V
234	2019-07-24	0.853	26.63	−0.45 ± 0.10	V
234	2019-07-29	0.910	27.42	−0.20 ± 0.14	V
234	2019-07-30	0.885	27.56	−0.44 ± 0.09	V
234	2019-07-31	0.896	27.69	−0.30 ± 0.09	V
234	2019-08-07	0.876	28.51	−0.33 ± 0.08	V
234	2021-01-06	0.912	9.73	−1.56 ± 0.11	V
234	2021-01-17	0.953	12.93	−1.55 ± 0.08	V
234	2021-01-19	0.948	13.52	−1.65 ± 0.08	V
235	2015-12-10	0.871	11.68	−1.48 ± 0.09	V
236	2015-02-22	0.125	11.50	−1.31 ± 0.09	V
236	2015-03-30	0.871	0.41	0.03 ± 0.08	V
236	2015-05-21	0.902	15.26	−1.24 ± 0.09	V
236	2016-06-07	0.989	5.02	−0.87 ± 0.10	V
236	2016-07-17	0.861	13.93	−1.30 ± 0.11	V

Table A.1. continued.

Asteroid Number	Date of observation	Fraction of day	Phase angle (deg)	P_r (%)	Filter
236	2016-07-26	0.863	16.52	−1.24 ± 0.10	V
236	2016-07-28	0.912	17.05	−1.45 ± 0.11	V
236	2017-07-17	0.079	25.69	0.09 ± 0.11	V
236	2016-07-05	0.922	9.98	−1.08 ± 0.13	V
236	2017-07-22	0.106	25.97	−0.06 ± 0.11	V
236	2017-07-29	0.117	26.23	−0.14 ± 0.10	V
236	2017-08-01	0.108	26.29	−0.07 ± 0.12	V
236	2019-01-28	0.037	6.59	−0.94 ± 0.09	V
236	2019-02-04	0.010	4.30	−0.69 ± 0.08	V
236	2019-04-14	0.874	16.40	−1.13 ± 0.11	V
236	2020-02-18	0.185	16.00	−1.37 ± 0.10	V
236	2020-02-19	0.164	15.88	−1.42 ± 0.12	V
236	2020-04-07	0.051	4.16	−0.69 ± 0.13	V
236	2020-04-15	0.032	1.72	−0.53 ± 0.09	V
236	2020-04-23	0.009	2.34	−0.48 ± 0.08	V
236	2020-05-20	0.882	11.02	−1.39 ± 0.11	V
236	2021-07-28	0.974	5.35	−0.69 ± 0.08	V
236	2021-08-17	0.907	12.22	−1.35 ± 0.09	V
236	2021-09-19	0.815	21.96	−0.84 ± 0.09	V
237	2020-01-01	0.953	6.47	−0.90 ± 0.10	V
238	2017-08-02	0.928	16.75	−1.75 ± 0.16	V
238	2016-06-07	0.870	12.45	−0.79 ± 0.22	V
238	2017-07-04	0.873	10.41	−1.59 ± 0.12	V
238	2017-07-12	0.900	14.72	−1.57 ± 0.10	V
238	2017-07-22	0.875	14.72	−1.57 ± 0.10	V
238	2017-07-26	0.907	15.53	−1.42 ± 0.16	V
238	2017-08-03	0.921	16.91	−1.24 ± 0.15	V
238	2017-08-14	0.831	18.31	−0.84 ± 0.12	V
238	2019-12-29	0.012	6.91	−1.34 ± 0.08	V
238	2020-02-21	0.825	17.04	−1.15 ± 0.11	V
238	2021-04-19	0.908	8.19	−1.38 ± 0.08	V
240	2019-08-09	0.024	17.51	−1.18 ± 0.09	V
240	2021-04-08	0.875	15.54	−1.19 ± 0.11	V
241	2017-07-30	0.063	13.51	−1.08 ± 0.08	V
241	2017-07-09	0.064	18.49	−0.47 ± 0.09	V
241	2017-07-16	0.104	17.11	−0.30 ± 0.13	V
241	2017-07-29	0.094	13.79	−1.08 ± 0.08	V
241	2017-08-12	0.040	9.25	−1.30 ± 0.11	V
241	2017-08-16	0.066	7.81	−1.31 ± 0.08	V
241	2020-01-06	0.141	13.91	−0.97 ± 0.09	V
241	2020-02-21	0.072	2.08	−0.52 ± 0.09	V
243	2019-08-02	0.123	11.05	−0.91 ± 0.16	V
245	2019-10-05	0.917	14.32	−0.45 ± 0.10	V
245	2019-11-05	0.726	21.14	0.11 ± 0.10	V
246	2016-12-09	0.120	10.85	−0.23 ± 0.09	V
246	2017-12-20	0.223	21.18	0.09 ± 0.09	V
246	2016-12-08	0.076	11.12	−0.27 ± 0.15	V
246	2019-07-24	0.067	14.62	−0.10 ± 0.11	V
246	2019-07-29	0.073	12.82	−0.31 ± 0.08	V
246	2019-07-31	0.070	12.06	−0.35 ± 0.08	V
246	2019-10-02	0.862	14.66	−0.33 ± 0.09	V
246	2021-01-19	0.858	16.99	−0.11 ± 0.09	V
247	2019-08-08	0.072	19.54	−0.10 ± 0.08	V
247	2019-10-03	0.984	6.15	−1.08 ± 0.08	V
247	2019-10-09	0.944	9.39	−1.22 ± 0.08	V
247	2019-11-08	0.866	21.97	0.57 ± 0.10	V
247	2019-12-31	0.835	27.65	2.48 ± 0.08	V
247	2021-02-10	0.104	10.71	−1.25 ± 0.10	V
252	2019-08-05	0.017	4.99	−0.95 ± 0.09	V

Table A.1. continued.

Asteroid Number	Date of observation	Fraction of day	Phase angle (deg)	P_r (%)	Filter
256	2017-07-06	0.028	7.88	−1.63 ± 0.11	V
256	2017-07-28	0.969	7.45	−1.36 ± 0.10	V
256	2017-08-14	0.940	11.49	−1.67 ± 0.16	V
257	2015-12-11	0.834	14.70	−1.62 ± 0.16	V
257	2021-11-30	0.043	8.74	−1.51 ± 0.08	V
258	2019-12-30	0.058	11.05	−0.34 ± 0.08	V
258	2020-02-23	0.929	14.86	−0.48 ± 0.09	V
258	2021-04-22	0.885	7.38	−0.68 ± 0.09	V
259	2017-12-22	0.112	9.73	−1.19 ± 0.11	V
259	2019-04-04	0.055	5.89	−0.91 ± 0.08	V
259	2019-06-15	0.882	19.77	0.08 ± 0.11	V
260	2019-05-31	0.063	3.64	−0.44 ± 0.09	V
261	2020-04-06	0.042	16.34	−0.59 ± 0.09	V
261	2020-05-05	0.976	2.96	−0.91 ± 0.10	V
261	2021-08-21	0.059	12.70	−1.03 ± 0.08	V
263	2019-12-30	0.016	1.32	−0.63 ± 0.10	V
264	2020-04-07	0.076	5.34	−0.99 ± 0.12	V
266	2019-06-10	0.071	11.48	−1.67 ± 0.09	V
266	2019-07-19	0.955	7.50	−1.33 ± 0.09	V
266	2019-07-29	0.941	10.37	−1.49 ± 0.10	V
266	2019-08-09	0.898	13.63	−1.43 ± 0.08	V
268	2016-12-12	0.157	20.88	0.63 ± 0.12	V
268	2019-08-05	0.105	10.44	−1.32 ± 0.11	V
270	2021-11-19	0.017	14.96	−0.32 ± 0.09	V
273	2015-07-23	0.964	17.87	−0.42 ± 0.09	V
273	2018-03-23	0.104	8.14	−0.91 ± 0.10	V
275	2019-11-05	0.802	13.96	−1.00 ± 0.14	V
276	2016-08-03	0.911	9.15	−0.96 ± 0.11	V
276	2016-08-14	0.895	8.49	−0.86 ± 0.09	V
276	2015-07-23	0.896	15.74	−0.38 ± 0.09	V
276	2020-04-24	0.995	0.96	0.00 ± 0.09	V
276	2021-08-16	0.854	13.93	−0.62 ± 0.17	V
277	2020-02-19	0.103	11.49	−0.93 ± 0.36	V
278	2020-04-07	0.990	17.71	−0.18 ± 0.09	V
279	2021-11-23	0.849	9.28	−0.98 ± 0.09	V
283	2019-07-22	0.054	9.11	−0.76 ± 0.28	V
283	2019-07-23	0.072	8.73	−1.00 ± 0.11	V
283	2019-07-30	0.023	6.01	−0.91 ± 0.09	V
283	2019-07-31	0.028	5.60	−0.82 ± 0.10	V
283	2021-01-06	0.884	11.84	−0.92 ± 0.09	V
284	2016-07-12	0.945	11.62	−1.81 ± 0.08	V
284	2016-07-26	0.879	17.72	−0.77 ± 0.09	V
284	2016-07-20	0.903	14.06	−1.28 ± 0.10	V
284	2016-07-22	0.985	15.90	−1.15 ± 0.10	V
286	2019-06-08	0.921	12.98	−1.61 ± 0.66	V
287	2019-08-05	0.089	13.60	−0.70 ± 0.08	V
287	2021-01-13	0.015	3.52	−0.56 ± 0.08	V
289	2016-02-05	0.974	15.57	−0.09 ± 0.11	V
289	2019-07-23	0.058	11.84	−0.16 ± 0.14	V
289	2019-07-30	0.081	9.11	−0.37 ± 0.10	V
289	2019-07-31	0.052	8.71	−0.30 ± 0.09	V
289	2019-10-02	0.828	18.95	0.22 ± 0.09	V
290	2021-11-24	0.131	31.49	1.11 ± 0.12	V
293	2019-01-28	0.836	20.44	−0.48 ± 0.14	V
293	2019-02-05	0.803	20.87	−0.13 ± 0.11	V
293	2019-02-06	0.805	20.91	−0.34 ± 0.11	V
293	2019-02-12	0.866	21.01	−0.22 ± 0.20	V
293	2020-03-03	0.087	9.30	−1.85 ± 0.09	V
293	2020-04-08	0.071	14.78	−1.48 ± 0.15	V

Table A.1. continued.

Asteroid Number	Date of observation	Fraction of day	Phase angle (deg)	P_r (%)	Filter
293	2020-05-04	0.910	20.26	0.02 ± 0.17	V
297	2021-12-01	0.051	5.39	−0.57 ± 0.09	V
298	2021-01-14	0.908	15.34	−0.29 ± 0.10	V
303	2021-11-29	0.830	15.44	−0.82 ± 0.09	V
304	2015-07-17	0.943	19.89	0.30 ± 0.09	V
306	2016-12-10	0.953	6.38	−0.53 ± 0.14	V
306	2016-12-09	0.023	6.75	−0.47 ± 0.09	V
306	2017-01-18	0.993	12.48	−0.45 ± 0.09	V
306	2015-07-14	0.004	4.59	−0.29 ± 0.10	V
306	2018-05-20	0.909	21.27	0.46 ± 0.09	V
306	2019-08-08	0.119	24.68	0.43 ± 0.09	V
306	2019-10-05	0.998	5.39	−0.58 ± 0.11	V
306	2019-12-26	0.827	25.57	0.66 ± 0.11	V
308	2016-08-10	0.117	21.37	0.12 ± 0.13	V
308	2016-08-16	0.113	20.72	−0.09 ± 0.10	V
308	2016-12-02	0.835	15.08	−1.28 ± 0.09	V
308	2016-12-11	0.844	17.18	−0.93 ± 0.09	V
308	2019-04-08	0.043	9.35	−1.58 ± 0.09	V
308	2019-06-12	0.950	16.23	−1.21 ± 0.09	V
313	2015-07-18	0.980	5.89	−1.52 ± 0.10	V
313	2015-07-14	0.026	6.67	−1.77 ± 0.09	V
313	2016-08-13	0.138	23.78	1.04 ± 0.11	V
313	2016-08-12	0.105	23.85	1.17 ± 0.11	V
313	2016-12-01	0.900	20.60	0.03 ± 0.10	V
313	2019-08-01	0.056	9.48	−2.01 ± 0.11	V
313	2019-10-08	0.890	17.02	−1.09 ± 0.10	V
313	2019-10-10	0.845	17.45	−0.81 ± 0.10	V
314	2019-08-01	0.912	9.86	−1.39 ± 0.15	V
317	2019-08-05	0.052	14.90	−0.24 ± 0.09	V
317	2021-01-06	0.048	11.76	−0.09 ± 0.10	V
321	2019-12-31	0.970	4.87	−0.78 ± 0.19	V
322	2016-08-03	0.046	21.55	0.22 ± 0.10	V
322	2016-12-12	0.822	27.20	1.44 ± 0.11	V
322	2016-07-26	0.086	23.41	0.54 ± 0.10	V
322	2021-08-27	0.149	28.00	1.72 ± 0.10	V
322	2021-11-17	0.978	5.28	−0.90 ± 0.09	V
323	2021-01-06	0.165	18.18	−0.10 ± 0.09	V
323	2021-03-01	0.990	13.48	−0.14 ± 0.10	V
324	2015-03-27	0.987	11.99	−1.48 ± 0.10	V
324	2019-01-28	0.983	4.61	−1.14 ± 0.08	V
324	2019-02-04	0.950	7.18	−1.48 ± 0.09	V
324	2020-02-22	0.123	9.48	−1.85 ± 10.00	V
324	2020-03-03	0.045	6.82	−1.39 ± 0.08	V
325	2021-11-19	0.831	15.99	−0.46 ± 0.09	V
328	2021-11-20	0.902	11.03	−1.10 ± 0.08	V
329	2019-10-10	0.172	23.12	1.04 ± 0.15	V
329	2021-02-28	0.186	23.97	1.55 ± 0.17	V
329	2021-04-22	0.048	14.99	−0.62 ± 0.09	V
329	2021-04-24	0.108	14.42	−0.57 ± 0.14	V
332	2019-10-08	0.146	17.44	−0.59 ± 0.10	V
334	2016-12-13	0.872	10.00	−1.46 ± 0.10	V
335	2016-06-07	0.006	6.82	−1.28 ± 0.10	V
335	2019-01-28	0.075	7.26	−1.25 ± 0.08	V
335	2019-02-07	0.020	3.08	−0.82 ± 0.08	V
335	2021-11-18	0.945	6.91	−1.06 ± 0.10	V
336	2017-08-10	0.013	22.06	1.00 ± 0.10	V
336	2017-08-13	0.027	21.19	0.58 ± 0.13	V
336	2017-08-14	0.058	20.87	0.51 ± 0.09	V
336	2017-08-15	0.072	20.55	0.28 ± 0.11	V

Table A.1. continued.

Asteroid Number	Date of observation	Fraction of day	Phase angle (deg)	P_r (%)	Filter
336	2017-08-16	0.099	20.22	0.14 ± 0.10	V
336	2017-07-28	0.017	25.06	2.08 ± 0.09	V
336	2019-01-28	0.006	3.75	−1.02 ± 0.08	V
336	2019-02-05	0.955	5.61	−1.33 ± 0.09	V
337	2017-12-22	0.803	26.27	0.84 ± 0.20	V
337	2015-02-25	0.853	18.22	−0.32 ± 0.10	R
337	2019-01-28	0.165	21.21	0.05 ± 0.09	V
337	2019-02-05	0.137	18.68	−0.36 ± 0.09	V
337	2019-02-11	0.100	16.44	−0.71 ± 0.08	V
337	2021-11-20	0.990	7.31	−1.04 ± 0.09	V
338	2016-07-27	0.072	15.12	−0.79 ± 0.09	V
338	2016-12-13	0.814	20.02	−0.10 ± 0.10	V
338	2019-02-12	0.100	10.67	−0.85 ± 0.08	V
338	2021-08-27	0.081	6.94	−0.92 ± 0.08	V
339	2017-07-07	0.042	12.99	−1.03 ± 0.18	V
339	2017-07-14	0.972	10.80	−1.12 ± 0.10	V
339	2017-07-30	0.998	5.36	−0.64 ± 0.12	V
339	2017-08-01	0.013	4.76	−0.67 ± 0.13	V
341	2016-08-08	0.108	30.43	0.75 ± 0.13	V
341	2016-12-12	0.872	26.62	0.29 ± 0.17	V
345	2016-12-11	0.884	22.13	0.39 ± 0.09	V
345	2016-08-11	0.107	25.36	1.35 ± 0.09	V
345	2018-03-23	0.997	3.85	−0.86 ± 0.08	V
345	2019-07-24	0.006	8.61	−1.38 ± 0.09	V
345	2019-07-31	0.991	7.10	−1.37 ± 0.10	V
345	2019-10-07	0.784	23.06	0.54 ± 0.10	V
345	2019-11-08	0.781	24.79	1.10 ± 0.21	V
346	2021-02-28	0.132	16.52	−0.30 ± 0.09	V
346	2021-04-23	0.004	3.59	−0.60 ± 0.08	V
346	2021-05-05	0.954	5.29	−0.58 ± 0.08	V
347	2021-04-23	0.091	17.13	−0.53 ± 0.09	V
348	2021-01-18	0.821	17.91	−0.34 ± 0.12	V
348	2021-01-18	0.821	11.49	−1.15 ± 0.09	V
349	2019-01-28	0.102	10.92	−0.33 ± 0.08	V
349	2019-02-05	0.122	8.51	−0.42 ± 0.08	V
350	2016-06-01	0.969	6.29	−1.43 ± 0.10	V
350	2016-06-09	0.975	7.67	−1.56 ± 0.09	V
350	2020-04-09	0.946	19.66	−0.24 ± 0.10	V
350	2020-05-06	0.858	19.62	−0.64 ± 0.37	V
350	2020-05-07	0.846	19.58	−0.17 ± 0.12	V
350	2021-04-12	0.054	8.79	−1.66 ± 0.09	V
354	2016-08-01	0.891	13.59	−0.29 ± 0.09	V
354	2016-08-08	0.830	15.05	−0.21 ± 0.09	V
354	2016-06-01	0.074	11.26	−0.48 ± 0.09	V
354	2016-07-26	0.896	12.20	−0.34 ± 0.09	V
354	2019-02-09	0.825	20.56	0.10 ± 0.08	V
354	2019-02-12	0.828	20.99	−0.04 ± 0.08	V
354	2020-02-18	0.162	20.08	0.10 ± 0.09	V
354	2020-03-03	0.130	17.35	−0.21 ± 0.08	V
354	2020-04-09	0.130	9.90	−0.48 ± 0.09	V
354	2020-05-08	0.941	13.93	−0.17 ± 0.08	V
354	2020-05-17	0.853	15.95	−0.20 ± 0.10	V
354	2020-05-20	0.851	16.59	−0.07 ± 0.08	V
354	2021-08-16	0.884	9.46	−0.57 ± 0.08	V
354	2021-08-21	0.858	10.91	−0.47 ± 0.09	V
355	2021-09-23	0.114	20.52	0.08 ± 0.10	V
355	2021-11-29	0.916	9.27	−0.61 ± 0.08	V
356	2021-01-13	0.989	9.57	−1.59 ± 0.08	V
358	2020-04-08	0.006	11.67	−1.35 ± 0.14	V

Table A.1. continued.

Asteroid Number	Date of observation	Fraction of day	Phase angle (deg)	P_r (%)	Filter
359	2021-08-22	0.069	18.29	−0.53 ± 0.10	V
359	2021-11-29	0.791	21.84	0.02 ± 0.10	V
360	2021-11-14	0.017	7.54	−1.12 ± 0.08	V
361	2017-12-22	0.169	15.26	−0.46 ± 0.13	V
362	2019-10-05	0.008	1.40	−0.42 ± 0.09	V
363	2020-01-01	0.064	6.39	−1.70 ± 0.08	V
363	2021-04-24	0.968	5.43	−1.26 ± 0.11	V
365	2017-08-16	0.080	11.30	−1.67 ± 0.13	V
365	2017-07-09	0.034	20.69	0.11 ± 0.12	V
365	2017-08-03	0.087	15.67	−0.94 ± 0.12	V
365	2017-08-04	0.067	15.37	−1.13 ± 0.13	V
365	2017-08-15	0.046	11.68	−1.64 ± 0.09	V
365	2020-04-15	0.002	2.05	−0.55 ± 0.12	V
365	2021-08-11	0.852	15.72	−0.89 ± 0.19	V
366	2021-04-08	0.924	7.80	−2.03 ± 0.10	V
368	2017-07-28	0.909	12.92	−1.08 ± 0.13	V
368	2017-07-13	0.942	7.44	−1.28 ± 0.14	V
368	2017-07-14	0.925	7.80	−1.18 ± 0.09	V
369	2018-05-24	0.058	8.64	−0.77 ± 0.09	V
370	2017-07-13	0.008	4.36	−1.15 ± 0.13	V
372	2016-08-11	0.008	5.18	−1.27 ± 0.08	V
372	2016-07-26	0.103	10.09	−1.62 ± 0.10	V
375	2018-05-20	0.870	16.86	−0.43 ± 0.09	V
375	2021-11-18	0.979	9.38	−1.22 ± 0.09	V
376	2020-02-18	0.024	2.58	−0.39 ± 0.09	V
376	2021-08-13	0.095	18.43	−0.32 ± 0.09	V
377	2016-07-27	0.018	4.84	−1.24 ± 0.09	V
377	2016-08-05	0.052	4.08	−0.98 ± 0.10	V
377	2021-11-18	0.879	15.46	−1.29 ± 0.09	V
379	2021-01-06	0.783	17.34	−0.74 ± 0.08	V
380	2018-05-24	0.862	11.20	−2.01 ± 0.17	V
381	2016-06-02	0.989	6.54	−1.24 ± 0.09	V
381	2016-07-27	0.851	18.58	−0.12 ± 0.09	V
385	2016-07-28	0.103	14.13	−0.59 ± 0.09	V
385	2021-11-18	0.797	15.90	−0.17 ± 0.09	V
386	2016-12-05	0.178	19.10	−0.42 ± 0.12	V
386	2016-12-10	0.117	18.83	−0.39 ± 0.13	V
386	2018-05-23	0.901	11.05	−1.77 ± 0.10	V
386	2019-04-14	0.135	19.30	−0.42 ± 0.09	V
386	2019-05-30	0.064	15.84	−1.21 ± 0.08	V
386	2019-07-16	0.976	8.89	−1.54 ± 0.09	V
386	2019-07-22	0.936	9.40	−1.77 ± 0.10	V
386	2019-07-23	0.949	9.54	−1.75 ± 0.08	V
386	2019-07-30	0.907	10.72	−1.77 ± 0.08	V
386	2019-11-06	0.734	20.41	−0.23 ± 0.09	V
387	2016-12-01	0.197	17.89	−1.24 ± 0.09	V
387	2017-07-25	0.854	25.52	−0.62 ± 0.10	V
387	2017-07-30	0.861	25.31	−0.49 ± 0.12	V
387	2017-01-18	0.202	20.59	−1.11 ± 0.08	V
387	2017-07-03	0.866	25.56	−0.38 ± 0.13	V
387	2017-07-03	0.866	25.56	−0.32 ± 0.11	R
387	2017-07-19	0.852	25.68	−0.40 ± 0.16	V
387	2017-07-19	0.852	25.68	−0.32 ± 0.11	R
387	2016-04-13	0.858	17.80	−1.54 ± 0.10	V
387	2015-10-10	0.149	16.47	−1.37 ± 0.09	V
387	2015-12-09	0.161	12.97	−1.53 ± 0.09	V
387	2016-04-10	0.931	17.74	−1.43 ± 0.10	V
387	2017-08-02	0.825	25.16	−0.48 ± 0.13	V
387	2017-08-02	0.825	25.16	−0.63 ± 0.18	R

Table A.1. continued.

Asteroid Number	Date of observation	Fraction of day	Phase angle (deg)	P_r (%)	Filter
387	2017-08-05	0.832	24.98	−0.51 ± 0.08	V
387	2019-10-09	0.111	17.58	−1.39 ± 0.11	V
387	2019-12-26	0.031	4.96	−0.81 ± 0.09	V
387	2019-12-29	0.974	5.36	−0.95 ± 0.09	V
387	2020-04-07	0.811	16.15	−1.24 ± 0.12	V
387	2021-01-17	0.116	10.75	−1.30 ± 0.10	V
387	2021-04-08	0.850	16.61	−1.37 ± 0.09	V
387	2021-04-24	0.868	18.92	−1.11 ± 0.10	V
388	2016-08-03	0.065	14.29	−0.95 ± 0.10	V
389	2019-11-06	0.173	19.80	−0.11 ± 0.09	V
389	2019-12-29	0.028	1.62	−0.52 ± 0.08	V
391	2021-08-11	0.918	26.68	0.78 ± 0.08	V
391	2021-08-21	0.877	28.33	1.08 ± 0.09	V
391	2021-09-24	0.809	34.15	1.59 ± 0.13	V
392	2017-12-22	0.036	9.73	−1.72 ± 0.10	V
393	2018-05-06	0.968	6.34	−1.44 ± 0.09	V
393	2019-11-08	0.061	2.88	−0.81 ± 0.10	V
396	2019-04-13	0.953	8.12	−1.05 ± 0.57	V
396	2021-11-24	0.003	1.38	−0.37 ± 0.09	V
399	2021-11-29	0.998	5.85	−0.81 ± 0.09	V
402	2015-10-10	0.775	17.35	−1.74 ± 0.10	V
402	2015-12-10	0.717	19.36	−1.50 ± 0.13	V
402	2016-12-01	0.921	6.78	−1.06 ± 0.09	V
402	2016-12-27	0.923	14.07	−1.71 ± 0.09	V
402	2016-12-28	0.949	14.42	−1.80 ± 0.09	V
402	2017-01-03	0.911	16.35	−1.79 ± 0.09	V
402	2017-01-06	0.960	17.28	−1.99 ± 0.12	V
402	2017-01-16	0.839	19.90	−1.58 ± 0.09	V
402	2015-10-14	0.807	18.05	−1.70 ± 0.10	V
402	2016-12-07	0.020	7.45	−1.16 ± 0.09	V
402	2017-01-17	0.902	20.15	−1.39 ± 0.10	V
402	2016-12-09	0.051	8.17	−1.46 ± 0.10	V
402	2016-12-12	0.952	8.99	−1.34 ± 0.12	V
402	2017-01-24	0.825	21.58	−1.41 ± 0.10	V
402	2018-05-06	0.012	9.99	−1.35 ± 0.09	V
403	2019-10-02	0.967	4.53	−0.64 ± 0.09	V
403	2019-11-06	0.831	14.33	−0.58 ± 0.15	V
404	2020-02-21	0.186	26.57	1.96 ± 0.09	V
404	2020-04-06	0.029	16.17	−1.22 ± 0.08	V
404	2020-05-25	0.967	15.38	−1.07 ± 0.08	V
405	2021-11-30	0.940	5.88	−1.39 ± 0.09	V
407	2019-11-06	0.218	21.67	0.26 ± 0.17	V
409	2019-10-07	0.157	17.81	−0.55 ± 0.10	V
409	2019-11-08	0.091	7.87	−1.75 ± 0.09	V
409	2019-12-29	0.907	13.23	−1.37 ± 0.08	V
409	2020-02-23	0.818	21.14	0.42 ± 0.09	V
409	2021-02-10	0.083	13.96	−1.22 ± 0.08	V
409	2021-05-04	0.907	21.17	0.37 ± 0.16	V
410	2017-12-22	0.130	13.81	−1.59 ± 0.12	V
410	2019-04-12	0.126	25.09	1.36 ± 0.09	V
410	2021-11-20	0.025	13.44	−1.52 ± 0.09	V
412	2021-04-22	0.998	7.94	−1.29 ± 0.09	V
417	2018-05-24	0.033	3.11	−0.85 ± 0.13	V
418	2017-07-06	0.067	19.71	−0.14 ± 0.10	V
418	2017-08-01	0.061	11.53	−1.04 ± 0.14	V
418	2021-08-16	0.949	9.60	−1.25 ± 0.08	V
419	2017-07-26	0.994	8.38	−1.10 ± 0.10	V
419	2017-08-12	0.021	4.40	−0.99 ± 0.09	V
419	2017-07-21	0.029	10.88	−0.98 ± 0.09	V

Table A.1. continued.

Asteroid Number	Date of observation	Fraction of day	Phase angle (deg)	P_r (%)	Filter
419	2017-07-03	0.048	19.27	0.72 ± 0.14	V
419	2017-07-13	0.036	14.83	−0.48 ± 0.14	V
419	2017-07-22	0.074	10.35	−0.99 ± 0.09	V
419	2019-12-30	0.104	11.79	−0.83 ± 0.09	V
419	2020-03-03	0.004	11.99	−0.79 ± 0.09	V
419	2020-04-08	0.880	19.48	1.03 ± 0.11	V
420	2016-07-29	0.046	10.96	−0.94 ± 0.13	V
420	2019-02-07	0.959	6.93	−0.84 ± 0.09	V
422	2019-08-09	0.092	25.71	0.16 ± 0.10	V
423	2019-08-10	0.146	15.36	−0.84 ± 0.10	V
423	2019-10-05	0.987	5.98	−1.24 ± 0.09	V
423	2019-12-26	0.804	18.44	−0.38 ± 0.09	V
423	2021-01-14	0.888	11.69	−1.11 ± 0.09	V
425	2020-02-19	0.980	3.79	−0.71 ± 0.09	V
426	2015-07-17	0.011	17.27	−0.47 ± 0.09	V
426	2015-07-18	0.019	17.20	−0.63 ± 0.13	V
426	2016-12-05	0.958	8.05	−1.01 ± 0.09	V
426	2016-12-10	0.847	7.89	−1.17 ± 0.11	V
426	2016-12-11	0.973	7.92	−1.14 ± 0.09	V
429	2019-11-08	0.981	5.10	−0.96 ± 0.13	V
431	2020-01-01	0.927	6.84	−1.60 ± 0.09	V
432	2021-11-18	0.995	9.64	−0.70 ± 0.09	V
433	2016-08-11	0.979	9.53	−0.74 ± 0.09	V
433	2016-08-16	0.003	7.11	−0.64 ± 0.09	V
433	2016-12-02	0.778	40.99	1.92 ± 0.09	V
433	2016-07-26	0.053	19.04	−0.33 ± 0.10	V
433	2016-07-28	0.051	17.92	−0.50 ± 0.09	V
433	2019-01-28	0.879	42.63	2.09 ± 0.08	V
433	2019-02-05	0.847	45.46	2.31 ± 0.08	V
433	2019-02-09	0.810	46.68	2.45 ± 0.08	V
433	2019-04-08	0.855	50.38	2.90 ± 0.10	V
434	2017-08-04	0.012	26.21	0.32 ± 0.14	V
434	2017-07-28	0.871	25.12	0.31 ± 0.10	V
434	2017-07-30	0.940	25.42	0.12 ± 0.18	V
434	2017-08-14	0.917	27.89	0.23 ± 0.09	V
434	2017-07-22	0.918	24.38	0.20 ± 0.10	V
434	2017-08-11	0.876	27.36	0.28 ± 0.11	V
434	2017-08-05	0.885	26.35	−0.22 ± 0.28	V
434	2019-02-06	0.016	12.83	−0.18 ± 0.09	V
434	2019-02-09	0.969	12.99	−0.11 ± 0.11	V
435	2021-11-30	0.964	8.17	−1.23 ± 0.08	V
437	2016-07-18	0.100	19.04	−0.09 ± 0.08	V
437	2016-07-26	0.976	15.11	−0.20 ± 0.09	V
437	2016-08-16	0.016	8.24	−0.04 ± 0.10	V
439	2018-05-23	0.010	5.39	−0.90 ± 0.20	V
441	2019-08-05	0.973	4.08	−0.83 ± 0.09	V
443	2019-08-09	0.055	18.34	−0.73 ± 0.09	V
443	2019-10-09	0.916	10.98	−0.92 ± 0.08	V
444	2015-07-17	0.876	17.42	−0.63 ± 0.09	V
444	2015-05-21	0.017	6.55	−1.11 ± 0.08	V
444	2015-07-13	0.921	15.80	−0.65 ± 0.09	V
444	2016-08-02	0.102	26.02	1.49 ± 0.09	V
444	2016-08-14	0.112	25.10	1.19 ± 0.09	V
444	2016-12-02	0.855	16.27	−0.81 ± 0.08	V
444	2016-12-09	0.845	18.23	−0.55 ± 0.08	V
444	2016-12-11	0.916	18.71	−0.36 ± 0.10	V
444	2017-01-18	0.779	23.06	0.72 ± 0.08	V
444	2019-04-14	0.048	1.29	−0.24 ± 0.09	V
444	2021-11-18	0.069	12.01	−1.11 ± 0.08	V

Table A.1. continued.

Asteroid Number	Date of observation	Fraction of day	Phase angle (deg)	P_r (%)	Filter
446	2016-12-09	0.994	4.99	−0.56 ± 0.13	V
446	2021-12-01	0.160	15.01	−0.24 ± 0.09	V
451	2019-01-28	0.196	14.17	−1.19 ± 0.08	V
451	2019-02-06	0.133	12.22	−1.44 ± 0.08	V
451	2019-04-08	0.916	11.97	−1.34 ± 0.09	V
451	2019-06-10	0.915	11.48	−1.67 ± 0.09	V
451	2020-02-24	0.209	17.58	−0.68 ± 0.09	V
451	2020-04-06	0.107	14.19	−1.18 ± 0.09	V
451	2020-04-17	0.136	11.88	−1.68 ± 0.23	V
451	2020-05-08	0.009	6.21	−1.57 ± 0.13	V
451	2020-05-17	0.061	3.81	−1.18 ± 0.09	V
453	2021-11-23	0.966	2.93	−0.45 ± 0.09	V
455	2021-04-24	0.025	3.84	−0.91 ± 0.10	V
456	2017-07-05	0.061	20.20	−0.03 ± 0.11	V
456	2017-08-12	0.059	11.83	−0.35 ± 0.12	V
456	2017-08-13	0.980	11.57	−0.54 ± 0.14	V
456	2020-02-25	0.831	13.21	−0.58 ± 0.15	V
456	2021-07-28	0.860	19.99	0.12 ± 0.09	V
458	2016-04-10	0.982	16.15	−1.85 ± 0.11	V
458	2018-05-24	0.078	8.22	−1.89 ± 0.23	V
458	2019-08-10	0.072	12.30	−2.07 ± 0.08	V
458	2021-01-06	0.091	11.34	−1.84 ± 0.09	V
459	2020-01-06	0.895	18.81	−0.39 ± 0.11	V
460	2016-08-21	0.966	5.51	−1.45 ± 0.14	V
460	2016-08-06	0.999	3.68	−1.44 ± 0.10	V
460	2016-08-14	0.953	3.19	−1.20 ± 0.11	V
460	2018-01-12	0.104	10.38	−1.50 ± 0.33	V
460	2019-04-04	0.993	6.29	−1.38 ± 0.32	V
463	2019-10-10	0.114	23.13	−0.11 ± 0.18	V
466	2021-08-20	0.913	4.56	−0.81 ± 0.10	V
468	2021-11-23	0.821	20.82	−0.10 ± 0.12	V
470	2021-08-16	0.981	5.45	−0.66 ± 0.09	V
471	2016-12-05	0.197	20.16	0.10 ± 0.11	V
471	2016-12-21	0.023	18.62	−0.07 ± 0.10	V
471	2018-05-23	0.853	9.42	−0.48 ± 0.09	V
472	2021-01-11	0.052	6.22	−0.69 ± 0.08	V
474	2021-05-08	0.023	10.41	−1.71 ± 10.00	V
476	2020-02-24	0.939	9.90	−1.52 ± 0.09	V
477	2020-02-19	0.083	10.20	−0.64 ± 0.13	V
478	2015-07-18	0.909	7.80	−0.73 ± 0.13	V
478	2015-07-21	0.938	8.60	−0.74 ± 0.09	V
478	2015-09-29	0.810	17.82	−0.10 ± 0.13	V
478	2016-07-29	0.006	14.68	−0.62 ± 0.10	V
478	2020-05-06	0.122	11.65	−0.64 ± 0.13	V
478	2020-05-20	0.050	7.71	−0.89 ± 0.11	V
478	2021-08-21	0.938	5.98	−0.75 ± 0.10	V
479	2017-07-21	0.002	1.60	−0.40 ± 0.09	V
480	2020-01-07	0.923	9.80	−0.61 ± 0.08	V
480	2020-02-21	0.803	19.81	0.12 ± 0.10	V
481	2021-05-07	0.980	3.29	−0.76 ± 0.08	V
482	2017-08-04	0.879	20.91	0.14 ± 0.13	V
482	2017-07-06	0.908	16.27	−0.09 ± 0.10	V
484	2020-04-24	0.141	17.21	−0.18 ± 0.12	V
485	2017-07-07	0.925	7.03	−0.65 ± 0.12	V
485	2017-07-18	0.063	5.96	−0.62 ± 0.09	V
485	2020-04-07	0.942	14.36	−0.18 ± 0.09	V
485	2021-04-23	0.129	14.89	−0.39 ± 0.10	V
486	2021-04-12	0.093	17.94	−0.22 ± 0.09	V
487	2017-12-22	0.147	16.26	−0.46 ± 0.11	V

Table A.1. continued.

Asteroid Number	Date of observation	Fraction of day	Phase angle (deg)	P_r (%)	Filter
487	2019-04-12	0.112	10.12	−1.00 ± 0.09	V
487	2021-11-19	0.039	15.57	−0.34 ± 0.08	V
489	2018-05-06	0.989	6.42	−0.97 ± 0.09	V
489	2019-06-01	0.103	14.99	−0.85 ± 0.10	V
489	2019-08-02	0.903	6.18	−0.78 ± 0.09	V
490	2018-01-15	0.969	11.27	−0.69 ± 0.25	V
490	2019-04-08	0.019	5.40	−1.21 ± 0.10	V
490	2020-05-17	0.076	14.87	−1.62 ± 10.00	V
490	2021-11-18	0.841	14.76	−1.41 ± 0.09	V
491	2015-07-21	0.859	11.93	−0.89 ± 0.10	V
491	2016-08-10	0.081	9.29	−1.16 ± 0.12	V
491	2020-04-17	0.012	6.69	−1.14 ± 0.10	V
491	2021-08-20	0.858	13.44	−0.85 ± 0.12	V
497	2019-01-30	0.099	8.90	−1.03 ± 0.09	V
500	2015-07-17	0.978	7.91	−0.61 ± 0.09	V
502	2021-01-11	0.121	19.18	−0.10 ± 0.08	V
503	2020-02-18	0.013	5.59	−1.26 ± 0.08	V
505	2020-04-23	0.085	10.15	−1.07 ± 0.10	V
507	2019-12-30	0.988	3.37	−0.66 ± 0.08	V
508	2021-02-28	0.112	14.39	−1.50 ± 0.12	V
508	2021-05-04	0.933	7.20	−1.40 ± 0.09	V
509	2017-07-07	0.003	16.47	−0.31 ± 0.13	V
509	2017-07-26	0.029	12.35	−0.62 ± 0.10	V
509	2017-08-13	0.945	8.44	−0.76 ± 0.11	V
509	2021-05-05	0.988	2.34	−0.57 ± 0.10	V
510	2017-07-22	0.949	15.71	−1.11 ± 0.10	V
510	2017-07-03	0.918	9.18	−1.32 ± 0.14	V
510	2017-07-21	0.907	15.33	−1.22 ± 0.09	V
510	2017-07-26	0.932	17.15	−0.96 ± 0.09	V
510	2017-07-30	0.913	18.52	−0.83 ± 0.09	V
510	2017-08-12	0.864	22.37	0.13 ± 0.12	V
510	2021-05-03	0.014	7.02	−1.37 ± 0.11	V
511	2015-02-25	0.098	9.78	−1.68 ± 0.08	V
511	2020-01-01	0.029	6.14	−1.63 ± 0.08	V
511	2021-05-04	0.987	8.83	−1.64 ± 0.08	V
513	2019-12-27	0.906	10.98	−1.15 ± 0.09	V
513	2020-02-19	0.781	20.48	−0.47 ± 0.12	V
516	2020-02-18	0.132	6.01	−0.71 ± 0.09	V
516	2021-08-12	0.070	9.72	−0.73 ± 0.08	V
517	2021-11-19	0.069	15.83	−0.31 ± 0.09	V
532	2015-07-18	0.874	21.44	0.04 ± 0.11	V
532	2019-02-09	0.012	6.13	−0.68 ± 0.08	V
532	2019-05-30	0.844	25.37	0.60 ± 0.08	V
534	2019-10-08	0.108	16.11	−0.43 ± 0.09	V
534	2020-01-01	0.848	15.87	−0.56 ± 0.12	V
534	2020-01-01	0.848	15.87	−0.64 ± 0.11	V
535	2021-11-13	0.914	2.71	−0.80 ± 0.08	V
542	2021-05-03	0.882	12.56	−0.58 ± 0.15	V
547	2019-08-02	0.990	10.18	−1.36 ± 0.09	V
547	2019-08-06	0.940	9.69	−1.44 ± 0.09	V
547	2019-10-07	0.831	22.74	0.79 ± 0.12	V
550	2016-08-12	0.063	23.00	0.14 ± 0.12	V
554	2019-02-11	0.163	20.07	−0.35 ± 0.09	V
554	2021-11-19	0.998	22.26	0.58 ± 0.09	V
556	2019-07-30	0.046	5.78	−0.79 ± 0.09	V
556	2021-01-19	0.912	14.52	−0.76 ± 0.09	V
558	2020-04-17	0.100	9.28	−0.91 ± 0.17	V
558	2020-04-22	0.063	7.79	−1.08 ± 0.09	V
558	2020-05-05	0.015	4.56	−0.64 ± 0.13	V

Table A.1. continued.

Asteroid Number	Date of observation	Fraction of day	Phase angle (deg)	P_r (%)	Filter
564	2019-04-01	0.098	18.01	−2.00 ± 0.11	V
566	2019-11-08	0.967	9.06	−1.14 ± 0.11	V
567	2021-05-07	0.942	11.68	−1.10 ± 0.09	V
570	2021-12-01	0.096	12.06	−1.61 ± 0.08	V
576	2019-11-08	0.027	5.67	−0.95 ± 0.09	V
579	2021-01-06	0.835	15.08	−0.66 ± 0.09	V
582	2017-07-03	0.960	10.87	−0.38 ± 0.15	V
582	2020-02-22	0.078	1.39	−0.36 ± 0.09	V
582	2020-04-09	0.016	20.93	0.21 ± 0.08	V
582	2021-05-04	0.091	16.37	−0.38 ± 0.09	V
582	2021-08-26	0.834	18.23	−0.14 ± 0.22	V
583	2019-11-06	0.111	11.44	−1.43 ± 0.09	V
585	2020-04-11	0.036	9.24	−1.62 ± 0.09	V
585	2021-08-21	0.971	2.38	−0.11 ± 0.22	V
589	2018-03-23	0.176	16.90	−0.74 ± 0.32	V
589	2019-08-10	0.983	4.31	−0.98 ± 0.09	V
592	2019-08-09	0.115	15.31	−0.80 ± 0.10	V
593	2021-01-13	0.050	10.70	−1.26 ± 0.09	V
595	2020-03-04	0.037	5.37	−1.00 ± 0.09	V
595	2020-04-07	0.021	12.59	−0.71 ± 0.11	V
595	2020-05-05	0.951	16.76	−0.48 ± 0.14	V
597	2021-11-21	0.026	4.01	−0.57 ± 0.08	V
599	2016-04-10	0.025	10.09	−1.51 ± 0.13	V
599	2019-01-30	0.824	20.58	−1.35 ± 0.09	V
599	2019-02-04	0.777	20.88	−1.39 ± 0.09	V
599	2019-02-06	0.863	20.98	−1.25 ± 0.09	V
599	2019-04-08	0.819	16.89	−1.66 ± 0.12	V
599	2021-04-12	0.994	4.98	−0.83 ± 0.09	V
599	2021-04-24	0.944	8.25	−1.39 ± 0.14	V
606	2015-12-10	0.120	19.80	−1.13 ± 0.24	V
606	2015-12-11	0.108	19.60	−1.30 ± 0.14	V
606	2019-10-07	0.177	25.09	−0.25 ± 0.20	V
606	2019-12-30	0.084	8.79	−1.93 ± 0.08	V
606	2020-01-07	0.020	5.20	−1.15 ± 0.10	V
606	2020-02-22	0.960	14.97	−2.02 ± 0.22	V
606	2020-02-24	0.818	15.50	−1.70 ± 0.15	V
611	2015-12-11	0.027	19.28	−0.89 ± 0.10	V
611	2017-07-13	0.882	17.67	−1.20 ± 0.17	V
611	2017-07-26	0.867	18.05	−1.53 ± 0.19	V
611	2017-08-02	0.853	17.99	−2.81 ± 0.75	V
611	2019-08-08	0.095	16.87	−1.52 ± 0.09	V
611	2019-10-02	0.048	1.32	−0.47 ± 0.09	V
611	2019-10-03	0.003	1.70	−0.43 ± 0.09	V
611	2019-10-09	0.982	4.17	−0.75 ± 0.09	V
618	2018-05-25	0.931	9.01	−1.36 ± 0.17	V
622	2021-05-04	0.011	4.32	−0.62 ± 0.14	V
625	2017-12-22	0.990	5.62	−0.48 ± 0.11	V
625	2020-04-08	0.129	14.9	−0.64 ± 0.12	V
625	2020-04-22	0.092	11.15	−0.95 ± 0.13	V
625	2020-05-25	0.039	9.30	−0.62 ± 0.12	V
625	2021-11-13	0.973	7.95	−0.48 ± 0.09	V
626	2021-08-22	0.095	31.01	4.45 ± 0.09	V
628	2020-04-09	0.166	20.16	0.60 ± 0.20	V
628	2020-05-06	0.080	13.39	−0.45 ± 0.10	V
628	2020-05-20	0.018	8.48	−0.62 ± 0.08	V
631	2021-09-23	0.089	13.86	−0.48 ± 0.10	V
634	2019-06-02	0.016	7.08	−1.59 ± 0.14	V
635	2019-08-02	0.028	4.20	−0.76 ± 0.09	V
635	2019-08-06	0.979	3.91	−0.78 ± 0.10	V

Table A.1. continued.

Asteroid Number	Date of observation	Fraction of day	Phase angle (deg)	P_r (%)	Filter
635	2019-08-08	0.009	3.96	−0.70 ± 0.09	V
638	2020-04-08	0.100	12.68	−1.15 ± 0.14	V
639	2017-07-29	0.001	2.47	−0.56 ± 0.10	V
639	2017-07-12	0.967	5.95	−1.07 ± 0.09	V
639	2020-03-04	0.993	10.66	−0.69 ± 0.10	V
639	2020-04-09	0.907	16.95	0.08 ± 0.15	V
642	2015-10-10	0.958	4.11	−0.95 ± 0.09	V
642	2016-12-07	0.051	6.55	−1.33 ± 0.12	V
642	2016-12-12	0.980	4.98	−1.18 ± 0.12	V
642	2017-01-06	0.016	8.49	−1.57 ± 0.14	V
642	2017-01-03	0.949	7.50	−1.56 ± 0.12	V
642	2016-12-01	0.030	8.42	−1.73 ± 0.11	V
642	2018-03-24	0.039	1.54	−0.30 ± 0.10	V
653	2020-04-23	0.122	14.58	−0.97 ± 0.09	V
653	2020-05-05	0.059	11.57	−0.68 ± 0.14	V
653	2020-05-21	0.009	7.10	−1.04 ± 0.10	V
654	2021-08-20	0.968	8.92	−1.50 ± 0.10	V
654	2021-09-23	0.833	13.4	−1.41 ± 0.09	V
654	2021-11-20	0.756	21.98	0.52 ± 0.09	V
656	2021-04-19	0.976	2.33	−0.60 ± 0.10	V
660	2018-03-22	0.164	24.37	0.42 ± 0.09	V
660	2019-10-09	0.026	7.79	−0.67 ± 0.09	V
660	2021-01-11	0.028	6.57	−0.59 ± 0.08	V
661	2021-11-30	0.885	9.99	−0.96 ± 0.14	V
663	2021-08-17	0.932	9.12	−0.87 ± 0.10	V
664	2021-05-08	0.959	5.09	−0.59 ± 0.08	V
667	2020-04-09	0.108	8.12	−1.31 ± 0.11	V
670	2021-11-19	0.917	12.28	−0.62 ± 0.10	V
673	2017-08-13	0.098	20.74	−1.55 ± 0.23	V
673	2017-08-10	0.078	20.91	−1.38 ± 0.23	V
673	2021-08-17	0.975	1.70	−0.34 ± 0.09	V
674	2020-05-06	0.952	19.79	0.02 ± 0.09	V
675	2019-10-07	0.120	17.12	−0.31 ± 0.08	V
675	2020-02-20	0.792	26.01	0.45 ± 0.08	V
675	2021-05-03	0.850	15.46	−0.42 ± 0.08	V
677	2019-11-04	0.022	3.61	−0.40 ± 0.10	V
678	2019-11-06	0.006	6.99	−0.80 ± 0.09	V
678	2019-12-26	0.866	25.44	0.47 ± 0.08	V
679	2015-07-13	0.963	3.72	−0.59 ± 0.09	V
679	2016-12-01	0.171	22.27	−0.89 ± 0.09	V
679	2016-12-27	0.167	14.94	−1.62 ± 0.10	V
679	2016-12-21	0.114	17.01	−1.49 ± 0.10	V
679	2016-12-28	0.199	14.57	−1.66 ± 0.09	V
679	2016-12-09	0.151	20.39	−1.27 ± 0.10	V
679	2017-01-16	0.997	7.26	−1.16 ± 0.08	V
679	2017-01-18	0.063	6.52	−1.25 ± 0.10	V
679	2019-04-08	0.160	19.92	−1.16 ± 0.18	V
679	2019-05-29	0.046	11.16	−1.83 ± 0.09	V
679	2019-06-15	0.993	6.70	−1.09 ± 0.17	V
679	2019-07-19	0.903	13.81	−1.49 ± 0.13	V
679	2019-07-23	0.903	15.19	−1.67 ± 0.13	V
679	2019-08-08	0.872	19.96	−1.21 ± 0.09	V
679	2021-01-06	0.998	3.45	−0.55 ± 0.09	V
679	2021-01-17	0.020	2.63	−0.30 ± 0.09	V
683	2019-07-31	0.940	6.29	−1.06 ± 0.09	V
690	2015-07-24	0.051	21.70	0.56 ± 0.13	V
690	2021-08-27	0.126	22.42	0.89 ± 0.08	V
690	2021-11-14	0.004	3.40	−0.87 ± 0.08	V
691	2021-05-03	0.920	11.75	−1.44 ± 0.12	V

Table A.1. continued.

Asteroid Number	Date of observation	Fraction of day	Phase angle (deg)	P_r (%)	Filter
692	2021-04-08	0.993	8.55	−0.50 ± 0.20	V
702	2019-07-29	0.100	16.75	−0.76 ± 0.09	V
702	2019-11-08	0.837	14.85	−1.17 ± 0.09	V
704	2017-07-07	0.068	22.62	2.25 ± 0.11	V
704	2017-07-25	0.044	21.57	1.88 ± 0.09	V
704	2017-08-01	0.037	20.80	1.54 ± 0.13	V
704	2017-07-22	0.084	21.84	2.05 ± 0.10	V
704	2017-12-22	0.765	22.14	2.08 ± 0.10	V
707	2019-10-07	0.909	12.93	−0.36 ± 0.09	V
712	2021-11-16	0.749	25.87	1.59 ± 0.08	V
713	2019-06-12	0.015	7.30	−1.05 ± 10.00	V
714	2017-07-10	0.003	15.80	−0.21 ± 0.09	V
714	2017-07-30	0.044	10.73	−0.48 ± 0.11	V
714	2017-08-03	0.036	9.86	−0.67 ± 0.08	V
714	2021-08-11	0.991	8.48	−0.83 ± 0.10	V
720	2019-10-10	0.005	0.43	−0.08 ± 0.08	V
720	2021-02-23	0.879	16.01	0.29 ± 0.44	V
727	2016-06-07	0.948	10.39	−0.92 ± 0.11	V
727	2020-04-14	0.064	12.02	−0.96 ± 0.10	V
727	2020-04-23	0.060	9.92	−0.98 ± 0.08	V
727	2020-05-20	0.980	9.07	−0.68 ± 0.09	V
727	2020-05-25	0.998	10.09	−1.01 ± 0.11	V
729	2015-12-11	0.759	18.10	−1.33 ± 0.10	V
729	2016-12-01	0.077	13.86	−1.20 ± 0.10	V
729	2016-12-08	0.115	9.86	−1.18 ± 0.15	V
729	2016-12-12	0.053	8.56	−0.84 ± 0.13	V
729	2016-12-05	0.071	10.82	−1.24 ± 0.10	V
729	2016-12-06	0.047	10.50	−1.17 ± 0.10	V
729	2016-12-13	0.081	8.22	−1.06 ± 0.09	V
729	2016-12-27	0.984	4.35	−0.64 ± 0.09	V
729	2017-01-16	0.895	7.99	−1.11 ± 0.09	V
729	2016-12-10	0.044	9.21	−0.88 ± 0.15	V
729	2016-12-23	0.981	5.17	−0.89 ± 0.09	V
729	2016-12-28	0.069	4.21	−0.70 ± 0.09	V
729	2016-12-04	0.056	11.14	−1.04 ± 0.16	V
729	2016-12-07	0.090	10.18	−1.18 ± 0.10	V
729	2017-12-19	0.200	21.33	−0.67 ± 0.12	V
729	2017-01-03	0.053	4.37	−0.66 ± 0.09	V
729	2017-01-06	0.054	4.96	−0.80 ± 0.13	V
729	2017-01-18	0.030	8.72	−1.10 ± 0.10	V
729	2018-03-08	0.046	18.60	−1.10 ± 0.10	V
729	2018-03-22	0.122	15.61	−1.19 ± 0.09	V
729	2018-05-06	0.052	13.22	−1.17 ± 0.09	V
729	2018-05-23	0.918	16.89	−1.17 ± 0.09	V
729	2018-05-25	0.867	17.33	−1.18 ± 0.14	V
729	2021-12-01	0.201	20.51	−0.91 ± 0.11	V
732	2020-04-26	0.046	10.21	−0.73 ± 1.06	V
739	2018-05-23	0.043	14.13	−1.01 ± 0.09	V
740	2020-04-10	0.046	7.54	−1.09 ± 0.09	V
741	2021-04-08	0.966	6.83	−1.16 ± 0.13	V
747	2018-03-21	0.152	11.80	−1.25 ± 0.09	V
747	2019-06-08	0.011	6.74	−1.22 ± 0.10	V
747	2019-07-19	0.925	8.99	−0.90 ± 0.10	V
747	2019-07-24	0.896	10.24	−1.31 ± 0.13	V
747	2021-01-06	0.815	29.21	2.50 ± 0.08	V
751	2017-12-22	0.158	14.80	−1.38 ± 0.10	V
751	2021-11-30	0.152	19.34	−0.41 ± 0.09	V
752	2021-04-19	0.937	11.03	−1.34 ± 0.10	V
753	2015-12-11	0.183	23.96	−0.12 ± 0.13	V

Table A.1. continued.

Asteroid Number	Date of observation	Fraction of day	Phase angle (deg)	P_r (%)	Filter
753	2017-07-28	0.122	24.68	−0.18 ± 0.31	V
753	2017-07-30	0.110	24.68	−0.06 ± 0.17	V
753	2017-08-02	0.123	24.65	0.32 ± 0.14	V
753	2017-08-12	0.107	24.29	0.05 ± 0.20	V
753	2019-01-30	0.152	6.11	−0.61 ± 0.11	V
753	2019-02-04	0.972	7.50	−0.91 ± 0.12	V
753	2019-04-08	0.880	23.09	−0.02 ± 0.12	V
754	2019-08-02	0.942	10.20	−1.37 ± 0.09	V
754	2021-11-30	0.107	16.61	−0.90 ± 0.12	V
755	2021-05-04	0.963	7.44	−1.05 ± 0.09	V
758	2020-04-16	0.037	2.15	−0.77 ± 0.08	V
758	2020-05-17	0.916	9.43	−1.08 ± 0.09	V
760	2021-09-20	0.166	15.85	−0.26 ± 0.09	V
760	2021-11-30	0.986	6.48	−0.66 ± 0.09	V
762	2019-07-24	0.044	5.44	−1.21 ± 0.10	V
762	2019-07-29	0.035	3.89	−1.08 ± 0.09	V
770	2019-11-06	0.076	13.03	−0.49 ± 0.09	V
776	2020-03-04	0.063	8.06	−1.77 ± 0.08	V
776	2020-05-06	0.015	15.48	−1.20 ± 0.11	V
776	2021-04-12	0.124	11.48	−1.78 ± 0.09	V
779	2016-08-01	0.953	6.03	−0.64 ± 0.08	V
779	2016-07-26	0.047	5.05	−0.79 ± 0.09	V
779	2021-08-22	0.120	25.88	0.72 ± 0.10	V
780	2020-04-17	0.051	8.98	−1.71 ± 0.19	V
780	2020-05-04	0.991	7.85	−1.36 ± 0.14	V
780	2021-08-12	0.955	6.82	−1.31 ± 0.09	V
781	2020-04-25	0.057	8.60	−1.30 ± 0.14	V
783	2015-07-21	0.003	15.40	−1.40 ± 0.09	V
786	2020-02-19	0.803	15.65	−0.89 ± 0.17	V
786	2021-04-19	0.883	17.05	−0.28 ± 0.09	V
787	2016-08-22	0.107	10.31	−0.70 ± 0.10	V
787	2016-07-29	0.083	19.89	−0.07 ± 0.10	V
787	2021-11-21	0.108	16.12	−0.24 ± 0.10	V
790	2021-08-11	0.964	10.02	−1.06 ± 0.08	V
795	2019-11-06	0.892	13.19	−1.17 ± 0.15	V
796	2021-09-20	0.137	28.91	1.08 ± 0.09	V
796	2021-11-20	0.997	7.87	−0.97 ± 0.08	V
796	2021-11-27	0.910	10.54	−0.83 ± 0.10	V
797	2019-10-10	0.047	7.79	−0.67 ± 0.10	V
798	2017-07-21	0.942	5.84	−0.94 ± 0.09	V
798	2017-07-27	0.964	7.39	−0.98 ± 0.09	V
798	2017-08-11	0.924	11.69	−0.76 ± 0.11	V
798	2017-07-04	0.997	5.65	−0.73 ± 0.10	V
798	2017-07-25	0.919	6.83	−1.03 ± 0.11	V
798	2017-08-12	0.928	11.97	−1.05 ± 0.13	V
799	2021-05-03	0.043	8.87	−1.69 ± 0.09	V
803	2021-09-23	0.032	8.73	−0.83 ± 0.10	V
804	2020-04-08	0.978	13.49	−1.03 ± 0.10	V
808	2019-08-01	0.111	10.98	−0.79 ± 0.11	V
814	2020-04-24	0.113	9.58	−1.15 ± 0.14	V
818	2021-09-23	0.064	9.38	−1.61 ± 0.12	V
818	2021-11-19	0.872	14.85	−1.99 ± 0.16	V
824	2016-12-04	0.885	11.41	−2.15 ± 0.14	V
824	2016-12-13	0.947	13.76	−2.59 ± 0.23	V
824	2017-01-09	0.814	18.11	−1.71 ± 0.19	V
824	2017-01-18	0.825	18.71	−1.62 ± 0.15	V
824	2015-07-15	0.933	3.74	−0.92 ± 0.10	V
824	2015-07-13	0.053	3.35	−0.80 ± 0.10	V
824	2019-04-01	0.048	5.66	−1.58 ± 0.10	V

Table A.1. continued.

Asteroid Number	Date of observation	Fraction of day	Phase angle (deg)	P_r (%)	Filter
824	2021-11-18	0.041	6.53	−1.39 ± 0.11	V
838	2019-07-19	0.989	5.26	−1.25 ± 0.10	V
838	2019-08-01	0.986	7.87	−1.46 ± 0.21	V
844	2019-10-08	0.069	11.25	−1.29 ± 0.10	V
847	2017-07-30	0.020	4.91	−0.71 ± 0.11	V
847	2017-08-12	0.003	1.35	−0.61 ± 0.11	V
849	2015-07-18	0.891	13.04	−0.86 ± 0.11	V
849	2015-07-17	0.922	13.19	−0.71 ± 0.09	V
849	2020-05-05	0.992	3.76	−0.76 ± 0.09	V
856	2019-06-01	0.066	9.29	−1.06 ± 0.09	V
856	2019-06-08	0.976	9.04	−1.09 ± 0.09	V
857	2021-11-24	0.088	9.87	−0.52 ± 0.25	V
861	2019-06-10	0.954	5.93	−1.10 ± 0.10	V
861	2019-06-12	0.983	6.59	−1.13 ± 0.15	V
863	2016-07-29	0.860	14.92	−0.14 ± 0.11	V
863	2016-06-01	0.017	8.23	−0.34 ± 0.10	V
863	2016-06-09	0.014	7.15	−0.40 ± 0.09	V
863	2020-01-01	0.087	6.99	−0.48 ± 0.11	V
863	2020-01-07	0.058	4.90	−0.40 ± 0.09	V
863	2020-01-07	0.058	4.89	−0.39 ± 0.09	V
863	2020-02-23	0.991	11.73	−0.41 ± 0.11	V
895	2016-08-03	0.968	7.48	−1.11 ± 0.10	V
895	2016-08-18	0.988	9.49	−0.78 ± 0.17	V
895	2017-07-14	0.069	19.48	0.21 ± 0.10	V
900	2019-07-30	0.945	11.98	−1.15 ± 0.13	V
906	2017-12-22	0.966	4.80	−0.92 ± 0.13	V
907	2021-11-20	0.965	5.28	−0.92 ± 0.09	V
908	2015-12-08	0.833	22.01	−0.38 ± 0.09	V
908	2016-12-04	0.187	25.36	0.64 ± 0.10	V
908	2021-05-03	0.957	11.28	−1.09 ± 0.12	V
909	2020-02-19	0.129	10.85	−1.01 ± 0.09	V
909	2020-04-10	0.077	5.67	−0.87 ± 0.12	V
909	2021-04-19	0.107	11.10	−1.21 ± 0.10	V
913	2020-04-26	0.124	11.93	−0.62 ± 0.09	V
914	2019-06-10	0.985	12.57	−1.77 ± 0.08	V
914	2019-06-15	0.005	10.90	−1.90 ± 0.09	V
914	2019-07-22	0.922	18.65	−0.51 ± 0.10	V
914	2019-08-09	0.870	24.91	1.48 ± 0.09	V
914	2019-11-05	0.764	29.26	3.10 ± 0.09	V
924	2021-01-18	0.773	21.13	0.69 ± 0.10	V
928	2017-07-21	0.068	11.92	−1.70 ± 0.20	V
934	2021-12-05	0.004	10.74	−0.90 ± 0.10	V
950	2020-05-19	0.068	18.28	−0.39 ± 0.14	V
951	2021-08-16	0.918	12.89	−0.61 ± 0.11	V
957	2021-11-30	0.849	14.76	−0.72 ± 0.10	V
972	2017-12-22	0.886	17.08	−1.09 ± 0.13	V
976	2021-07-29	0.063	9.96	−1.91 ± 0.14	V
980	2017-08-10	0.123	14.55	−1.29 ± 0.14	V
980	2017-08-01	0.135	21.27	−0.99 ± 0.14	V
980	2016-07-04	0.996	3.02	−0.61 ± 0.09	V
980	2016-07-26	0.004	7.98	−1.03 ± 0.11	V
980	2016-08-10	0.915	14.54	−1.18 ± 0.13	V
980	2016-07-22	0.900	6.01	−0.77 ± 0.10	V
980	2017-12-21	0.922	3.22	−0.58 ± 0.11	V
980	2017-12-22	0.961	3.40	−0.61 ± 0.09	V
980	2016-08-05	0.921	12.48	−1.32 ± 0.10	V
980	2016-12-02	0.747	22.30	−0.78 ± 0.09	V
980	2021-08-26	0.999	19.47	−1.04 ± 0.08	V
980	2021-11-18	0.813	21.77	−0.81 ± 0.09	V

Table A.1. continued.

Asteroid Number	Date of observation	Fraction of day	Phase angle (deg)	P_r (%)	Filter
980	2021-12-02	0.791	23.92	−0.52 ± 0.08	V
984	2016-07-26	0.070	22.01	0.32 ± 0.10	V
984	2016-07-28	0.079	21.60	0.15 ± 0.10	V
984	2016-12-01	0.827	24.94	0.58 ± 0.09	V
984	2017-01-17	0.754	24.34	0.62 ± 0.10	V
984	2016-08-17	0.992	15.84	−0.15 ± 0.11	V
984	2016-07-16	0.090	23.75	−0.27 ± 0.10	V
984	2019-02-06	0.168	15.28	−0.17 ± 0.21	V
984	2019-04-13	0.981	4.80	−0.99 ± 0.15	V
984	2021-11-20	0.939	7.90	−0.47 ± 0.09	V
994	2021-08-18	0.140	17.65	−0.42 ± 0.09	V
1013	2021-05-04	0.882	24.30	0.65 ± 0.09	V
1021	2016-06-07	0.032	5.07	−0.98 ± 0.11	V
1021	2020-04-10	0.135	8.79	−0.78 ± 0.15	V
1021	2020-04-22	0.037	6.65	−1.36 ± 0.12	V
1021	2020-04-25	0.090	6.28	−1.02 ± 0.18	V
1021	2020-05-17	0.012	7.59	−1.07 ± 0.10	V
1031	2020-05-27	0.075	13.45	−1.59 ± 0.10	V
1036	2021-01-06	0.969	14.15	−0.27 ± 0.09	V
1040	2017-07-20	0.111	21.21	−1.06 ± 0.45	V
1040	2016-08-06	0.921	4.14	−0.12 ± 0.12	V
1040	2016-08-12	0.971	4.71	−0.39 ± 0.13	V
1040	2016-08-22	0.963	6.94	−1.04 ± 0.14	V
1040	2017-12-19	0.005	16.03	−1.21 ± 0.21	V
1040	2019-02-05	0.044	12.43	−1.02 ± 0.12	V
1040	2019-02-06	0.072	12.18	−0.97 ± 0.13	V
1040	2019-04-14	0.929	14.30	−1.01 ± 0.74	V
1048	2021-04-08	0.945	12.56	−1.62 ± 0.08	V
1055	2019-06-10	0.024	13.85	−0.57 ± 0.09	V
1059	2019-06-08	0.886	18.75	−0.38 ± 0.12	V
1070	2019-11-04	0.987	7.26	−1.49 ± 0.24	V
1098	2021-11-29	0.869	14.50	−0.81 ± 0.10	V
1146	2020-05-17	0.111	26.00	0.88 ± 0.12	V
1164	2021-02-28	0.077	1.67	−0.22 ± 0.17	V
1165	2019-06-04	0.027	9.17	−1.14 ± 0.10	V
1166	2019-04-12	0.147	24.37	0.33 ± 0.23	V
1166	2019-05-29	0.023	11.20	−1.04 ± 0.10	V
1166	2019-06-11	0.018	8.16	−0.70 ± 0.13	V
1166	2019-06-15	0.956	8.26	−0.63 ± 0.10	V
1189	2021-11-18	0.002	6.58	−1.06 ± 0.13	V
1222	2021-09-23	0.864	16.42	−0.52 ± 0.13	V
1246	2017-07-25	0.980	6.52	−0.71 ± 0.10	V
1246	2017-08-13	0.909	10.79	−0.72 ± 0.13	V
1246	2017-07-17	0.026	9.60	−0.93 ± 0.12	R
1248	2020-04-09	0.050	13.14	−0.51 ± 0.10	V
1263	2020-04-08	0.040	15.07	−0.78 ± 0.18	V
1284	2016-12-09	0.191	22.95	−0.53 ± 0.12	V
1284	2015-12-09	0.870	25.20	−0.19 ± 0.09	V
1284	2015-10-10	0.869	9.23	−1.93 ± 0.10	V
1284	2016-12-10	0.145	22.89	−0.55 ± 0.27	V
1294	2017-12-21	0.970	5.14	−1.17 ± 0.24	V
1303	2020-02-23	0.109	10.05	−0.65 ± 0.09	V
1303	2020-04-30	0.889	18.52	0.35 ± 0.16	V
1303	2020-05-06	0.984	19.20	0.83 ± 0.17	V
1322	2021-08-26	0.914	20.79	−0.07 ± 0.17	V
1330	2021-02-03	0.944	8.13	−1.52 ± 0.17	V
1332	2016-04-10	0.119	8.90	−2.10 ± 0.31	V
1332	2017-07-12	0.061	8.82	−1.69 ± 0.17	V
1353	2020-05-20	0.125	12.53	−0.79 ± 0.10	V

Table A.1. continued.

Asteroid Number	Date of observation	Fraction of day	Phase angle (deg)	P_r (%)	Filter
1372	2015-02-26	0.787	19.96	−0.91 ± 0.15	V
1406	2016-12-04	0.994	11.06	−0.44 ± 0.13	V
1406	2018-03-25	0.031	5.55	−1.11 ± 0.18	V
1434	2020-04-22	0.999	7.42	−0.62 ± 0.17	V
1469	2021-07-29	0.103	14.12	−1.01 ± 0.13	V
1504	2021-05-07	0.038	6.33	−0.39 ± 0.15	V
1531	2019-10-07	0.009	9.00	−0.81 ± 0.11	V
1620	2019-10-04	0.852	45.28	2.51 ± 0.20	V
1620	2019-10-08	0.789	44.62	1.95 ± 0.15	V
1627	2018-03-19	0.182	26.09	0.63 ± 0.34	V
1627	2018-05-25	0.977	29.37	0.82 ± 0.10	V
1627	2021-12-11	0.930	7.04	−0.83 ± 0.14	V
1627	2021-12-13	0.024	6.55	−0.76 ± 0.21	V
1627	2021-12-14	0.020	6.13	−0.67 ± 0.14	V
1627	2021-12-15	0.016	5.72	−0.67 ± 0.15	V
1627	2021-12-16	0.029	5.34	−0.59 ± 0.17	V
1627	2021-12-17	0.045	4.99	−0.64 ± 0.23	V
1627	2021-12-18	0.016	4.70	−0.62 ± 0.15	V
1627	2021-12-19	0.057	4.44	−0.80 ± 0.31	V
1627	2021-12-20	0.066	4.24	0.34 ± 0.67	V
1639	2021-07-30	0.102	18.71	−0.24 ± 0.13	V
1675	2021-02-03	0.896	18.02	−0.21 ± 0.13	V
1702	2015-05-22	0.974	7.39	−1.08 ± 0.66	V
1702	2016-08-02	0.022	12.08	−1.01 ± 0.13	V
1702	2016-08-22	0.037	5.75	−0.72 ± 0.10	V
1712	2020-05-25	0.091	10.12	−1.27 ± 0.19	V
1819	2020-04-14	0.103	16.63	−0.73 ± 0.14	V
1819	2020-05-06	0.049	13.41	−1.01 ± 0.18	V
1819	2020-05-27	0.005	12.98	−0.80 ± 0.10	V
1862	2021-12-03	0.775	61.71	4.42 ± 0.25	V
1862	2021-12-11	0.849	51.31	3.09 ± 0.28	V
1981	2018-03-08	0.938	38.10	1.82 ± 0.08	V
1981	2018-03-19	0.976	63.59	4.93 ± 0.09	V
1981	2018-03-21	0.787	75.89	6.00 ± 0.12	V
1981	2018-03-22	0.791	83.19	7.27 ± 0.09	V
2031	2019-11-05	0.892	22.71	0.20 ± 0.20	V
2050	2020-05-21	0.941	26.73	1.00 ± 0.12	V
2085	2017-07-04	0.075	12.28	−2.03 ± 0.18	V
2085	2017-07-12	0.019	9.51	−2.21 ± 0.73	V
2354	2015-12-11	0.927	3.54	−0.65 ± 0.11	V
2382	2019-11-06	0.039	7.15	−1.78 ± 0.14	V
2448	2016-12-21	0.180	17.35	−0.64 ± 0.14	V
2448	2016-12-04	0.116	20.27	0.06 ± 0.15	V
2448	2017-01-18	0.094	8.37	−1.69 ± 0.11	V
2448	2018-03-24	0.134	23.18	0.56 ± 0.29	V
2448	2018-05-17	0.117	15.26	−2.75 ± 10.00	V
2511	2018-03-23	0.945	7.55	−0.10 ± 0.21	V
2512	2019-11-06	0.148	17.68	−0.63 ± 0.29	V
2660	2021-08-26	0.876	15.75	−0.38 ± 0.15	V
2732	2016-12-06	0.101	8.86	−0.77 ± 0.34	V
2962	2020-04-23	0.033	4.91	−0.50 ± 0.09	V
3127	2019-11-05	0.960	10.91	−1.05 ± 0.19	V
3178	2021-02-28	0.036	9.15	−0.95 ± 0.11	V
3200	2017-12-20	0.756	109.39	39.69 ± 0.17	V
3200	2017-12-15	0.865	49.70	10.78 ± 0.08	R
3200	2017-12-19	0.825	101.81	38.54 ± 0.12	V
3200	2017-12-20	0.756	110.02	41.68 ± 0.15	V
3200	2017-12-17	0.845	78.82	27.95 ± 0.14	R
3200	2017-12-15	0.865	50.26	11.00 ± 0.08	R

Table A.1. continued.

Asteroid Number	Date of observation	Fraction of day	Phase angle (deg)	P_r (%)	Filter
3200	2017-12-14	0.755	36.85	5.45 ± 0.09	R
3200	2017-12-19	0.825	101.65	37.58 ± 0.11	R
3200	2017-12-20	0.756	109.85	40.99 ± 0.13	V
3200	2017-12-19	0.825	101.87	38.59 ± 0.13	V
3200	2017-12-19	0.825	101.90	38.67 ± 0.12	V
3200	2017-12-19	0.825	101.94	39.22 ± 0.13	V
3200	2017-12-15	0.865	48.66	10.78 ± 0.09	V
3200	2017-12-15	0.865	48.66	9.99 ± 9.99	R
3200	2017-12-20	0.756	109.29	39.58 ± 0.10	V
3200	2017-12-20	0.756	109.92	41.38 ± 0.14	V
3200	2017-12-17	0.845	77.21	27.17 ± 0.12	I
3200	2017-12-15	0.865	49.13	10.68 ± 0.09	R
3200	2017-12-15	0.865	49.77	11.03 ± 0.09	V
3200	2017-12-15	0.865	49.77	9.99 ± 9.99	R
3200	2017-12-15	0.865	50.32	11.34 ± 0.08	V
3200	2017-12-15	0.865	50.32	9.99 ± 9.99	R
3200	2017-12-17	0.845	77.72	25.04 ± 0.24	R
3200	2017-12-19	0.825	101.67	37.55 ± 0.28	R
3200	2017-12-20	0.756	109.33	38.73 ± 0.52	V
3200	2017-12-20	0.756	109.43	39.35 ± 0.12	V
3200	2017-12-17	0.845	78.27	25.53 ± 0.12	V
3200	2017-12-20	0.756	110.10	40.99 ± 0.19	V
3200	2017-12-20	0.756	109.36	39.14 ± 0.24	V
3200	2017-12-17	0.845	78.34	26.42 ± 0.13	R
3200	2017-12-15	0.865	49.49	10.14 ± 0.11	I
3200	2017-12-15	0.865	49.85	11.55 ± 0.08	B
3200	2017-12-15	0.865	49.85	9.99 ± 9.99	V
3200	2017-12-15	0.865	49.85	9.99 ± 9.99	R
3200	2017-12-14	0.755	37.53	5.08 ± 0.09	B
3200	2017-12-19	0.825	101.63	37.44 ± 0.17	R
3200	2017-12-15	0.865	48.91	10.19 ± 0.11	I
3200	2017-12-17	0.845	78.76	27.20 ± 0.13	V
3200	2017-12-14	0.755	36.92	5.71 ± 0.08	I
3200	2017-12-17	0.845	78.42	27.68 ± 0.12	I
3200	2017-12-19	0.825	101.78	38.40 ± 0.12	V
3200	2017-12-19	0.825	101.84	38.68 ± 0.12	V
3200	2017-12-17	0.845	78.57	27.25 ± 0.13	R
3200	2017-12-15	0.865	50.59	10.95 ± 0.09	I
3200	2017-12-15	0.865	50.87	11.89 ± 0.08	V
3200	2017-12-15	0.865	50.87	9.99 ± 9.99	R
3200	2017-12-15	0.865	49.19	10.89 ± 0.08	V
3200	2017-12-15	0.865	49.19	9.99 ± 9.99	R
3200	2017-12-15	0.865	48.73	11.27 ± 0.08	B
3200	2017-12-15	0.865	48.73	9.99 ± 9.99	V
3200	2017-12-15	0.865	48.73	9.99 ± 9.99	R
3200	2017-12-15	0.865	49.31	11.33 ± 0.08	B
3200	2017-12-15	0.865	49.31	9.99 ± 9.99	V
3200	2017-12-15	0.865	49.31	9.99 ± 9.99	R
3200	2017-12-17	0.845	77.04	25.94 ± 0.12	V
3200	2017-12-15	0.865	50.41	11.89 ± 0.09	B
3200	2017-12-15	0.865	50.41	9.99 ± 9.99	V
3200	2017-12-15	0.865	50.41	9.99 ± 9.99	R
3200	2017-12-21	0.737	116.21	41.91 ± 0.29	V
3200	2017-12-20	0.756	109.49	40.71 ± 0.15	V
3200	2017-12-15	0.865	48.59	10.50 ± 0.09	R
3200	2017-12-17	0.845	77.12	26.65 ± 0.14	R
3200	2017-12-19	0.825	101.57	36.22 ± 0.18	V
3200	2017-12-19	0.825	101.62	37.38 ± 0.19	R
3200	2017-12-15	0.865	50.96	12.40 ± 0.08	B

Table A.1. continued.

Asteroid Number	Date of observation	Fraction of day	Phase angle (deg)	P_r (%)	Filter
3200	2017-12-15	0.865	50.96	9.99 ± 9.99	V
3200	2017-12-15	0.865	50.96	9.99 ± 9.99	R
3200	2017-12-20	0.756	109.89	41.61 ± 0.32	V
3200	2017-12-20	0.756	109.46	40.12 ± 0.18	V
3200	2017-12-20	0.756	109.82	41.48 ± 0.14	V
3200	2017-12-14	0.755	36.79	5.27 ± 0.09	V
3200	2017-12-15	0.865	51.17	11.13 ± 0.09	I
3200	2017-12-17	0.845	77.63	25.56 ± 0.11	V
3200	2017-12-17	0.845	78.51	26.39 ± 0.12	V
3200	2017-12-17	0.845	77.42	24.55 ± 0.14	B
3200	2017-12-17	0.845	78.66	28.41 ± 0.11	I
3200	2017-12-20	0.756	109.54	41.24 ± 0.15	V
3200	2017-12-15	0.865	50.82	11.66 ± 0.08	R
3200	2017-12-20	0.756	110.05	41.39 ± 0.16	V
3200	2017-12-15	0.865	50.04	10.41 ± 0.09	I
3200	2017-12-17	0.845	78.03	24.15 ± 0.15	B
3200	2017-12-20	0.756	109.95	41.34 ± 0.18	V
3200	2017-12-20	0.756	109.98	41.11 ± 0.29	V
3200	2017-12-17	0.845	77.82	26.98 ± 0.12	I
3269	2016-12-05	0.003	12.48	−0.92 ± 0.34	V
3295	2019-11-06	0.961	11.50	−1.87 ± 0.14	V
3674	2021-08-18	0.099	32.83	1.33 ± 0.10	V
3674	2021-11-20	0.848	33.27	1.53 ± 0.09	V
3800	2018-05-12	0.021	22.00	1.24 ± 10.00	V
3800	2018-05-17	0.927	22.00	0.34 ± 0.19	V
4205	2021-07-30	0.023	20.09	0.07 ± 0.28	V
4905	2021-07-29	0.984	9.93	0.14 ± 0.18	V
5131	2019-01-28	0.952	20.14	0.91 ± 10.00	V
5131	2019-01-30	0.017	22.85	0.40 ± 0.13	V
5131	2019-02-06	0.958	31.68	1.02 ± 0.29	V
5131	2019-02-11	0.965	37.55	0.70 ± 0.26	V
5131	2019-02-12	0.925	38.61	1.62 ± 0.14	V
5817	2019-10-08	0.031	24.42	0.45 ± 0.11	V
6147	2019-10-08	0.941	8.43	−0.87 ± 0.36	V
6364	2019-10-07	0.046	8.91	−0.45 ± 0.11	V
6979	2019-10-10	0.952	4.03	−0.60 ± 0.14	V
7358	2021-12-12	0.007	15.05	−0.44 ± 0.12	V
7505	2017-12-20	0.852	28.64	0.99 ± 0.10	V
8256	2017-12-19	0.063	11.06	−0.29 ± 0.13	V
12008	2021-07-29	0.893	30.98	0.73 ± 0.10	V
18736	2019-02-05	0.909	17.86	−0.21 ± 0.09	V
18736	2019-02-11	0.053	22.41	0.01 ± 0.12	V
18736	2019-02-12	0.997	23.06	0.27 ± 0.13	V
24473	2019-04-12	0.001	1.71	−0.08 ± 0.13	V
25916	2018-05-17	0.014	19.48	−0.04 ± 0.13	V
35107	2020-02-18	0.069	7.90	−0.33 ± 0.29	V
35107	2020-02-19	0.015	8.68	0.01 ± 0.24	V
52800	2017-12-20	0.918	32.40	1.41 ± 0.22	V
162149	2021-12-18	0.076	6.14	−1.20 ± 0.16	V
326732	2021-07-29	0.025	27.89	3.26 ± 0.15	V
354030	2019-10-04	0.092	28.55	4.38 ± 0.12	V
354030	2019-10-07	0.083	30.36	5.06 ± 0.24	V
418849	2017-12-20	0.051	37.37	1.29 ± 0.32	V

Appendix B: Unpublished CASLEO data used in this paper

Table B.1. List of unpublished polarimetric measurements of asteroids obtained using the 2.15m telescope of the El Leoncito observatory (San Juan, Argentina) between 1995 and 2004, plus a small number of measurements obtained in another observing run in 2013. The Table lists for each object its identification number, the epoch of observation (expressed as year, month, day and fraction of day), the phase angle, the measured P_r, its error, and the adopted filter (in all cases chosen among the standard Johnson-Cousin *UBVRI* filters).

Asteroid Number	Date of observation	Fraction of day	Phase angle (deg)	P_r (%)	Filter
000001	1997-07-09	0.367	16.75	-0.388 ± 0.055	U
000001	1997-07-09	0.367	16.75	-0.369 ± 0.028	B
000001	1997-07-09	0.367	16.75	-0.306 ± 0.025	V
000001	1997-07-09	0.367	16.75	-0.300 ± 0.017	R
000001	1997-07-09	0.367	16.75	-0.241 ± 0.033	I
000001	2002-10-07	0.191	5.15	-1.803 ± 0.174	U
000001	2002-10-07	0.191	5.15	-1.667 ± 0.079	B
000001	2002-10-07	0.191	5.15	-1.487 ± 0.025	V
000001	2002-10-07	0.191	5.15	-1.506 ± 0.027	R
000001	2002-10-07	0.191	5.15	-1.431 ± 0.055	I
000002	2003-08-25	0.331	17.60	-0.270 ± 0.094	U
000002	2003-08-25	0.331	17.60	-0.216 ± 0.042	B
000002	2003-08-25	0.331	17.60	-0.249 ± 0.039	V
000002	2003-08-25	0.331	17.60	-0.206 ± 0.036	R
000002	2003-08-25	0.331	17.60	-0.088 ± 0.039	I
000002	2003-08-24	0.332	17.77	-0.354 ± 0.123	U
000002	2003-08-24	0.332	17.77	-0.162 ± 0.044	B
000002	2003-08-24	0.332	17.77	-0.164 ± 0.039	V
000002	2003-08-24	0.332	17.77	-0.182 ± 0.045	R
000002	2003-08-24	0.332	17.77	-0.120 ± 0.083	I
000002	2003-08-23	0.340	17.93	-0.280 ± 0.201	U
000002	2003-08-23	0.340	17.93	-0.058 ± 0.040	B
000002	2003-08-23	0.340	17.93	-0.086 ± 0.024	V
000002	2003-08-23	0.340	17.93	-0.129 ± 0.033	R
000002	2003-08-23	0.340	17.93	-0.079 ± 0.108	I
000002	2003-08-22	0.364	18.09	0.209 ± 0.184	U
000002	2003-08-22	0.364	18.09	-0.138 ± 0.071	B
000002	2003-08-22	0.364	18.09	-0.042 ± 0.073	V
000002	2003-08-22	0.364	18.09	-0.126 ± 0.032	R
000002	1995-02-03	0.042	25.90	0.975 ± 0.140	U
000002	1995-02-03	0.042	25.90	1.674 ± 0.121	B
000002	1995-02-03	0.042	25.90	1.605 ± 0.102	V
000002	1995-02-03	0.042	25.90	1.652 ± 0.098	R
000002	1995-02-03	0.042	25.90	1.632 ± 0.149	I
000002	1995-02-04	0.043	25.93	1.472 ± 0.089	B
000002	1995-02-04	0.043	25.93	1.563 ± 0.138	V
000002	1995-02-04	0.043	25.93	1.652 ± 0.063	R
000002	1995-02-04	0.043	25.93	1.715 ± 0.140	I
000002	1995-02-05	0.044	25.95	1.131 ± 0.134	U
000002	1995-02-05	0.044	25.95	1.512 ± 0.078	B
000002	1995-02-05	0.044	25.95	1.535 ± 0.053	V
000002	1995-02-05	0.044	25.95	1.714 ± 0.042	R
000002	1995-02-05	0.044	25.95	1.562 ± 0.091	I
000002	1995-02-06	0.038	25.96	1.139 ± 0.079	U
000002	1995-02-06	0.038	25.96	1.710 ± 0.106	B
000002	1995-02-06	0.038	25.96	1.618 ± 0.138	V
000002	1995-02-06	0.038	25.96	1.713 ± 0.042	R
000002	1995-02-06	0.038	25.96	1.629 ± 0.094	I
000003	1999-07-15	0.039	14.92	-0.385 ± 0.138	U
000003	1999-07-15	0.039	14.92	-0.724 ± 0.198	B

Table B.1. continued.

Asteroid Number	Date of observation	Fraction of day	Phase angle (deg)	P_r (%)	Filter
000003	1999-07-15	0.039	14.92	−0.987 ± 0.062	V
000003	1999-07-15	0.039	14.92	−1.119 ± 0.362	R
000003	1999-07-16	0.060	15.07	−0.325 ± 0.049	V
000003	1999-07-16	0.060	15.07	−0.350 ± 0.107	R
000003	1999-07-16	0.060	15.07	−0.509 ± 0.042	I
000003	2013-07-28	0.220	5.80	−0.673 ± 0.050	V
000004	1996-03-17	0.250	22.32	0.072 ± 0.140	U
000004	1996-03-17	0.250	22.32	0.031 ± 0.128	B
000004	1996-03-17	0.250	22.32	0.017 ± 0.030	V
000004	1996-03-17	0.250	22.32	0.004 ± 0.042	R
000004	1996-03-17	0.250	22.32	−0.105 ± 0.073	I
000004	1996-03-15	0.344	22.74	0.435 ± 0.121	U
000004	1996-03-15	0.344	22.74	0.171 ± 0.152	B
000004	1996-03-15	0.344	22.74	0.024 ± 0.035	V
000004	1996-03-15	0.344	22.74	0.082 ± 0.018	R
000004	1996-03-15	0.344	22.74	−0.048 ± 0.066	I
000005	2002-10-09	0.285	13.33	−0.337 ± 0.072	U
000005	2002-10-09	0.285	13.33	−0.434 ± 0.065	B
000005	2002-10-09	0.285	13.33	−0.590 ± 0.035	V
000005	2002-10-09	0.285	13.33	−0.597 ± 0.031	R
000005	2002-10-09	0.285	13.33	−0.802 ± 0.072	I
000005	2004-07-01	0.002	22.02	0.471 ± 0.114	U
000005	2004-07-01	0.002	22.02	0.376 ± 0.085	B
000005	2004-07-01	0.002	22.02	0.116 ± 0.078	V
000005	2004-07-01	0.002	22.02	0.127 ± 0.071	R
000005	2004-07-01	0.002	22.02	−0.081 ± 0.082	I
000005	2004-06-30	0.005	22.12	0.027 ± 0.174	U
000005	2004-06-30	0.005	22.12	0.294 ± 0.157	B
000005	2004-06-30	0.005	22.12	0.363 ± 0.258	V
000005	2004-06-30	0.005	22.12	0.392 ± 0.247	R
000005	2004-06-30	0.005	22.12	0.645 ± 0.248	I
000005	2004-07-03	0.963	22.43	0.541 ± 0.220	U
000005	2004-07-03	0.963	22.43	0.389 ± 0.107	B
000005	2004-07-03	0.963	22.43	0.050 ± 0.037	V
000005	2004-07-03	0.963	22.43	0.252 ± 0.079	R
000005	2004-07-03	0.963	22.43	0.135 ± 0.124	I
000006	1999-12-14	0.181	11.12	−0.462 ± 0.061	U
000006	1999-12-14	0.181	11.12	−0.769 ± 0.099	B
000006	1999-12-14	0.181	11.12	−0.784 ± 0.023	V
000006	1999-12-14	0.181	11.12	−0.912 ± 0.035	R
000006	1999-12-14	0.181	11.12	−0.742 ± 0.023	I
000006	1995-11-29	0.081	23.08	0.513 ± 0.129	B
000006	1995-11-29	0.081	23.08	0.092 ± 0.039	V
000006	1995-11-29	0.081	23.08	0.081 ± 0.047	R
000006	1995-11-29	0.081	23.08	−0.162 ± 0.093	I
000006	1995-11-30	0.078	23.33	0.515 ± 0.223	U
000006	1995-11-30	0.078	23.33	0.253 ± 0.115	B
000006	1995-11-30	0.078	23.33	0.166 ± 0.064	V
000006	1995-11-30	0.078	23.33	0.095 ± 0.061	R
000006	1995-11-30	0.078	23.33	−0.015 ± 0.036	I
000006	1995-12-01	0.075	23.56	−0.095 ± 9.999	V
000006	2002-10-09	0.035	27.15	0.859 ± 0.247	U
000006	2002-10-09	0.035	27.15	0.630 ± 0.115	B
000006	2002-10-09	0.035	27.15	0.546 ± 0.060	V
000006	2002-10-09	0.035	27.15	0.572 ± 0.036	R
000006	2002-10-09	0.035	27.15	0.551 ± 0.067	I
000008	2013-07-27	0.199	4.00	−0.509 ± 0.040	V
000009	1995-03-26	0.160	8.18	−0.814 ± 0.074	U
000009	1995-03-26	0.160	8.18	−0.704 ± 0.037	B

Table B.1. continued.

Asteroid Number	Date of observation	Fraction of day	Phase angle (deg)	P_r (%)	Filter
000009	1995-03-26	0.160	8.18	−0.687 ± 0.054	V
000009	1995-03-26	0.160	8.18	−0.944 ± 0.032	I
000009	1995-03-28	0.153	9.00	−0.734 ± 0.083	U
000009	1995-03-28	0.153	9.00	−0.804 ± 0.022	B
000009	1995-03-28	0.153	9.00	−0.671 ± 0.044	V
000009	1995-03-28	0.153	9.00	−0.866 ± 0.031	R
000009	1995-03-28	0.153	9.00	−1.087 ± 0.074	I
000009	1995-02-05	0.321	16.51	−0.333 ± 0.200	U
000009	1995-02-05	0.321	16.51	−0.486 ± 0.015	B
000009	1995-02-05	0.321	16.51	−0.404 ± 0.031	V
000009	1995-02-05	0.321	16.51	−0.617 ± 0.053	R
000009	1995-02-05	0.321	16.51	−0.749 ± 0.091	I
000009	1995-02-02	0.329	17.55	−0.097 ± 0.123	U
000009	1995-02-02	0.329	17.55	−0.339 ± 0.070	B
000009	1995-02-02	0.329	17.55	−0.387 ± 0.068	V
000009	1995-02-02	0.329	17.55	−0.482 ± 0.021	R
000009	1995-02-02	0.329	17.55	−0.611 ± 0.050	I
000009	2003-03-10	0.363	21.60	0.406 ± 0.196	U
000009	2003-03-10	0.363	21.60	0.214 ± 0.095	B
000009	2003-03-10	0.363	21.60	−0.213 ± 0.048	V
000009	2003-03-10	0.363	21.60	−0.181 ± 0.038	R
000009	2003-03-10	0.363	21.60	−0.278 ± 0.031	I
000009	2004-06-27	0.412	24.29	1.087 ± 0.122	U
000009	2004-06-27	0.412	24.29	0.409 ± 0.088	B
000009	2004-06-27	0.412	24.29	−0.024 ± 0.071	V
000009	2004-06-27	0.412	24.29	−0.015 ± 0.052	R
000009	2004-06-27	0.412	24.29	−0.121 ± 0.081	I
000010	1996-11-15	0.066	10.91	−1.466 ± 0.266	B
000010	1996-11-15	0.066	10.91	−1.270 ± 0.046	V
000010	1996-11-15	0.066	10.91	−1.171 ± 0.105	R
000010	1996-11-15	0.066	10.91	−0.823 ± 0.176	I
000010	1996-11-16	0.063	11.15	−1.307 ± 0.144	V
000010	1996-11-16	0.063	11.15	−1.053 ± 0.049	R
000010	1996-11-16	0.063	11.15	−1.454 ± 0.122	I
000010	1996-11-18	0.057	11.60	−1.502 ± 0.277	B
000010	1996-11-18	0.057	11.60	−0.899 ± 0.149	V
000010	1996-11-18	0.057	11.60	−0.921 ± 0.044	R
000010	1996-11-18	0.057	11.60	−1.171 ± 0.252	I
000010	2004-02-16	0.068	12.45	−1.064 ± 0.101	U
000010	2004-02-16	0.068	12.45	−1.237 ± 0.087	B
000010	2004-02-16	0.068	12.45	−1.111 ± 0.040	V
000010	2004-02-16	0.068	12.45	−1.063 ± 0.024	R
000010	2004-02-16	0.068	12.45	−0.948 ± 0.037	I
000010	2002-10-07	0.279	9.94	−1.846 ± 0.254	U
000010	2002-10-07	0.279	9.94	−1.455 ± 0.128	B
000010	2002-10-07	0.279	9.94	−1.508 ± 0.048	V
000010	2002-10-07	0.279	9.94	−1.343 ± 0.038	R
000010	2002-10-07	0.279	9.94	−1.300 ± 0.087	I
000012	2002-03-05	0.093	12.52	−0.805 ± 0.197	U
000012	2002-03-05	0.093	12.52	−0.575 ± 0.047	B
000012	2002-03-05	0.093	12.52	−0.705 ± 0.049	V
000012	2002-03-05	0.093	12.52	−0.793 ± 0.040	R
000012	2002-03-05	0.093	12.52	−0.697 ± 0.080	I
000012	2002-03-06	0.090	12.83	−0.570 ± 0.169	U
000012	2002-03-06	0.090	12.83	−0.669 ± 0.108	B
000012	2002-03-06	0.090	12.83	−0.846 ± 0.027	V
000012	2002-03-06	0.090	12.83	−0.825 ± 0.025	R
000012	2002-03-06	0.090	12.83	−0.916 ± 0.044	I
000012	1995-03-28	0.057	16.22	−0.223 ± 0.200	U

Table B.1. continued.

Asteroid Number	Date of observation	Fraction of day	Phase angle (deg)	P_r (%)	Filter
000012	1995-03-28	0.057	16.22	−0.468 ± 0.123	B
000012	1995-03-28	0.057	16.22	−0.359 ± 0.176	V
000012	1995-03-28	0.057	16.22	−0.385 ± 0.088	R
000012	1995-03-28	0.057	16.22	−0.908 ± 0.235	I
000012	2003-03-10	0.380	27.61	1.265 ± 0.121	U
000012	2003-03-10	0.380	27.61	1.024 ± 0.126	B
000012	2003-03-10	0.380	27.61	0.656 ± 0.061	V
000012	2003-03-10	0.380	27.61	0.654 ± 0.063	R
000012	2003-03-10	0.380	27.61	0.302 ± 0.096	I
000012	1996-11-14	0.036	30.97	2.033 ± 0.111	B
000012	1996-11-14	0.036	30.97	1.803 ± 0.164	V
000012	1996-11-14	0.036	30.97	1.479 ± 0.262	R
000012	1995-02-07	0.216	5.61	−0.223 ± 0.093	U
000012	1995-02-07	0.216	5.61	−0.432 ± 0.085	B
000012	1995-02-07	0.216	5.61	−0.459 ± 0.116	V
000012	1995-02-07	0.216	5.61	−0.612 ± 0.043	R
000012	1995-02-07	0.216	5.61	−0.683 ± 0.122	I
000012	1995-02-06	0.220	5.87	−0.669 ± 0.184	U
000012	1995-02-06	0.220	5.87	−0.551 ± 0.093	B
000012	1995-02-06	0.220	5.87	−0.517 ± 0.058	V
000012	1995-02-06	0.220	5.87	−0.514 ± 0.113	R
000012	1995-02-06	0.220	5.87	−0.624 ± 0.134	I
000012	1995-02-05	0.223	6.14	−0.015 ± 0.154	U
000012	1995-02-05	0.223	6.14	−0.565 ± 0.077	B
000012	1995-02-05	0.223	6.14	−0.757 ± 0.111	V
000012	1995-02-05	0.223	6.14	−0.638 ± 0.045	R
000012	1995-02-05	0.223	6.14	−0.680 ± 0.059	I
000012	1995-02-04	0.226	6.43	−0.994 ± 0.355	B
000012	1995-02-04	0.226	6.43	−0.787 ± 0.195	V
000012	1995-02-04	0.226	6.43	−0.909 ± 0.115	R
000012	1995-02-04	0.226	6.43	−0.916 ± 0.239	I
000012	1995-02-03	0.230	6.75	−0.236 ± 0.090	U
000012	1995-02-03	0.230	6.75	−0.133 ± 0.074	B
000012	1995-02-03	0.230	6.75	−0.340 ± 0.240	V
000012	1995-02-03	0.230	6.75	−0.602 ± 0.113	R
000012	1995-02-03	0.230	6.75	−0.518 ± 0.139	I
000012	1995-02-02	0.233	7.06	−0.365 ± 0.229	U
000012	1995-02-02	0.233	7.06	−0.623 ± 0.156	B
000012	1995-02-02	0.233	7.06	−0.522 ± 0.078	V
000012	1995-02-02	0.233	7.06	−0.672 ± 0.027	R
000012	1995-02-02	0.233	7.06	−0.855 ± 0.103	I
000016	2002-03-05	0.192	1.03	−0.337 ± 0.075	U
000016	2002-03-05	0.192	1.03	−0.427 ± 0.036	B
000016	2002-03-05	0.192	1.03	−0.440 ± 0.019	V
000016	2002-03-05	0.192	1.03	−0.454 ± 0.013	R
000016	2002-03-05	0.192	1.03	−0.441 ± 0.037	I
000016	2004-06-28	0.312	14.04	−0.723 ± 0.299	U
000016	2004-06-28	0.312	14.04	−0.974 ± 0.111	B
000016	2004-06-28	0.312	14.04	−0.777 ± 0.156	V
000016	2004-06-28	0.312	14.04	−0.848 ± 0.079	R
000016	2004-06-28	0.312	14.04	−1.120 ± 0.115	I
000016	2002-03-06	0.189	1.41	−0.095 ± 0.222	U
000016	2002-03-06	0.189	1.41	0.121 ± 0.140	B
000016	2002-03-06	0.189	1.41	0.005 ± 0.038	V
000016	2002-03-06	0.189	1.41	0.043 ± 0.037	R
000016	2002-03-06	0.189	1.41	0.051 ± 0.097	I
000016	2004-06-27	0.315	14.31	−0.781 ± 0.116	U
000016	2004-06-27	0.315	14.31	−0.824 ± 0.050	B
000016	2004-06-27	0.315	14.31	−0.970 ± 0.024	V

Table B.1. continued.

Asteroid Number	Date of observation	Fraction of day	Phase angle (deg)	P_r (%)	Filter
000016	2004-06-27	0.315	14.31	-1.032 ± 0.042	R
000016	2004-06-27	0.315	14.31	-1.009 ± 0.073	I
000016	2002-03-07	0.186	1.78	-0.495 ± 0.138	U
000016	2002-03-07	0.186	1.78	-0.536 ± 0.041	B
000016	2002-03-07	0.186	1.78	-0.524 ± 0.034	V
000016	2002-03-07	0.186	1.78	-0.598 ± 0.029	R
000016	2002-03-07	0.186	1.78	-0.581 ± 0.049	I
000016	2003-08-25	0.036	18.06	-0.429 ± 0.179	U
000016	2003-08-25	0.036	18.06	-0.394 ± 0.126	B
000016	2003-08-25	0.036	18.06	-0.534 ± 0.022	V
000016	2003-08-25	0.036	18.06	-0.493 ± 0.062	R
000016	2003-08-25	0.036	18.06	-0.623 ± 0.084	I
000016	2003-08-24	0.027	18.12	-0.193 ± 0.173	U
000016	2003-08-24	0.027	18.12	-0.372 ± 0.100	B
000016	2003-08-24	0.027	18.12	-0.560 ± 0.037	V
000016	2003-08-24	0.027	18.12	-0.659 ± 0.052	R
000016	2003-08-24	0.027	18.12	-0.712 ± 0.056	I
000016	2003-08-23	0.022	18.18	-0.396 ± 0.153	U
000016	2003-08-23	0.022	18.18	-0.475 ± 0.102	B
000016	2003-08-23	0.022	18.18	-0.514 ± 0.048	V
000016	2003-08-23	0.022	18.18	-0.505 ± 0.052	R
000016	2003-08-23	0.022	18.18	-0.538 ± 0.097	I
000016	2003-08-22	0.055	18.22	-0.560 ± 0.259	U
000016	2003-08-22	0.055	18.22	-0.552 ± 0.110	B
000016	2003-08-22	0.055	18.22	-0.458 ± 0.075	V
000016	2003-08-22	0.055	18.22	-0.430 ± 0.036	R
000016	2003-08-22	0.055	18.22	-0.523 ± 0.072	I
000018	2004-02-15	0.293	11.68	-0.726 ± 0.098	U
000018	2004-02-15	0.293	11.68	-0.882 ± 0.132	B
000018	2004-02-15	0.293	11.68	-0.869 ± 0.045	V
000018	2004-02-15	0.293	11.68	-0.909 ± 0.071	R
000018	2004-02-15	0.293	11.68	-0.976 ± 0.050	I
000018	1995-10-18	0.162	20.51	0.011 ± 0.139	U
000018	1995-10-18	0.162	20.51	-0.085 ± 0.078	B
000018	1995-10-18	0.162	20.51	-0.100 ± 0.153	V
000018	1995-10-18	0.162	20.51	-0.078 ± 0.064	R
000018	1995-10-18	0.162	20.51	-0.176 ± 0.072	I
000018	1995-10-19	0.196	20.97	-0.093 ± 0.149	U
000018	1995-10-19	0.196	20.97	-0.177 ± 0.053	B
000018	1995-10-19	0.196	20.97	-0.157 ± 0.080	V
000018	1995-10-19	0.196	20.97	-0.088 ± 0.066	R
000018	1995-10-19	0.196	20.97	-0.061 ± 0.147	I
000019	2003-03-08	0.238	2.30	0.359 ± 0.222	V
000019	2003-03-08	0.238	2.30	0.224 ± 0.216	R
000019	2003-03-08	0.238	2.30	-0.045 ± 0.276	I
000019	2003-03-10	0.107	3.13	-0.529 ± 0.126	U
000019	2003-03-10	0.107	3.13	-1.074 ± 0.115	B
000019	2003-03-10	0.107	3.13	-1.152 ± 0.144	V
000019	2003-03-10	0.107	3.13	-1.136 ± 0.125	R
000031	2004-06-27	0.303	10.30	-1.138 ± 0.236	B
000031	2004-06-27	0.303	10.30	-1.323 ± 0.136	V
000031	2004-06-27	0.303	10.30	-1.168 ± 0.067	R
000031	2004-06-27	0.303	10.30	-1.728 ± 0.205	I
000041	2013-07-27	0.184	12.00	-1.780 ± 0.050	V
000041	2013-07-28	0.147	12.20	-1.744 ± 0.030	V
000041	2013-07-29	0.147	12.40	-1.629 ± 0.040	V
000044	2004-06-27	0.031	19.37	0.288 ± 0.265	U
000044	2004-06-27	0.031	19.37	0.135 ± 0.126	B
000044	2004-06-27	0.031	19.37	0.065 ± 0.089	V

Table B.1. continued.

Asteroid Number	Date of observation	Fraction of day	Phase angle (deg)	P_r (%)	Filter
000044	2004-06-27	0.031	19.37	−0.015 ± 0.060	R
000044	2004-06-27	0.031	19.37	−0.230 ± 0.165	I
000044	2004-06-28	0.028	19.57	−0.132 ± 0.263	U
000044	2004-06-28	0.028	19.57	−0.047 ± 0.199	B
000044	2004-06-28	0.028	19.57	0.404 ± 0.166	V
000044	2004-06-28	0.028	19.57	0.303 ± 0.106	R
000044	2004-06-28	0.028	19.57	0.334 ± 0.195	I
000044	2004-06-29	0.025	19.75	0.338 ± 0.257	U
000044	2004-06-29	0.025	19.75	−0.029 ± 0.114	B
000044	2004-06-29	0.025	19.75	−0.139 ± 0.170	V
000044	2004-06-29	0.025	19.75	−0.015 ± 0.089	R
000044	2004-06-29	0.025	19.75	−0.008 ± 0.089	I
000044	2004-07-01	0.020	20.10	−0.212 ± 0.158	U
000044	2004-07-01	0.020	20.10	0.257 ± 0.135	B
000044	2004-07-01	0.020	20.10	−0.174 ± 0.151	V
000044	2004-07-01	0.020	20.10	−0.111 ± 0.128	R
000044	2004-07-01	0.020	20.10	−0.185 ± 0.170	I
000044	2004-07-04	0.012	20.58	0.095 ± 0.147	U
000044	2004-07-04	0.012	20.58	0.032 ± 0.052	B
000044	2004-07-04	0.012	20.58	0.019 ± 0.067	V
000044	2004-07-04	0.012	20.58	0.016 ± 0.042	R
000044	2004-07-04	0.012	20.58	0.030 ± 0.068	I
000044	2004-02-16	0.347	24.34	0.697 ± 0.364	V
000044	1998-10-13	0.196	2.77	−0.180 ± 0.121	V
000044	1998-10-13	0.196	2.77	−0.045 ± 0.145	R
000044	1998-10-13	0.196	2.77	0.024 ± 0.236	I
000044	1998-10-12	0.116	3.01	0.296 ± 0.295	U
000044	1998-10-12	0.116	3.01	−0.198 ± 0.174	B
000044	1998-10-12	0.116	3.01	−0.266 ± 0.076	V
000044	1998-10-12	0.116	3.01	−0.258 ± 0.056	R
000044	1998-10-12	0.116	3.01	−0.273 ± 0.142	I
000047	2013-07-27	0.211	2.90	−0.881 ± 0.040	V
000047	2013-07-28	0.161	3.00	−0.869 ± 0.040	V
000047	2013-07-29	0.161	3.10	−0.926 ± 0.060	V
000048	2004-07-01	0.093	10.33	−1.732 ± 0.282	U
000048	2004-07-01	0.093	10.33	−2.069 ± 0.124	B
000048	2004-07-01	0.093	10.33	−2.131 ± 9.999	V
000048	2004-07-01	0.093	10.33	−2.181 ± 0.073	R
000048	2004-07-01	0.093	10.33	−2.031 ± 0.231	I
000048	2004-06-29	0.099	9.83	−1.756 ± 0.163	B
000048	2004-06-29	0.099	9.83	−2.023 ± 0.059	V
000048	2004-06-29	0.099	9.83	−1.973 ± 0.037	R
000048	2004-06-29	0.099	9.83	−1.779 ± 0.096	I
000051	2012-07-21	0.374	17.90	−0.548 ± 0.020	V
000051	2012-10-22	0.108	19.20	−0.237 ± 0.069	V
000053	2002-03-06	0.203	1.40	−0.185 ± 0.118	U
000053	2002-03-06	0.203	1.40	−0.371 ± 0.049	B
000053	2002-03-06	0.203	1.40	−0.399 ± 0.026	V
000053	2002-03-06	0.203	1.40	−0.424 ± 0.028	R
000053	2002-03-06	0.203	1.40	−0.393 ± 0.050	I
000053	2002-03-05	0.207	1.47	−0.445 ± 0.127	U
000053	2002-03-05	0.207	1.47	−0.437 ± 0.060	B
000053	2002-03-05	0.207	1.47	−0.438 ± 0.020	V
000053	2002-03-05	0.207	1.47	−0.351 ± 0.030	R
000053	2002-03-05	0.207	1.47	−0.416 ± 0.035	I
000053	2002-03-07	0.200	1.52	−0.404 ± 0.126	U
000053	2002-03-07	0.200	1.52	−0.493 ± 0.056	B
000053	2002-03-07	0.200	1.52	−0.471 ± 0.017	V
000053	2002-03-07	0.200	1.52	−0.508 ± 0.026	R

Table B.1. continued.

Asteroid Number	Date of observation	Fraction of day	Phase angle (deg)	P_r (%)	Filter
000053	2002-03-07	0.200	1.52	−0.542 ± 0.053	I
000073	1997-05-02	0.102	11.53	−0.762 ± 0.063	V
000073	1997-05-02	0.102	11.53	−0.603 ± 0.098	R
000073	1997-05-02	0.102	11.53	−0.406 ± 0.178	I
000073	2003-08-23	0.295	14.07	−0.389 ± 0.215	B
000073	2003-08-23	0.295	14.07	−0.543 ± 0.051	V
000073	2003-08-23	0.295	14.07	−0.507 ± 0.072	R
000073	2003-08-23	0.295	14.07	−0.580 ± 0.113	I
000078	2013-07-27	0.283	4.50	−1.009 ± 0.060	V
000078	2013-07-28	0.245	4.20	−1.006 ± 0.050	V
000085	2012-10-21	0.185	5.10	−1.253 ± 0.030	V
000087	2002-03-05	0.322	10.72	−1.599 ± 0.466	U
000087	2002-03-05	0.322	10.72	−0.743 ± 0.190	B
000087	2002-03-05	0.322	10.72	−0.920 ± 0.187	V
000087	2002-03-05	0.322	10.72	−1.226 ± 0.044	R
000087	2002-03-05	0.322	10.72	−1.372 ± 0.220	I
000091	2003-08-23	0.185	1.79	−0.296 ± 0.211	U
000091	2003-08-23	0.185	1.79	−0.472 ± 0.082	B
000091	2003-08-23	0.185	1.79	−0.575 ± 0.050	V
000091	2003-08-23	0.185	1.79	−0.469 ± 0.048	R
000091	2003-08-23	0.185	1.79	−0.768 ± 0.115	I
000091	2003-08-24	0.159	2.25	−0.323 ± 0.203	U
000091	2003-08-24	0.159	2.25	−0.740 ± 0.114	B
000091	2003-08-24	0.159	2.25	−0.720 ± 0.048	V
000091	2003-08-24	0.159	2.25	−0.585 ± 0.057	R
000091	2003-08-24	0.159	2.25	−0.798 ± 0.099	I
000091	1995-10-19	0.261	10.19	−2.166 ± 0.323	B
000091	1995-10-19	0.261	10.19	−1.178 ± 0.264	V
000091	1995-10-19	0.261	10.19	−1.650 ± 0.153	R
000091	1995-10-19	0.261	10.19	−1.304 ± 0.282	I
000094	2013-07-29	0.318	17.90	−0.338 ± 0.070	V
000106	2013-07-27	0.054	16.00	−1.320 ± 0.050	V
000106	2013-07-29	0.067	16.10	−1.047 ± 0.180	V
000113	2003-03-10	0.259	16.58	0.001 ± 0.021	U
000113	2003-03-10	0.259	16.58	0.137 ± 0.095	B
000113	2003-03-10	0.259	16.58	−0.200 ± 0.059	V
000113	2003-03-10	0.259	16.58	−0.242 ± 0.055	R
000113	2003-03-10	0.259	16.58	−0.441 ± 0.134	I
000113	2003-03-08	0.347	17.30	0.036 ± 0.182	U
000113	2003-03-08	0.347	17.30	0.010 ± 0.073	B
000113	2003-03-08	0.347	17.30	−0.072 ± 0.054	V
000113	2003-03-08	0.347	17.30	−0.134 ± 0.060	R
000113	2003-03-08	0.347	17.30	−0.166 ± 0.097	I
000113	1996-04-24	0.332	20.12	−0.124 ± 0.187	B
000113	1996-04-24	0.332	20.12	0.167 ± 0.157	V
000113	1996-04-24	0.332	20.12	0.308 ± 0.119	R
000113	1996-04-24	0.332	20.12	0.039 ± 0.137	I
000113	1997-07-09	0.416	23.23	0.257 ± 0.176	V
000113	1997-07-09	0.416	23.23	0.174 ± 0.166	R
000113	1996-03-17	0.382	26.62	0.676 ± 0.070	V
000113	1996-03-17	0.382	26.62	0.488 ± 0.077	R
000113	1996-03-17	0.382	26.62	0.497 ± 0.139	I
000113	2012-10-22	0.312	14.20	−0.210 ± 0.070	V
000118	1999-07-15	0.266	8.81	−0.439 ± 0.269	B
000118	1999-07-15	0.266	8.81	−0.797 ± 0.308	V
000118	1996-11-14	0.234	9.05	−0.581 ± 0.141	B
000118	1996-11-14	0.234	9.05	−0.651 ± 0.115	V
000118	1996-11-14	0.234	9.05	−0.735 ± 0.070	R
000118	1996-11-14	0.234	9.05	−0.878 ± 0.086	I

Table B.1. continued.

Asteroid Number	Date of observation	Fraction of day	Phase angle (deg)	P_r (%)	Filter
000125	1999-07-16	0.322	16.29	−0.918 ± 0.367	U
000125	1999-07-16	0.322	16.29	−0.850 ± 0.381	B
000125	1999-07-16	0.322	16.29	−0.706 ± 0.145	V
000125	1999-07-16	0.322	16.29	−0.321 ± 0.184	R
000125	1999-07-16	0.322	16.29	−0.229 ± 0.250	I
000125	2003-08-22	0.006	22.04	0.139 ± 0.218	B
000125	2003-08-22	0.006	22.04	0.195 ± 0.112	V
000125	2003-08-22	0.006	22.04	0.310 ± 0.094	R
000125	2003-08-22	0.006	22.04	0.003 ± 0.155	I
000128	1995-11-30	0.114	10.19	−1.480 ± 0.299	B
000128	1995-11-30	0.114	10.19	−1.476 ± 0.036	V
000128	1995-11-30	0.114	10.19	−1.417 ± 0.080	R
000128	1995-11-30	0.114	10.19	−1.488 ± 0.106	I
000128	1995-10-19	0.305	10.38	−1.555 ± 0.387	U
000128	1995-10-19	0.305	10.38	−1.938 ± 0.153	B
000128	1995-10-19	0.305	10.38	−1.601 ± 0.130	V
000128	1995-10-19	0.305	10.38	−1.422 ± 0.131	R
000128	1995-10-19	0.305	10.38	−1.074 ± 0.178	I
000128	1995-12-01	0.111	10.61	−1.627 ± 0.242	U
000128	1995-12-01	0.111	10.61	−1.660 ± 0.136	B
000128	1995-12-01	0.111	10.61	−1.460 ± 0.075	V
000128	1995-12-01	0.111	10.61	−1.435 ± 0.027	R
000128	1995-12-01	0.111	10.61	−1.515 ± 0.095	I
000128	1995-10-18	0.326	10.72	−1.743 ± 0.168	B
000128	1995-10-18	0.326	10.72	−1.844 ± 0.117	V
000128	1995-10-18	0.326	10.72	−1.522 ± 0.078	R
000128	1995-10-18	0.326	10.72	−1.477 ± 0.131	I
000128	2003-08-25	0.013	20.33	0.556 ± 0.158	B
000128	2003-08-25	0.013	20.33	0.149 ± 0.092	V
000128	2003-08-25	0.013	20.33	0.198 ± 0.104	R
000128	2003-08-25	0.013	20.33	0.371 ± 0.107	I
000128	1995-11-29	0.117	9.77	−1.011 ± 0.207	U
000128	1995-11-29	0.117	9.77	−1.346 ± 0.095	B
000128	1995-11-29	0.117	9.77	−1.480 ± 0.027	V
000128	1995-11-29	0.117	9.77	−1.494 ± 0.031	R
000128	1995-11-29	0.117	9.77	−1.495 ± 0.066	I
000129	2012-10-22	0.361	12.90	−0.458 ± 0.070	V
000131	2009-02-19	0.226	9.20	−0.332 ± 0.037	V
000131	2009-02-18	0.217	9.60	−0.484 ± 0.040	V
000131	1995-10-18	0.111	18.57	0.103 ± 0.165	V
000131	1995-10-18	0.111	18.57	−0.024 ± 0.147	R
000131	1995-10-20	0.055	19.01	0.141 ± 0.230	V
000131	1995-10-20	0.055	19.01	−0.111 ± 0.263	R
000131	2003-08-22	0.365	20.73	0.152 ± 0.143	V
000131	2003-08-22	0.365	20.73	−0.007 ± 0.087	R
000131	2003-08-22	0.365	20.73	0.169 ± 0.302	I
000131	1995-11-30	0.016	22.80	0.566 ± 0.183	R
000131	2010-09-03	0.118	12.10	−0.716 ± 0.130	V
000131	2010-09-04	0.181	12.50	−0.790 ± 0.110	V
000131	2010-09-05	0.123	12.90	−0.625 ± 0.080	V
000132	1995-03-28	0.157	27.00	1.547 ± 0.129	U
000132	1995-03-28	0.157	27.00	1.011 ± 0.092	B
000132	1995-03-28	0.157	27.00	0.917 ± 0.055	V
000132	1995-03-28	0.157	27.00	0.832 ± 0.080	R
000132	1995-03-28	0.157	27.00	0.918 ± 0.280	I
000132	1995-03-26	0.163	27.39	1.423 ± 0.079	U
000132	1995-03-26	0.163	27.39	1.193 ± 0.067	B
000132	1995-03-26	0.163	27.39	1.044 ± 0.093	V
000132	1995-03-26	0.163	27.39	1.100 ± 0.120	I

Table B.1. continued.

Asteroid Number	Date of observation	Fraction of day	Phase angle (deg)	P_r (%)	Filter
000132	1995-02-07	0.301	35.06	0.813 ± 0.172	U
000132	1995-02-07	0.301	35.06	2.299 ± 0.209	B
000132	1995-02-07	0.301	35.06	2.235 ± 0.064	V
000132	1995-02-07	0.301	35.06	2.002 ± 0.056	R
000132	1995-02-06	0.303	35.16	0.947 ± 0.136	U
000132	1995-02-06	0.303	35.16	2.096 ± 0.088	B
000132	1995-02-06	0.303	35.16	2.100 ± 0.059	V
000132	1995-02-06	0.303	35.16	2.021 ± 0.049	R
000132	1995-02-06	0.303	35.16	2.023 ± 0.123	I
000132	1995-02-05	0.306	35.26	2.203 ± 0.229	B
000132	1995-02-05	0.306	35.26	2.342 ± 0.106	V
000132	1995-02-05	0.306	35.26	2.342 ± 0.067	R
000132	1995-02-05	0.306	35.26	2.141 ± 0.091	I
000132	1995-02-04	0.308	35.36	2.263 ± 0.186	B
000132	1995-02-04	0.308	35.36	2.026 ± 0.274	V
000132	1995-02-04	0.308	35.36	2.306 ± 0.211	R
000132	1995-02-02	0.313	35.55	1.323 ± 0.192	U
000132	1995-02-02	0.313	35.55	2.428 ± 0.053	B
000132	1995-02-02	0.313	35.55	2.418 ± 0.111	V
000132	1995-02-02	0.313	35.55	2.093 ± 0.050	R
000132	1995-02-02	0.313	35.55	2.136 ± 0.108	I
000134	2004-06-28	0.345	16.71	−0.679 ± 0.328	U
000134	2004-06-28	0.345	16.71	−1.155 ± 0.191	B
000134	2004-06-28	0.345	16.71	−1.016 ± 0.076	V
000134	2004-06-28	0.345	16.71	−0.904 ± 0.104	R
000134	2004-06-28	0.345	16.71	−1.063 ± 0.233	I
000134	1999-07-16	0.012	19.01	−0.007 ± 0.212	V
000134	1999-07-16	0.012	19.01	0.226 ± 0.245	R
000134	2012-07-24	0.304	5.30	−1.119 ± 0.030	V
000138	2004-02-14	0.394	21.41	0.301 ± 0.104	V
000138	2004-02-14	0.394	21.41	0.351 ± 0.056	R
000138	2004-02-14	0.394	21.41	0.469 ± 0.247	I
000138	1997-07-09	0.334	21.57	0.855 ± 0.203	U
000138	1997-07-09	0.334	21.57	0.430 ± 0.126	B
000138	1997-07-09	0.334	21.57	0.220 ± 0.045	V
000138	1997-07-09	0.334	21.57	0.219 ± 0.032	R
000138	1997-07-09	0.334	21.57	0.174 ± 0.080	I
000138	2004-06-27	0.007	23.93	0.941 ± 0.202	V
000138	2004-06-27	0.007	23.93	0.923 ± 0.352	R
000138	2004-06-27	0.007	23.93	0.547 ± 0.355	I
000138	2004-06-28	0.991	24.22	0.502 ± 0.195	B
000138	2004-06-28	0.991	24.22	0.680 ± 0.105	V
000138	2004-06-28	0.991	24.22	0.573 ± 0.084	R
000138	2004-06-30	0.014	24.37	1.056 ± 0.269	B
000138	2004-06-30	0.014	24.37	0.807 ± 0.155	V
000138	2004-06-30	0.014	24.37	0.568 ± 0.158	R
000138	2004-06-30	0.014	24.37	0.980 ± 0.241	I
000138	1997-05-02	0.388	28.89	1.543 ± 0.245	B
000138	1997-05-02	0.388	28.89	0.968 ± 0.122	V
000138	1997-05-02	0.388	28.89	1.026 ± 0.049	R
000138	1997-05-02	0.388	28.89	0.887 ± 0.205	I
000139	2013-07-27	0.372	16.30	−0.922 ± 0.140	V
000139	2013-07-29	0.363	16.10	−0.856 ± 0.070	V
000141	2010-04-20	0.023	16.60	−0.046 ± 0.006	V
000141	2012-10-21	0.026	25.40	1.429 ± 0.030	V
000150	1997-05-02	0.182	0.96	−0.257 ± 0.249	U
000150	1997-05-02	0.182	0.96	−0.269 ± 0.155	B
000150	1997-05-02	0.182	0.96	−0.323 ± 0.074	V
000150	1997-05-02	0.182	0.96	−0.263 ± 0.094	R

Table B.1. continued.

Asteroid Number	Date of observation	Fraction of day	Phase angle (deg)	P_r (%)	Filter
000150	1997-05-02	0.182	0.96	−0.237 ± 0.194	I
000158	1996-11-17	0.181	0.39	−0.561 ± 0.249	V
000158	1996-11-17	0.181	0.39	−0.578 ± 0.132	R
000158	1996-11-18	0.178	0.56	−0.149 ± 0.149	B
000158	1996-11-18	0.178	0.56	−0.293 ± 0.050	V
000158	1996-11-18	0.178	0.56	−0.347 ± 0.046	R
000158	1996-11-18	0.178	0.56	−0.257 ± 0.087	I
000158	2003-03-10	0.205	0.59	−0.102 ± 0.143	B
000158	2003-03-10	0.205	0.59	−0.107 ± 0.068	V
000158	2003-03-10	0.205	0.59	−0.139 ± 0.071	R
000158	2003-03-10	0.205	0.59	0.033 ± 0.150	I
000158	2003-03-08	0.275	1.20	−0.605 ± 0.070	V
000158	2003-03-08	0.275	1.20	−0.435 ± 0.083	R
000158	2003-03-08	0.275	1.20	0.015 ± 0.165	I
000158	1999-07-16	0.024	16.46	−0.295 ± 0.336	V
000158	1999-07-16	0.024	16.46	−0.322 ± 0.344	R
000158	1999-07-16	0.024	16.46	−0.172 ± 0.329	I
000169	1999-07-16	0.368	23.72	1.255 ± 0.232	V
000169	1999-07-16	0.368	23.72	0.525 ± 0.213	R
000169	1999-07-16	0.368	23.72	0.649 ± 0.347	I
000170	1996-03-17	0.177	14.06	−0.407 ± 0.137	V
000170	1996-03-17	0.177	14.06	−0.421 ± 0.082	R
000170	1996-03-17	0.177	14.06	−0.692 ± 0.298	I
000170	1996-03-15	0.276	14.57	−0.293 ± 0.104	V
000170	1996-03-15	0.276	14.57	−0.324 ± 0.101	R
000170	1996-03-15	0.276	14.57	−0.878 ± 0.316	I
000170	2004-02-14	0.308	17.69	−0.667 ± 0.295	B
000170	2004-02-14	0.308	17.69	−0.223 ± 0.128	V
000170	2004-02-14	0.308	17.69	−0.239 ± 0.147	R
000170	2004-02-14	0.308	17.69	−0.074 ± 0.249	I
000170	1997-05-02	0.363	21.80	0.134 ± 0.221	V
000170	1997-05-02	0.363	21.80	−0.041 ± 0.107	R
000170	1996-04-24	0.134	9.55	−1.227 ± 0.117	V
000170	1996-04-24	0.134	9.55	−1.097 ± 0.113	R
000170	1997-07-09	0.270	9.58	−0.648 ± 0.118	V
000170	1997-07-09	0.270	9.58	−0.734 ± 0.090	R
000170	1997-07-08	0.274	9.97	−0.621 ± 0.379	B
000170	1997-07-08	0.274	9.97	−0.736 ± 0.137	V
000170	1997-07-08	0.274	9.97	−0.747 ± 0.112	R
000172	2010-04-20	0.355	18.30	−0.955 ± 0.039	V
000178	2003-03-10	0.286	21.70	0.353 ± 0.145	V
000178	2003-03-10	0.286	21.70	0.212 ± 0.183	R
000178	2003-03-10	0.286	21.70	0.104 ± 0.224	I
000178	2012-10-23	0.195	3.70	−1.393 ± 0.060	V
000183	1998-10-11	0.296	31.37	1.778 ± 0.271	U
000183	1998-10-11	0.296	31.37	1.293 ± 0.113	B
000183	1998-10-11	0.296	31.37	1.185 ± 0.058	V
000183	1998-10-11	0.296	31.37	1.098 ± 0.048	R
000183	1998-10-11	0.296	31.37	0.925 ± 0.080	I
000183	2012-10-21	0.356	30.10	1.181 ± 0.030	V
000186	2006-08-27	0.258	13.09	−0.023 ± 0.093	U
000186	2006-08-27	0.258	13.09	−0.118 ± 0.049	B
000186	2006-08-27	0.258	13.09	−0.286 ± 0.024	V
000186	2006-08-27	0.258	13.09	−0.280 ± 0.023	R
000186	2006-08-27	0.258	13.09	−0.390 ± 0.064	I
000186	1995-10-18	0.137	25.21	1.597 ± 0.334	U
000186	1995-10-18	0.137	25.21	1.373 ± 0.263	B
000186	1995-10-18	0.137	25.21	1.196 ± 0.079	V
000186	1995-10-18	0.137	25.21	1.017 ± 0.080	R

Table B.1. continued.

Asteroid Number	Date of observation	Fraction of day	Phase angle (deg)	P_r (%)	Filter
000186	1995-10-18	0.137	25.21	0.835 ± 0.144	I
000186	1995-10-19	0.170	25.43	1.301 ± 0.192	B
000186	1995-10-19	0.170	25.43	1.093 ± 0.080	V
000186	1995-10-19	0.170	25.43	0.955 ± 0.082	R
000186	1995-10-19	0.170	25.43	1.482 ± 0.145	I
000186	1995-12-01	0.042	28.64	1.758 ± 0.129	V
000186	1995-12-01	0.042	28.64	1.770 ± 0.117	R
000186	1995-12-01	0.042	28.64	1.837 ± 0.301	I
000186	2002-10-10	0.040	29.56	1.474 ± 0.330	V
000186	2002-10-10	0.040	29.56	1.222 ± 0.231	R
000188	1996-03-16	0.091	14.46	−1.137 ± 0.250	V
000188	1996-03-16	0.091	14.46	−0.806 ± 0.167	R
000188	1998-10-13	0.062	16.56	−0.512 ± 0.196	R
000188	1998-10-13	0.062	16.56	−0.742 ± 0.272	I
000188	1998-10-12	0.141	16.28	−0.273 ± 0.343	U
000188	1998-10-12	0.141	16.28	−0.275 ± 0.128	B
000188	1998-10-12	0.141	16.28	−0.603 ± 0.059	V
000188	1998-10-12	0.141	16.28	−0.556 ± 0.050	R
000188	1998-10-12	0.141	16.28	−0.512 ± 0.089	I
000188	1996-04-26	0.059	18.13	0.966 ± 0.308	R
000188	1997-07-08	0.055	22.41	0.474 ± 0.372	B
000188	1997-07-08	0.055	22.41	0.104 ± 0.154	V
000188	1997-07-08	0.055	22.41	0.240 ± 0.098	R
000188	1997-07-08	0.055	22.41	−0.534 ± 0.318	I
000188	2012-10-22	0.155	6.90	−2.723 ± 0.070	V
000189	2004-06-27	0.258	10.02	−1.222 ± 0.353	U
000189	2004-06-27	0.258	10.02	−1.512 ± 0.271	B
000189	2004-06-27	0.258	10.02	−1.264 ± 0.098	V
000189	2004-06-27	0.258	10.02	−1.190 ± 0.112	R
000189	2004-06-27	0.258	10.02	−0.957 ± 0.184	I
000189	1996-04-24	0.321	16.65	−0.762 ± 0.125	V
000189	1996-04-24	0.321	16.65	−0.321 ± 0.044	R
000189	1996-04-24	0.321	16.65	−0.939 ± 0.210	I
000189	1996-03-16	0.375	22.91	0.262 ± 0.161	V
000189	1996-03-16	0.375	22.91	0.054 ± 0.135	R
000189	2004-06-28	0.255	9.63	−0.938 ± 0.132	R
000189	2012-10-23	0.044	20.60	−0.423 ± 0.060	V
000192	2007-09-03	0.011	25.73	0.552 ± 0.336	U
000192	2007-09-03	0.011	25.73	0.526 ± 0.103	B
000192	2007-09-03	0.011	25.73	−0.242 ± 0.335	V
000192	2007-09-03	0.011	25.73	−0.014 ± 0.183	R
000192	2007-09-03	0.011	25.73	−0.410 ± 0.357	I
000197	2002-10-09	0.025	23.17	0.775 ± 0.215	B
000197	2002-10-09	0.025	23.17	0.417 ± 0.068	V
000197	2002-10-09	0.025	23.17	0.338 ± 0.074	R
000197	2002-10-09	0.025	23.17	0.004 ± 0.060	I
000197	1998-10-11	0.226	9.61	−0.396 ± 0.240	B
000197	1998-10-11	0.226	9.61	−0.788 ± 0.083	V
000197	1998-10-11	0.226	9.61	−0.721 ± 0.069	R
000197	1998-10-11	0.226	9.61	−0.597 ± 0.124	I
000200	2004-02-14	0.274	9.71	−1.609 ± 0.374	U
000200	2004-02-14	0.274	9.71	−1.725 ± 0.177	B
000200	2004-02-14	0.274	9.71	−1.768 ± 0.072	V
000200	2004-02-14	0.274	9.71	−1.804 ± 0.088	R
000200	2004-02-14	0.274	9.71	−1.348 ± 0.214	I
000201	1996-03-15	0.229	0.90	−0.165 ± 0.309	U
000201	1996-03-15	0.229	0.90	0.089 ± 0.275	B
000201	1996-03-15	0.229	0.90	−0.347 ± 0.100	V
000201	1996-03-15	0.229	0.90	−0.426 ± 0.061	R

Table B.1. continued.

Asteroid Number	Date of observation	Fraction of day	Phase angle (deg)	P_r (%)	Filter
000201	1996-03-15	0.229	0.90	−0.323 ± 0.258	I
000201	1996-03-17	0.098	1.06	−0.435 ± 0.073	V
000201	1996-03-17	0.098	1.06	−0.419 ± 0.091	R
000201	1996-03-17	0.098	1.06	−0.188 ± 0.271	I
000201	2006-08-28	0.239	14.97	−0.751 ± 0.138	U
000201	2006-08-28	0.239	14.97	−1.487 ± 0.258	V
000201	2006-08-28	0.239	14.97	−1.077 ± 0.280	R
000204	2004-02-15	0.270	10.93	−0.316 ± 0.211	B
000204	2004-02-15	0.270	10.93	−0.834 ± 0.119	V
000204	2004-02-15	0.270	10.93	−0.813 ± 0.070	R
000204	2004-02-15	0.270	10.93	−0.761 ± 0.179	I
000210	2009-09-14	0.238	6.70	−0.792 ± 0.022	V
000210	2013-07-27	0.235	3.30	−0.807 ± 0.050	V
000210	2013-07-28	0.186	3.10	−0.668 ± 0.060	V
000213	2005-09-28	0.198	3.73	−1.288 ± 0.279	U
000213	2005-09-28	0.198	3.73	−1.040 ± 0.261	B
000213	2005-09-28	0.198	3.73	−1.503 ± 0.152	V
000213	2005-09-28	0.198	3.73	−1.545 ± 0.095	R
000213	2005-09-28	0.198	3.73	−1.611 ± 0.149	I
000214	1996-11-19	0.091	11.48	−0.164 ± 0.225	B
000214	1996-11-19	0.091	11.48	−0.123 ± 0.084	V
000214	1996-11-19	0.091	11.48	−0.193 ± 0.067	R
000214	1996-11-19	0.091	11.48	−0.118 ± 0.143	I
000216	1997-05-02	0.157	3.38	−0.409 ± 0.264	U
000216	1997-05-02	0.157	3.38	−0.656 ± 0.169	B
000216	1997-05-02	0.157	3.38	−0.628 ± 0.068	V
000216	1997-05-02	0.157	3.38	−0.854 ± 0.050	R
000216	1997-05-02	0.157	3.38	−0.905 ± 0.084	I
000216	1996-03-15	0.112	11.50	−1.109 ± 0.210	U
000216	1996-03-15	0.112	11.50	−0.906 ± 0.253	B
000216	1996-03-15	0.112	11.50	−0.893 ± 0.086	V
000216	1996-03-15	0.112	11.50	−0.989 ± 0.117	R
000216	1996-03-15	0.112	11.50	−0.792 ± 0.167	I
000216	1996-03-17	0.040	11.99	−1.236 ± 0.234	U
000216	1996-03-17	0.040	11.99	−1.191 ± 0.137	B
000216	1996-03-17	0.040	11.99	−0.895 ± 0.067	V
000216	1996-03-17	0.040	11.99	−0.903 ± 0.061	R
000216	1996-03-17	0.040	11.99	−1.123 ± 0.200	I
000216	2003-08-22	0.133	13.09	−1.114 ± 0.262	U
000216	2003-08-22	0.133	13.09	−0.651 ± 0.118	B
000216	2003-08-22	0.133	13.09	−0.842 ± 0.026	V
000216	2003-08-22	0.133	13.09	−0.938 ± 0.058	R
000216	2003-08-22	0.133	13.09	−0.970 ± 0.150	I
000216	2003-08-22	0.102	13.12	−0.532 ± 0.141	U
000216	2003-08-22	0.102	13.12	−0.755 ± 0.070	B
000216	2003-08-22	0.102	13.12	−0.826 ± 0.039	V
000216	2003-08-22	0.102	13.12	−0.939 ± 0.052	R
000216	2003-08-22	0.102	13.12	−0.927 ± 0.059	I
000216	2003-08-23	0.048	13.39	−0.712 ± 0.140	U
000216	2003-08-23	0.048	13.39	−0.670 ± 0.077	B
000216	2003-08-23	0.048	13.39	−0.805 ± 0.052	V
000216	2003-08-23	0.048	13.39	−0.829 ± 0.033	R
000216	2003-08-23	0.048	13.39	−0.943 ± 0.056	I
000216	2003-08-24	0.096	13.70	−0.688 ± 0.077	U
000216	2003-08-24	0.096	13.70	−0.668 ± 0.055	B
000216	2003-08-24	0.096	13.70	−0.751 ± 0.034	V
000216	2003-08-24	0.096	13.70	−0.810 ± 0.034	R
000216	2003-08-24	0.096	13.70	−0.830 ± 0.057	I
000216	2003-08-25	0.104	14.02	−0.607 ± 0.114	U

Table B.1. continued.

Asteroid Number	Date of observation	Fraction of day	Phase angle (deg)	P_r (%)	Filter
000216	2003-08-25	0.104	14.02	−0.662 ± 0.085	B
000216	2003-08-25	0.104	14.02	−0.778 ± 0.031	V
000216	2003-08-25	0.104	14.02	−0.842 ± 0.038	R
000216	2003-08-25	0.104	14.02	−0.783 ± 0.053	I
000219	2004-02-14	0.043	24.68	0.040 ± 0.299	V
000219	2004-02-14	0.043	24.68	0.296 ± 0.100	R
000219	2004-02-14	0.043	24.68	−1.139 ± 0.212	I
000219	2006-08-27	0.099	28.83	1.695 ± 0.263	U
000219	2006-08-27	0.099	28.83	1.008 ± 0.113	B
000219	2006-08-27	0.099	28.83	0.898 ± 0.076	V
000219	2006-08-27	0.099	28.83	0.841 ± 0.064	R
000219	2006-08-27	0.099	28.83	0.609 ± 0.095	I
000219	2006-08-30	0.150	29.36	0.977 ± 0.114	V
000219	2006-08-30	0.150	29.36	0.938 ± 0.121	R
000219	2006-08-30	0.150	29.36	0.917 ± 0.149	I
000219	2009-02-18	0.277	16.70	−0.061 ± 0.082	V
000219	2010-09-05	0.283	19.70	−0.057 ± 0.048	V
000220	1996-03-17	0.217	14.31	−1.136 ± 0.553	V
000220	1996-03-17	0.217	14.31	−1.393 ± 0.235	R
000221	2003-03-08	0.297	10.16	−1.311 ± 0.170	B
000221	2003-03-08	0.297	10.16	−0.983 ± 0.092	V
000221	2003-03-08	0.297	10.16	−1.009 ± 0.096	R
000221	2003-03-08	0.297	10.16	−1.175 ± 0.106	I
000221	1995-12-01	0.198	5.05	−1.077 ± 0.357	U
000221	1995-12-01	0.198	5.05	−0.969 ± 0.270	B
000221	1995-12-01	0.198	5.05	−0.728 ± 0.103	V
000221	1995-12-01	0.198	5.05	−0.946 ± 0.055	R
000221	1995-12-01	0.198	5.05	−0.982 ± 0.051	I
000222	2004-02-16	0.211	1.18	−0.341 ± 0.296	B
000222	2004-02-16	0.211	1.18	−0.745 ± 0.237	V
000222	2004-02-16	0.211	1.18	−0.494 ± 0.149	R
000222	2010-04-22	0.127	10.40	0.648 ± 0.153	V
000234	2003-03-10	0.068	14.14	−1.561 ± 0.332	V
000234	2003-03-10	0.068	14.14	−1.629 ± 0.274	R
000234	1997-07-09	0.101	18.49	−0.853 ± 0.299	U
000234	1997-07-09	0.101	18.49	−1.330 ± 0.154	B
000234	1997-07-09	0.101	18.49	−1.253 ± 0.068	V
000234	1997-07-09	0.101	18.49	−1.249 ± 0.045	R
000234	1997-07-09	0.101	18.49	−1.157 ± 0.173	I
000234	1997-05-02	0.321	19.89	−1.642 ± 0.384	U
000234	1997-05-02	0.321	19.89	−1.535 ± 0.130	B
000234	1997-05-02	0.321	19.89	−1.217 ± 0.067	V
000234	1997-05-02	0.321	19.89	−1.136 ± 0.067	R
000234	1997-05-02	0.321	19.89	−1.042 ± 0.131	I
000234	2004-06-28	0.004	23.68	−0.873 ± 0.239	V
000234	2004-06-28	0.004	23.68	−0.648 ± 0.142	R
000234	2004-06-28	0.004	23.68	−0.068 ± 0.235	I
000234	2012-10-21	0.074	30.80	0.017 ± 0.027	V
000237	1996-11-17	0.275	10.12	−0.669 ± 0.070	V
000237	1996-11-17	0.275	10.12	−0.695 ± 0.068	R
000237	1996-11-17	0.275	10.12	−0.806 ± 0.190	I
000237	1995-10-18	0.224	15.41	−0.341 ± 0.219	V
000237	1995-10-18	0.224	15.41	−0.234 ± 0.133	R
000237	1995-10-18	0.224	15.41	−0.761 ± 0.386	I
000237	1995-10-19	0.138	15.64	−0.308 ± 0.117	V
000237	1995-10-19	0.138	15.64	−0.271 ± 0.099	R
000237	1995-10-19	0.138	15.64	−0.934 ± 0.299	I
000237	1995-11-30	0.029	21.12	0.215 ± 0.305	V
000237	1995-11-30	0.029	21.12	0.042 ± 0.177	R

Table B.1. continued.

Asteroid Number	Date of observation	Fraction of day	Phase angle (deg)	P_r (%)	Filter
000237	1995-12-01	0.044	21.14	0.107 ± 0.307	V
000237	1995-12-01	0.044	21.14	0.115 ± 0.183	R
000238	2013-07-27	0.332	17.00	−1.234 ± 0.169	V
000238	2013-07-28	0.338	16.70	−1.180 ± 0.050	V
000246	2004-02-14	0.127	9.05	−0.480 ± 0.201	B
000246	2004-02-14	0.127	9.05	−0.570 ± 0.084	V
000246	2004-02-14	0.127	9.05	−0.536 ± 0.093	R
000246	2004-02-14	0.127	9.05	−0.779 ± 0.172	I
000253	1996-03-17	0.283	16.58	−0.116 ± 0.345	R
000263	1997-05-02	0.186	0.40	−0.303 ± 0.174	V
000263	1997-05-02	0.186	0.40	−0.341 ± 0.146	R
000263	1997-05-02	0.186	0.40	−0.053 ± 0.347	I
000271	2004-02-16	0.208	0.67	−0.192 ± 0.203	V
000271	2004-02-16	0.208	0.67	−0.301 ± 0.145	R
000273	1996-03-15	0.378	23.86	0.288 ± 0.287	V
000273	1996-03-15	0.378	23.86	0.704 ± 0.145	R
000278	2002-03-05	0.315	16.00	−0.073 ± 0.224	B
000278	2002-03-05	0.315	16.00	−0.548 ± 0.118	V
000278	2002-03-05	0.315	16.00	−0.313 ± 0.100	R
000278	2002-03-05	0.315	16.00	−1.116 ± 0.251	I
000282	2002-10-07	0.327	20.86	1.200 ± 0.225	V
000282	2002-10-07	0.327	20.86	1.104 ± 0.249	R
000288	2009-02-19	0.182	9.20	−0.763 ± 0.050	V
000288	1996-04-24	0.320	18.36	−0.031 ± 0.224	B
000288	1996-04-24	0.320	18.36	−0.564 ± 0.248	V
000288	1996-04-24	0.320	18.36	−0.205 ± 0.238	R
000288	1996-04-24	0.320	18.36	−0.350 ± 0.297	I
000288	1996-03-16	0.341	25.93	0.632 ± 0.116	V
000288	1996-03-16	0.341	25.93	0.447 ± 0.088	R
000288	1996-03-16	0.341	25.93	0.756 ± 0.220	I
000292	1999-07-15	0.070	15.92	−0.202 ± 0.237	V
000292	1999-07-15	0.070	15.92	−0.481 ± 0.273	R
000292	2003-08-25	0.002	23.70	0.313 ± 0.233	V
000292	2003-08-25	0.002	23.70	0.272 ± 0.231	R
000302	2002-10-07	0.187	0.83	0.214 ± 0.223	U
000302	2002-10-07	0.187	0.83	−0.326 ± 0.187	B
000302	2002-10-07	0.187	0.83	−0.269 ± 0.091	V
000302	2002-10-07	0.187	0.83	−0.205 ± 0.082	R
000302	2002-10-07	0.187	0.83	−0.147 ± 0.189	I
000305	2003-08-25	0.283	10.70	−0.971 ± 0.245	B
000305	2003-08-25	0.283	10.70	−0.641 ± 0.099	V
000305	2003-08-25	0.283	10.70	−0.527 ± 0.071	R
000305	2003-08-25	0.283	10.70	−0.737 ± 0.257	I
000306	2012-10-20	0.279	11.00	−0.507 ± 0.020	V
000324	2002-03-05	0.189	1.40	−0.626 ± 0.202	U
000324	2002-03-05	0.189	1.40	−0.415 ± 0.156	B
000324	2002-03-05	0.189	1.40	−0.575 ± 0.050	V
000324	2002-03-05	0.189	1.40	−0.550 ± 0.043	R
000324	2002-03-05	0.189	1.40	−0.475 ± 0.135	I
000324	2002-03-06	0.185	1.63	−0.586 ± 0.135	U
000324	2002-03-06	0.185	1.63	−0.556 ± 0.048	B
000324	2002-03-06	0.185	1.63	−0.651 ± 0.027	V
000324	2002-03-06	0.185	1.63	−0.668 ± 0.029	R
000324	2002-03-06	0.185	1.63	−0.624 ± 0.085	I
000324	2002-03-06	0.185	1.90	−0.721 ± 0.093	U
000324	2002-03-06	0.185	1.90	−0.670 ± 0.064	B
000324	2002-03-06	0.185	1.90	−0.676 ± 0.048	V
000324	2002-03-06	0.185	1.90	−0.689 ± 0.030	R
000324	2002-03-06	0.185	1.90	−0.534 ± 0.077	I

Table B.1. continued.

Asteroid Number	Date of observation	Fraction of day	Phase angle (deg)	P_r (%)	Filter
000324	2013-07-27	0.308	24.00	1.250 ± 0.050	V
000324	2013-07-28	0.372	23.70	1.149 ± 0.050	V
000324	2013-07-29	0.294	23.40	1.032 ± 0.040	V
000334	2013-07-28	0.026	14.70	−0.990 ± 0.060	V
000334	2013-07-29	0.105	14.80	−0.940 ± 0.050	V
000335	2012-07-24	0.071	25.50	2.673 ± 0.020	V
000338	2004-02-16	0.248	7.14	−1.148 ± 0.291	U
000338	2004-02-16	0.248	7.14	−0.771 ± 0.105	B
000338	2004-02-16	0.248	7.14	−0.969 ± 0.104	V
000338	2004-02-16	0.248	7.14	−0.973 ± 0.108	R
000338	2004-02-16	0.248	7.14	−1.154 ± 0.162	I
000341	1996-04-24	0.324	20.88	−0.013 ± 0.334	U
000341	1996-04-24	0.324	20.88	0.777 ± 0.179	B
000341	1996-04-24	0.324	20.88	0.537 ± 0.218	V
000341	1996-04-24	0.324	20.88	0.458 ± 0.199	R
000341	1996-11-18	0.022	29.11	0.906 ± 0.315	R
000341	2003-08-23	0.363	29.42	0.547 ± 0.188	V
000341	2003-08-23	0.363	29.42	0.531 ± 0.090	R
000345	2012-10-22	0.065	23.60	1.110 ± 0.080	V
000351	2002-10-07	0.267	10.46	−0.791 ± 0.219	B
000351	2002-10-07	0.267	10.46	−0.736 ± 0.092	V
000351	2002-10-07	0.267	10.46	−0.748 ± 0.068	R
000351	2002-10-07	0.267	10.46	−0.814 ± 0.109	I
000351	2004-02-15	0.297	13.15	−0.611 ± 0.173	B
000351	2004-02-15	0.297	13.15	−0.673 ± 0.230	V
000351	2004-02-15	0.297	13.15	−0.719 ± 0.084	R
000351	2004-02-15	0.297	13.15	−0.693 ± 0.154	I
000359	2003-08-22	0.291	19.98	−0.171 ± 0.308	B
000359	2003-08-22	0.291	19.98	−0.207 ± 0.144	V
000359	2003-08-22	0.291	19.98	−0.159 ± 0.145	R
000359	2003-08-22	0.291	19.98	−0.462 ± 0.317	I
000359	1998-10-12	0.064	25.20	1.458 ± 0.395	U
000359	1998-10-12	0.064	25.20	1.030 ± 0.213	B
000359	1998-10-12	0.064	25.20	1.002 ± 0.079	V
000359	1998-10-12	0.064	25.20	0.814 ± 0.098	R
000359	1998-10-12	0.064	25.20	1.176 ± 0.163	I
000367	2003-08-22	0.284	13.20	−0.454 ± 0.187	V
000367	2003-08-22	0.284	13.20	−0.324 ± 0.145	R
000367	2002-03-07	0.368	24.68	0.304 ± 0.141	V
000367	2002-03-07	0.368	24.68	0.146 ± 0.116	R
000374	2003-08-23	0.983	23.01	0.525 ± 0.138	V
000374	2003-08-23	0.983	23.01	0.281 ± 0.175	R
000374	2003-08-23	0.983	23.01	0.032 ± 0.226	I
000376	2003-03-08	0.325	19.70	−0.003 ± 0.138	B
000376	2003-03-08	0.325	19.70	0.114 ± 0.080	V
000376	2003-03-08	0.325	19.70	0.096 ± 0.107	R
000376	2003-03-08	0.325	19.70	−0.045 ± 0.135	I
000376	1996-03-18	0.228	8.47	−0.540 ± 0.370	U
000376	1996-03-18	0.228	8.47	−0.690 ± 0.089	B
000376	1996-03-18	0.228	8.47	−0.461 ± 0.056	V
000376	1996-03-18	0.228	8.47	−0.439 ± 0.111	R
000376	1996-03-18	0.228	8.47	−0.581 ± 0.173	I
000376	1996-03-17	0.155	8.87	−0.472 ± 0.278	B
000376	1996-03-17	0.155	8.87	−0.817 ± 0.204	V
000376	1996-03-17	0.155	8.87	−0.638 ± 0.090	R
000376	1996-03-17	0.155	8.87	−0.457 ± 0.223	I
000381	2012-10-20	0.210	5.70	−0.083 ± 0.131	V
000384	1999-07-16	0.196	10.11	−0.579 ± 0.182	R
000386	2004-07-04	0.152	10.19	−1.201 ± 0.304	U

Table B.1. continued.

Asteroid Number	Date of observation	Fraction of day	Phase angle (deg)	P_r (%)	Filter
000386	2004-07-04	0.152	10.19	−1.304 ± 0.084	B
000386	2004-07-04	0.152	10.19	−1.631 ± 0.069	V
000386	2004-07-04	0.152	10.19	−1.554 ± 0.049	R
000386	2004-07-04	0.152	10.19	−1.741 ± 0.086	I
000387	2013-07-27	0.160	9.80	−1.300 ± 0.040	V
000387	2013-07-28	0.126	10.20	−1.290 ± 0.100	V
000396	2002-10-09	0.105	10.58	−1.011 ± 0.320	B
000396	2002-10-09	0.105	10.58	−1.336 ± 0.089	V
000396	2002-10-09	0.105	10.58	−1.023 ± 0.094	R
000396	2002-10-09	0.105	10.58	−1.593 ± 0.262	I
000399	2002-03-05	0.274	10.60	−0.873 ± 0.257	B
000399	2002-03-05	0.274	10.60	−1.026 ± 0.125	V
000399	2002-03-05	0.274	10.60	−0.981 ± 0.069	R
000399	2002-03-05	0.274	10.60	−1.278 ± 0.273	I
000404	2013-07-28	0.401	19.40	−0.573 ± 0.277	V
000409	2004-02-14	0.101	12.80	−1.620 ± 0.161	U
000409	2004-02-14	0.101	12.80	−1.683 ± 0.134	B
000409	2004-02-14	0.101	12.80	−1.352 ± 0.086	V
000409	2004-02-14	0.101	12.80	−1.356 ± 0.056	R
000409	2004-02-14	0.101	12.80	−1.225 ± 0.101	I
000409	1996-03-15	0.127	13.75	−1.022 ± 0.295	U
000409	1996-03-15	0.127	13.75	−1.305 ± 0.080	B
000409	1996-03-15	0.127	13.75	−1.193 ± 0.052	V
000409	1996-03-15	0.127	13.75	−1.183 ± 0.026	R
000409	1996-03-15	0.127	13.75	−1.288 ± 0.063	I
000409	1996-03-17	0.024	14.35	−1.122 ± 0.231	U
000409	1996-03-17	0.024	14.35	−1.287 ± 0.107	B
000409	1996-03-17	0.024	14.35	−1.087 ± 0.045	V
000409	1996-03-17	0.024	14.35	−1.002 ± 0.062	R
000409	1996-03-17	0.024	14.35	−1.173 ± 0.105	I
000409	1999-12-14	0.281	18.43	−1.069 ± 0.181	U
000444	2010-04-20	0.241	3.70	−0.628 ± 0.030	V
000444	2004-02-16	0.112	9.80	−2.199 ± 0.196	B
000444	2004-02-16	0.112	9.80	−1.304 ± 0.181	V
000444	2004-02-16	0.112	9.80	−1.631 ± 0.136	R
000444	2010-09-04	0.991	18.20	−0.964 ± 0.159	V
000444	2012-10-23	0.360	20.90	0.260 ± 0.060	V
000451	2004-06-29	0.094	10.19	−1.112 ± 0.229	U
000451	2004-06-29	0.094	10.19	−1.617 ± 0.085	B
000451	2004-06-29	0.094	10.19	−1.359 ± 0.075	V
000451	2004-06-29	0.094	10.19	−1.555 ± 0.071	R
000451	2004-06-29	0.094	10.19	−1.523 ± 0.109	I
000451	2004-07-01	0.087	10.73	−0.860 ± 0.187	B
000451	2004-07-01	0.087	10.73	−0.394 ± 0.071	V
000451	2004-07-01	0.087	10.73	−0.246 ± 0.051	R
000451	2004-07-01	0.087	10.73	−0.366 ± 0.164	I
000451	2004-06-28	0.097	8.93	−1.599 ± 0.222	U
000451	2004-06-28	0.097	8.93	−1.596 ± 0.205	B
000451	2004-06-28	0.097	8.93	−1.583 ± 0.093	V
000451	2004-06-28	0.097	8.93	−1.467 ± 0.126	R
000451	2004-06-28	0.097	8.93	−1.228 ± 0.141	I
000456	2002-03-06	0.288	16.13	0.051 ± 0.313	U
000456	2002-03-06	0.288	16.13	−0.550 ± 0.143	B
000456	2002-03-06	0.288	16.13	−0.208 ± 0.080	V
000456	2002-03-06	0.288	16.13	−0.355 ± 0.040	R
000456	2002-03-06	0.288	16.13	−0.745 ± 0.111	I
000456	2003-08-22	0.208	8.89	−1.064 ± 0.388	B
000456	2003-08-22	0.208	8.89	−0.752 ± 0.099	V
000456	2003-08-22	0.208	8.89	−0.552 ± 0.105	R

Table B.1. continued.

Asteroid Number	Date of observation	Fraction of day	Phase angle (deg)	P_r (%)	Filter
000456	2003-08-22	0.208	8.89	−0.484 ± 0.225	I
000471	2013-07-29	0.020	16.40	−0.210 ± 0.050	V
000472	2003-08-22	0.320	18.88	−0.077 ± 0.188	V
000472	2003-08-22	0.320	18.88	−0.309 ± 0.192	R
000472	2003-08-22	0.320	18.88	−0.154 ± 0.291	I
000476	2013-07-28	0.285	8.60	−1.492 ± 0.070	V
000476	2013-07-29	0.200	8.30	−1.489 ± 0.090	V
000491	2002-03-05	0.193	1.67	−0.921 ± 0.238	B
000491	2002-03-05	0.193	1.67	−0.530 ± 0.099	V
000491	2002-03-05	0.193	1.67	−0.464 ± 0.083	R
000491	2002-03-05	0.193	1.67	−0.673 ± 0.214	I
000491	2002-03-06	0.190	1.69	−0.137 ± 0.161	V
000491	2002-03-06	0.190	1.69	−0.214 ± 0.173	R
000491	2002-03-07	0.187	1.80	−0.341 ± 0.290	B
000491	2002-03-07	0.187	1.80	−0.481 ± 0.074	V
000491	2002-03-07	0.187	1.80	−0.478 ± 0.091	R
000491	2002-03-07	0.187	1.80	−0.397 ± 0.319	I
000532	2012-10-20	0.158	8.30	−0.660 ± 0.020	V
000542	2003-08-22	0.239	7.46	−0.152 ± 0.323	B
000542	2003-08-22	0.239	7.46	−0.425 ± 0.090	V
000542	2003-08-22	0.239	7.46	−0.500 ± 0.115	R
000542	2003-08-22	0.239	7.46	−0.285 ± 0.348	I
000542	1999-12-13	0.228	9.08	−0.163 ± 0.221	V
000542	1999-12-13	0.228	9.08	−0.335 ± 0.105	R
000542	1999-12-13	0.228	9.08	−0.361 ± 0.213	I
000550	1996-11-15	0.321	15.82	−0.654 ± 0.206	V
000550	1996-11-15	0.321	15.82	−0.671 ± 0.173	R
000550	1996-11-14	0.345	16.05	−0.593 ± 0.189	V
000550	1996-11-14	0.345	16.05	−0.774 ± 0.156	R
000550	1995-10-20	0.121	24.16	0.638 ± 0.104	V
000550	1995-10-20	0.121	24.16	0.493 ± 0.153	R
000550	2003-08-22	0.086	27.73	1.293 ± 0.258	V
000550	2003-08-22	0.086	27.73	0.758 ± 0.227	R
000550	2003-08-22	0.086	27.73	0.972 ± 0.268	I
000554	2004-02-13	0.228	4.74	−0.433 ± 0.305	U
000554	2004-02-13	0.228	4.74	−0.864 ± 0.160	B
000554	2004-02-13	0.228	4.74	−0.934 ± 0.049	V
000554	2004-02-13	0.228	4.74	−0.901 ± 0.028	R
000554	2004-02-13	0.228	4.74	−1.142 ± 0.116	I
000572	2002-10-09	0.345	24.42	0.875 ± 0.364	B
000572	2002-10-09	0.345	24.42	0.374 ± 0.150	V
000572	2002-10-09	0.345	24.42	0.663 ± 0.093	R
000573	2002-03-05	0.194	0.63	−0.230 ± 0.188	V
000573	2002-03-05	0.194	0.63	−0.271 ± 0.131	R
000573	2002-03-06	0.191	1.00	−0.730 ± 0.179	V
000573	2002-03-06	0.191	1.00	−0.492 ± 0.163	R
000573	1999-07-17	0.327	14.99	−0.505 ± 0.355	V
000573	1999-07-17	0.327	14.99	−0.499 ± 0.233	R
000600	1999-12-13	0.290	9.89	−0.427 ± 0.193	V
000600	1999-12-13	0.290	9.89	−0.620 ± 0.120	R
000600	1999-12-13	0.290	9.89	−0.802 ± 0.383	I
000604	1996-03-16	0.198	0.54	0.080 ± 0.131	V
000604	1996-03-16	0.198	0.54	−0.185 ± 0.149	R
000604	1996-03-17	0.130	0.73	−0.551 ± 0.330	V
000604	1996-03-17	0.130	0.73	−0.332 ± 0.117	R
000604	1996-03-18	0.192	0.98	−0.313 ± 0.190	V
000604	1996-03-18	0.192	0.98	−0.116 ± 0.147	R
000625	1999-07-17	0.297	14.50	−0.663 ± 0.324	U
000625	1999-07-17	0.297	14.50	−0.645 ± 0.158	B

Table B.1. continued.

Asteroid Number	Date of observation	Fraction of day	Phase angle (deg)	P_r (%)	Filter
000625	1999-07-17	0.297	14.50	−0.466 ± 0.141	V
000625	1999-07-17	0.297	14.50	−0.590 ± 0.068	R
000625	1999-07-17	0.297	14.50	−0.485 ± 0.109	I
000625	1999-07-16	0.263	15.35	−0.600 ± 0.228	B
000625	1999-07-16	0.263	15.35	−0.425 ± 0.225	V
000625	1999-07-16	0.263	15.35	−0.324 ± 0.151	R
000625	1999-07-16	0.263	15.35	−0.381 ± 0.270	I
000625	2003-08-25	0.056	26.59	0.372 ± 0.130	V
000625	2003-08-25	0.056	26.59	0.431 ± 0.107	R
000625	2003-08-25	0.056	26.59	1.241 ± 0.323	I
000660	1999-12-14	0.135	15.89	−0.244 ± 0.249	B
000660	1999-12-14	0.135	15.89	0.058 ± 0.102	V
000660	1999-12-14	0.135	15.89	−0.195 ± 0.072	R
000660	1999-12-14	0.135	15.89	−0.607 ± 0.228	I
000660	2003-08-24	0.400	21.60	0.012 ± 0.096	V
000660	2003-08-24	0.400	21.60	0.172 ± 0.134	R
000660	2003-08-24	0.400	21.60	0.403 ± 0.354	I
000661	1999-07-17	0.256	14.48	−0.458 ± 0.238	V
000661	1999-07-17	0.256	14.48	−0.802 ± 0.140	R
000661	1999-07-16	0.294	14.50	−0.910 ± 0.163	R
000662	1999-12-13	0.125	10.76	−1.317 ± 0.333	V
000662	1999-12-13	0.125	10.76	−0.639 ± 0.163	R
000678	2009-02-19	0.337	17.00	−0.128 ± 0.073	V
000678	1999-12-14	0.328	22.37	−0.153 ± 0.310	B
000678	1999-12-14	0.328	22.37	−0.048 ± 0.101	V
000678	1999-12-14	0.328	22.37	0.365 ± 0.096	R
000678	1999-12-14	0.328	22.37	−0.294 ± 0.214	I
000704	2009-02-21	0.210	6.70	−1.307 ± 0.020	V
000704	2009-02-19	0.211	7.10	−1.226 ± 0.030	V
000704	2010-04-22	0.220	7.20	−1.247 ± 0.020	V
000704	2010-04-21	0.229	7.30	−1.184 ± 0.020	V
000704	2003-03-10	0.050	15.43	−0.050 ± 0.145	U
000704	2003-03-10	0.050	15.43	−0.118 ± 0.090	B
000704	2003-03-10	0.050	15.43	0.045 ± 0.044	V
000704	2003-03-10	0.050	15.43	0.038 ± 0.044	R
000704	2003-03-10	0.050	15.43	0.235 ± 0.097	I
000704	2004-07-03	0.970	16.54	0.358 ± 0.155	B
000704	2004-07-03	0.970	16.54	0.309 ± 0.127	V
000704	2004-07-03	0.970	16.54	0.187 ± 0.073	R
000704	2004-07-03	0.970	16.54	−0.011 ± 0.100	I
000704	2004-06-29	0.961	16.67	0.488 ± 0.364	U
000704	2004-06-29	0.961	16.67	0.180 ± 0.342	B
000704	2004-06-29	0.961	16.67	0.237 ± 0.199	R
000704	2004-06-29	0.961	16.67	0.556 ± 0.248	I
000737	2012-10-23	0.276	11.40	−0.719 ± 0.051	V
000769	1997-05-02	0.180	1.20	−0.174 ± 0.222	B
000769	1997-05-02	0.180	1.20	−0.411 ± 0.081	V
000769	1997-05-02	0.180	1.20	−0.258 ± 0.053	R
000769	1997-05-02	0.180	1.20	−0.372 ± 0.185	I
000787	1996-11-16	0.084	15.34	−0.472 ± 0.067	V
000787	1996-11-16	0.084	15.34	−0.300 ± 0.050	R
000787	1996-07-15	0.341	26.27	0.405 ± 0.211	V
000787	1996-07-15	0.341	26.27	0.480 ± 0.168	R
000787	1996-07-12	0.366	26.31	0.548 ± 0.361	V
000787	1996-07-12	0.366	26.31	0.479 ± 0.184	R
000787	2012-10-23	0.135	16.40	−0.335 ± 0.060	V
000791	2013-07-27	0.097	19.10	0.308 ± 0.060	V
000796	2003-03-10	0.328	18.20	−0.422 ± 0.190	V
000796	2003-03-10	0.328	18.20	−0.376 ± 0.172	R

Table B.1. continued.

Asteroid Number	Date of observation	Fraction of day	Phase angle (deg)	P_r (%)	Filter
000796	1995-10-18	0.076	30.85	1.654 ± 0.170	B
000796	1995-10-18	0.076	30.85	1.455 ± 0.100	V
000796	1995-10-18	0.076	30.85	1.398 ± 0.098	R
000796	1995-10-18	0.076	30.85	1.277 ± 0.156	I
000796	1995-10-19	0.058	31.00	1.599 ± 0.203	B
000796	1995-10-19	0.058	31.00	1.305 ± 0.135	V
000796	1995-10-19	0.058	31.00	1.204 ± 0.104	R
000796	1995-10-19	0.058	31.00	0.801 ± 0.252	I
000796	1995-12-01	0.045	33.25	1.855 ± 0.344	B
000796	1995-12-01	0.045	33.25	1.352 ± 0.041	V
000796	1995-12-01	0.045	33.25	1.984 ± 0.200	R
000796	1995-12-01	0.045	33.25	1.991 ± 0.175	I
000832	2003-08-23	0.186	0.71	−0.358 ± 0.139	V
000832	2003-08-23	0.186	0.71	−0.145 ± 0.166	R
000832	2003-08-24	0.114	0.59	−0.548 ± 0.138	V
000832	2003-08-24	0.114	0.59	−0.271 ± 0.169	R
000832	2003-08-25	0.156	0.81	−0.270 ± 0.202	V
000832	2003-08-25	0.156	0.81	−0.443 ± 0.155	R
000832	2003-08-25	0.156	0.81	−1.865 ± 0.166	I
000832	2003-08-22	0.187	1.00	−0.455 ± 0.158	V
000832	2003-08-22	0.187	1.00	−0.165 ± 0.152	R
000834	2004-02-15	0.273	0.98	−0.418 ± 0.194	V
000834	2004-02-15	0.273	0.98	−0.566 ± 0.187	R
000834	2004-02-14	0.201	1.00	−0.519 ± 0.243	V
000834	2004-02-14	0.201	1.00	−0.672 ± 0.193	R
000857	2004-06-28	0.254	9.83	−0.744 ± 0.159	V
000857	2004-06-28	0.254	9.83	−0.751 ± 0.149	R
000857	2004-06-28	0.254	9.83	−1.159 ± 0.323	I
000863	1995-10-19	0.222	10.96	−0.634 ± 0.174	V
000863	1995-10-19	0.222	10.96	−0.410 ± 0.159	R
000863	1995-10-18	0.346	11.07	−0.746 ± 0.269	V
000863	1995-10-18	0.346	11.07	−0.807 ± 0.142	R
000863	1995-11-29	0.132	11.44	−0.308 ± 0.197	V
000863	1995-11-29	0.132	11.44	−0.250 ± 0.120	R
000863	1995-11-29	0.132	11.44	−0.462 ± 0.360	I
000863	1995-11-30	0.129	11.59	−0.100 ± 0.136	V
000863	1995-11-30	0.129	11.59	−0.320 ± 0.174	R
000863	1995-12-01	0.126	11.73	−0.285 ± 0.217	V
000863	1995-12-01	0.126	11.73	−0.543 ± 0.137	R
000863	1996-11-18	0.326	15.89	−0.343 ± 0.158	R
000863	2012-10-21	0.249	10.10	−0.099 ± 0.050	V
001100	2002-10-09	0.177	0.79	−0.439 ± 0.196	V
001100	2002-10-09	0.177	0.79	0.005 ± 0.090	R
001105	1996-11-16	0.274	10.12	−1.203 ± 0.160	V
001105	1996-11-16	0.274	10.12	−1.097 ± 0.125	R
001105	1995-10-18	0.193	16.58	−0.524 ± 0.313	V
001105	1995-10-18	0.193	16.58	−0.617 ± 0.245	R
001105	1995-10-20	0.084	17.00	−0.779 ± 0.276	V
001105	1995-10-20	0.084	17.00	−0.986 ± 0.152	R
001201	2002-10-10	0.284	0.62	−0.050 ± 0.189	V
001201	2002-10-10	0.284	0.62	−0.386 ± 0.172	R
001263	2013-07-29	0.249	7.70	−1.250 ± 0.170	V
001659	2004-06-30	0.264	10.59	−0.474 ± 0.139	V
001659	2004-06-30	0.264	10.59	−0.727 ± 0.115	R
001659	2004-06-29	0.268	10.84	−0.870 ± 0.283	B
001659	2004-06-29	0.268	10.84	−0.626 ± 0.193	V
001659	2004-06-29	0.268	10.84	−0.764 ± 0.100	R
001659	2004-06-29	0.268	10.84	−0.922 ± 0.220	I
001659	1995-10-20	0.153	22.71	0.544 ± 0.120	V

Table B.1. continued.

Asteroid Number	Date of observation	Fraction of day	Phase angle (deg)	P_r (%)	Filter
001659	1995-10-20	0.153	22.71	0.427 ± 0.190	R
002126	2003-08-23	0.249	1.57	−1.012 ± 0.269	V
002126	2003-08-23	0.249	1.57	−0.212 ± 0.249	R
002126	2003-08-25	0.222	2.65	−0.710 ± 0.284	V
002126	2003-08-25	0.222	2.65	−0.794 ± 0.261	R
002209	2004-02-14	0.190	1.44	−0.046 ± 0.280	V
002209	2004-02-14	0.190	1.44	−0.480 ± 0.255	R
002271	2003-08-24	0.259	0.66	−0.785 ± 0.304	B
002271	2003-08-24	0.259	0.66	−0.069 ± 0.136	V
002271	2003-08-24	0.259	0.66	−0.225 ± 0.143	R
002271	2003-08-24	0.259	0.66	−0.064 ± 0.281	I
002271	2003-08-25	0.298	0.56	−0.476 ± 0.102	V
002271	2003-08-25	0.298	0.56	−0.252 ± 0.151	R
002271	2003-08-25	0.298	0.56	−0.035 ± 0.248	I
002271	2003-08-23	0.201	1.00	−0.283 ± 0.144	V
002271	2003-08-23	0.201	1.00	−0.390 ± 0.130	R
002271	2003-08-23	0.201	1.00	−0.891 ± 0.354	I